

@ Edward Oscar Amponsah-Abu
University of Cape Coast

UNIVERSITY OF CAPE COAST

**DESIGN AND CONSTRUCTION OF A PNEUMATIC TRANSFER
CONTROL UNIT FOR CYCLIC NEUTRON ACTIVATION
ANALYSIS**

BY

EDWARD OSCAR AMPONSAH-ABU

Thesis submitted to the Department of Physics of the School of Physical Sciences, College of Agriculture and Natural Sciences, University of Cape Coast, in partial fulfilment of the requirements for the award of Doctor of Philosophy degree in Physics

SEPTEMBER 2019

DECLARATION

Candidate's Declaration

I hereby declare that this thesis is the result of my own original research and that no part of it has been presented for another degree in this university or elsewhere.

Candidate's Signature: Date:

Name: Edward Oscar Amponsah-Abu

Supervisors' Declaration

We hereby declare that the preparation and presentation of the thesis were supervised in accordance with the guidelines on supervision of thesis laid down by the University of Cape Coast.

Principal Supervisor's Signature: Date:

Name: Prof. Benjamin Jabez Botwe Nyarko

Co-Supervisor's Signature: Date:

Name: Dr. Raymond Edziah

ABSTRACT

Pneumatic Transfer System (PTS) is an auxiliary system of Ghana Research Reactor -1 (GHARR-1) to transfer sample capsule in and out of the reactor irradiation sites. The PTS controller unit design and construction was carried out because the transfer system was not designed to operate in cyclic Neutron Activation Analysis (NAA) and as a result could not determine radionuclides whose half-lives are equal or less than 100 seconds. In addition, most of the components used to design the present one-shot conventional NAA controller unit are outmoded and out of market, posing threat to future maintenance. To address these situations, a Programmable Logic Controller (PLC) has been used to design and construct a control unit to facilitate a cyclic neutron activation analysis for the PTS. The design has been simulated successfully using a LOGO Soft Comfort software, version 8. Function block diagram programming language was used. The constructed control unit has been tested experimentally using 220 AC volts electric bulbs to represent solenoid valves. The results show that the sample-IN and sample-OUT bulbs come ON and go OFF to represent the solenoid valves' opening and closing for sample transfer. The results obtained from the study would eliminate the difficulty of getting up-to-date components to replace the outmoded ones in the PTS control. The study has shown that the computer based PLC controller unit for PTS is capable of facilitating both cyclic and conventional NAA application for GHARR-1 and especially, the Miniature Neutron Source Reactors.

KEY WORDS

Irradiation

Neutron Activation Analysis

Phototransistor

Pneumatic Transfer System

Programmable Logic Controller

Solenoid Valve

ACKNOWLEDGEMENTS

My sincerest gratitude goes to the Almighty God for his unending mercies and support throughout my life and in the execution of this thesis. I am very grateful to Rev. Dr. Akoto-Bamford who encouraged and urged me to pursue my PhD programme in respect of all odds.

I am especially indebted to my thesis supervisors, Prof. B. J. B. Nyarko and Dr. Raymond Edziah whose direction, criticisms and advice nurtured this work into fruition.

I also take this opportunity to express my appreciation to the Head and all lecturers of the Department of Physics of the School of Physical Sciences, College of Agriculture and Natural Sciences, University of Cape Coast for their support, advice and guidance throughout my stay in this University.

My sincere appreciation also goes to Mr. Kwame Gyamfi, Mr. Benjamin Ekow Mensah, Mr. Bernard Osei for their individual contributions towards the completion of this work. My special thanks also go to all the GHARR-1 Reactor Operating Team especially Mr. Henry Obeng, whose support and corporation helped to carry out all the experiments.

To Madam Patience Adu Serwaa, Prof. Shilo Osae, I appreciate your encouragements.

Finally, I wish to thank my family and friends for their support, especially, my wife Dinah Amponsah-Abu, my Children, Foster Owusu Amponsah and Anita Yeboaa Amponsah.

DEDICATION

In memory of my Parents, Opanyin Edward Johnson Abu-Bonsrah and

Madam Janet Adwapah

TABLE OF CONTENTS

| | Page |
|-------------------------------------|------|
| DECLARATION | ii |
| ABSTRACT | iii |
| KEY WORDS | iv |
| ACKNOWLEDGMENTS | v |
| DEDICATION | vi |
| LIST OF TABLES | xiii |
| LIST OF FIGURES | xiv |
| LIST OF ACRONYMS | xix |
| CHAPTER ONE : INTRODUCTION | |
| Background of the Study | 1 |
| Ghana Research Reactor -1 (GHARR-1) | 3 |
| Statement of the Problem | 8 |
| Objectives of the Study | 9 |
| Specific Research Objectives | 9 |
| Significance of the Study | 10 |
| Nuclear Power Programme of Ghana | 10 |
| Radiation Technology Centre | 10 |
| Tertiary Institutions | 10 |
| Delimitations | 11 |
| Limitations | 12 |
| Organization of the Study | 12 |
| Chapter Summary | 13 |

CHAPTER TWO : LITERATURE REVIEW

| | |
|--|----|
| Introduction | 14 |
| The Concept of Neutron Activation Analysis | 14 |
| Activation Process of Nuclides | 14 |
| Invention and early development of PLCs | 16 |
| PLC Programming | 20 |
| Cyclic Neutron Activation Analysis | 21 |
| Dalhousie University SLOWPOKE-2 Reactor (DUSR) facility-CANADA | 24 |
| Atomic Institute, Vienna University of Technology- TRIGA Mark II | 24 |
| Atomic Energy Commission of Syria – MNSR Facility | 26 |
| Equation of Cyclic Activation Analysis | 26 |
| Dead Time and Pile-up Correction | 28 |
| Chapter Summary | 30 |

CHAPTER THREE : MATERIALS AND METHODS

| | |
|---|----|
| Introduction | 32 |
| Logo 8 Siemens Programmable Controller Logic (PLC) Specifications | 32 |
| Web Server Support | 34 |
| Network Access Security | 35 |
| Program Copy Protection | 36 |
| Basic Components of GHARR-1 Pneumatic System | 36 |
| Solenoid Valves | 38 |
| Operation of the Solenoid | 39 |
| Schematic of CNAA of PTS | 41 |
| Pneumatic Transfer Loop System | 43 |

| | |
|--|----|
| Proposed PLC Controller Unit | 45 |
| Control Flow Chart of PTS | 46 |
| Control Flow Chart of a Cyclic Mode Operation with Conventional Mode Option | 47 |
| Block Diagram for the PLC Power Supply | 49 |
| Power Supply Characteristics | 52 |
| Output Power after Rectification | 52 |
| Rectification Efficiency | 53 |
| Output Frequency | 53 |
| Peak Voltage Calculation | 54 |
| Load Regulation | 54 |
| Flow Chart of an 8-way Relay Bank | 54 |
| Common-Emitter Phototransistor | 55 |
| Context Analysis Diagram | 57 |
| Characteristics of Logic used in the PLC FBD Program Interface | 57 |
| Latching Relays | 57 |
| OR Logic Function | 58 |
| AND Logic Function | 59 |
| NOT Logic Function | 60 |
| Wiping Relay (pulse output) Timer | 61 |
| On-Delay Timer | 61 |
| Asynchronous Pulse Generator | 62 |
| Up / Down Counter | 63 |
| State Transition Diagram | 64 |

| | |
|---|----|
| Data Flow Diagram | 65 |
| Design Requirements for Safety Systems and Components (SSCs) | 67 |
| Engineering Safety Features | 67 |
| Pre-Design Appraisal | 67 |
| Safety Considerations for the Design of an Experiment or Modification (IAEA SPECIFIC SAFETY GUIDE No. SSG-24, 2012). | 68 |
| Failure Mode and Effects Analysis for a Computer Based PLC Control Unit for PTS | 68 |
| Methodology for FMEA | 69 |
| Conceptual Full Scale Device Summary | 72 |
| Definitions Important for Understanding Various Items in Table 9 | 78 |
| List of Components for +12 / +24 VDC Power supply | 81 |
| Chapter Summary | 83 |
| CHAPTER FOUR : RESULTS AND DISCUSSION | |
| Introduction | 84 |
| Designed Circuits | 84 |
| Direct-on-Line Starter connection for the Air Compressor Control System | 84 |
| The PLC connections | 86 |
| Dual Voltage Regulated High Current Power Supply (1.25-30V/5A) | 87 |
| Power Supply Response Curves | 89 |
| Peak-to-Peak Voltage Response Curves for V_{RMS} (30 VAC/15 VAC) | 89 |
| Response Curve after Rectification | 90 |
| Smoothing Capacitor Response | 92 |
| Regulated Output Voltage Curve | 93 |

| | |
|--|-----|
| Normal Conventional NAA Operation | 94 |
| Relay Bank for the PLC Output Loads | 95 |
| CNAA Operational Mode | 96 |
| Function Block Diagrams (FBD) Programming Language | 97 |
| CNAA Mode Programme Designed | 97 |
| Conventional Mode Programme Designed | 100 |
| Common-Emitter Phototransistor Circuit Designed | 101 |
| Series Resistor Calculation for LED | 102 |
| Phototransistor Characteristics for Common-Emitter | 103 |
| Integration of Various Components of the Controller Unit | 105 |
| Controller Unit Casing Design | 107 |
| Construction of Controller Unit | 109 |
| Internal features of the PTS controller Unit | 110 |
| Front View of the Constructed PTS Controller Unit | 110 |
| Complete Designed and Construction of PTS Controller | 112 |
| PTS Controller with Bulbs for Simulation | 112 |
| Phototransistor Control Unit | 113 |
| Results and Discussions | 114 |
| Simulation of PTS Controller Designed Programme | 114 |
| Experimental Test Results | 121 |
| Compressor Contactor Coil Energized | 123 |
| Sample-IN Solenoid Valves Open, Bulbs “ON” | 124 |
| Sample-IN Phototransistor Switched | 125 |
| Sample-IN Bulbs go “OFF”, Irradiation Starts | 126 |

| | |
|--|-----|
| Sample Capsule is out of Phototransistor Detection Limit | 127 |
| Illumination Intensity of LED in Sample Capsule Slot | 127 |
| Irradiated Sample Transferred onto Detector for Counting | 128 |
| Irradiation Cycle Repeat, Sample-IN Bulbs “ON” | 129 |
| Web Server Support for Remote access | 129 |
| AnyDesk Remote Desktop Software | 135 |
| Chapter Summary | 138 |
| CHAPTER FIVE : SUMMARY, CONCLUSIONS AND RECOMMENDATIONS | |
| Overview | 139 |
| Summary | 140 |
| Conclusions | 141 |
| Recommendations | 142 |
| REFERENCES | 144 |
| APPENDICES | 151 |
| APPENDIX A | 152 |
| APPENDIX B | 155 |
| APPENDIX C | 156 |

LIST OF TABLES

| Table | Page |
|---|------|
| 1 Comparison of Highly Enriched Uranium (HEU) and Low Enriched Uranium (LEU) - Fuelled Reactor Core Specification | 5 |
| 2 Logic Table of the Latching Relay | 58 |
| 3 Logic Table of OR Function | 59 |
| 4 AND Function Logic Table | 60 |
| 5 NOT Function Logic Table | 61 |
| 6 Severity Classification and Description used in Failure Mode Effect Analysis (FMEA) | 70 |
| 7 Likelihood of Occurrence | 71 |
| 8 Likelihood of Detection of Failures | 72 |
| 9 Failure Mode and Effects Analysis for PTS Control Unit | 75 |
| 10 List of Components used in the Circuit | 82 |
| 11 Comparison of the Control Units | 138 |

LIST OF FIGURES

| Figure | Page |
|--|------|
| 1 The Existing Modified Pneumatic Transefer System Controller | 3 |
| 2 Vertical Cross Section of Ghana Research Reactor-1 | 7 |
| 3 The CrossSsectional View of Ghana Research Reactor-1 Core | 8 |
| 4 A Typical Activation Process of Nuclides | 15 |
| 5 A Programmable Logic Controller System | 18 |
| 6 Time Parameters of Cyclic Activation Analysis and the Variation of the Activity of Nuclides with time and number of cycles | 27 |
| 7 LOGO! Structure for module 0BA8 (LOGO! 12/24VDC RCE) | 33 |
| 8 Ghana Research Reactor-1 Pneumatic System | 36 |
| 9 Air Filter / Water Trap | 38 |
| 10 Solenoid Valves used in Ghana Research Reactor-1 Pneumatic Transfer System | 39 |
| 11 Electromagnetic Field Circuit | 41 |
| 12 Schematic Diagram of Pneumatic Transfer System with little Modification for Cyclic Neutron Activation Analysis | 42 |
| 13 Block Diagram of a Basic Gamma Spectrometry System | 43 |
| 14 Block Diagram of Pneumatic Transfer Loop System | 44 |
| 15 Diagram of the Proposed Controller Unit | 45 |
| 16 A Complete Block Diagram of Pneumatic Transfer System | 46 |
| 17 Flow Chart for Cyclic Mode Analysis with Conventional Mode Option | 47 |
| 18 Block Diagram of a Dual Regulated Voltage Power Supply | 49 |

| | | |
|----|---|----|
| 19 | Integrated Circuit LM 317 Functional Block Diagram | 51 |
| 20 | Output Voltage Regulation Diagram | 51 |
| 21 | Block Diagram of Proposed 8-way Relay Bank | 55 |
| 22 | Pictorial Diagram of a Phototransistor | 55 |
| 23 | Latching Relay | 58 |
| 24 | OR Logic Block | 58 |
| 25 | AND Logic Block | 59 |
| 26 | NOT Logic Block | 60 |
| 27 | Pulse Output Timer Block | 61 |
| 28 | On-Delay Timer Block | 62 |
| 29 | Asynchronous Pulse Generator Block | 62 |
| 30 | Up/Down Counter Block | 63 |
| 31 | Context Analysis Diagram | 64 |
| 32 | State Transition Diagram for Conventional Neutron Activation Analysis and Cyclic Mode Operation | 65 |
| 33 | Flow Chart for Cyclic and Conventional Modes of Analysis | 66 |
| 34 | A Complete Functional Block Diagram of Pneumatic Transfer System for Failure Mode Effect Analysis | 73 |
| 35 | Flow Chart for Cyclic Mode Analysis with Conventional Mode Option for Failure Mode Effect Analysis | 73 |
| 36 | Block Diagram of the Controller Unit for Failure Mode Effect Analysis | 74 |
| 37 | Legend of Figure 34, 35 and 36 | 74 |
| 38 | Schmitt Trigger Diagram for a Remote Control of Air | |

| | |
|---|-----|
| Compressor System by Programmable Logic Controller | 84 |
| 39 Schematic Diagrams of the Existing Pneumatic Transfer System | |
| Air-Compressor Connection | 86 |
| 40 Input and Output Connections of Programmable Logic Controller | 86 |
| 41 Dual Voltage Regulated Power Supply – 12/24 VDC | 87 |
| 42 Peak Voltage Response Curve of Transformer Output V_T for 30 V_{RMS} | 89 |
| 43 Peak Voltage Response Curve of Transformer Output V_T for 15 V_{RMS} | 90 |
| 44 Response after Rectification for +24 VDC Circuit | 91 |
| 45 Response after Rectification for +12 VDC Circuit | 92 |
| 46 Smoothing by Capacitor C_1 and before the Regulator for +24 VDC | 92 |
| 47 Smoothing by Capacitor C_5 and before the Regulator for +12 VDC | 93 |
| 48 Regulated Output Voltage for +24 VDC | 93 |
| 49 Regulated Output Voltage for +12 VDC | 94 |
| 50 Eight (8)-way Relay Bank | 96 |
| 51 The Designed Cyclic Mode Activation Programme | 98 |
| 52 Designed Conventional Mode Activation Programme | 100 |
| 53 Common-Emitter Phototransistor Circuit | 101 |
| 54 I-V Characteristics for Light Emitting Diode | 103 |
| 55 Load Line for $I_{C(Sat)} / V_{CE}$ | 104 |
| 56 Schematic Diagram of Pneumatic Transfer System Controller | 106 |
| 57 Side View 1 of the Pneumatic Transfer System of Programmable Logic Controller Control Unit Casing | 107 |
| 58 Side View 2 of the Pneumatic Transfer System of Programmable Logic Controller Control Unit Casing | 108 |

| | | |
|----|--|-----|
| 59 | The Front View of the Pneumatic Transfer System of Programmable Logic Controller Control Unit Casing | 108 |
| 60 | Back View of the Pneumatic Transfer System of Programmable Logic Controller Control Unit Casing | 109 |
| 61 | Top Cover of the Pneumatic Transfer System of Programmable Logic Controller Control Unit Casing | 109 |
| 62 | Constructed Pneumatic Transfer System Controller Unit | 110 |
| 63 | Front View of Pneumatic Transfer System Controller Unit | 111 |
| 64 | Designed and Constructed Pneumatic Transfer System Controller | 112 |
| 65 | Pneumatic Transfer System Controller with Bulbs to Simulate the Solenoid Valves | 113 |
| 66 | Phototransistor Control Unit with Sample Capsule | 114 |
| 67 | Compressor Contactor Coil and Solenoid Valves Energized | 116 |
| 68 | Irradiation Process; Light Flashes and Buzzer Beeps | 117 |
| 69 | Solenoid Valves S2/S4 Energized, Sample out of Irradiation Site | 118 |
| 70 | Counting of Samples | 119 |
| 71 | Irradiation Cycle Repeats and Solenoid Valves S1 and S3 Open (Second Cycle) | 120 |
| 72 | Contactoer Coil Energized, Compressor Starts | 123 |
| 73 | SAMPLE-IN Button Depressed, Solenoid Valves S1 and S3 Open | 124 |
| 74 | Phototransistor Detects Sample Capsule, Output +24 VDC | 125 |
| 75 | Solenoid Valves S1 and S3 Close; Sample Irradiation Starts with Flash Light / Beeps of Buzzer | 126 |
| 76 | Sample Capsule moved out the reach of Phototransistor | 127 |

| | | |
|----|---|-----|
| 77 | Illumination of Light Emitting Diode in the Sample Slot | 127 |
| 78 | Irradiated Sample Transferred to Detector | 128 |
| 79 | Irradiation Cycle is Repeated | 129 |
| 80 | Log on to Display the Information to be Monitored | 131 |
| 81 | The Pneumatic Transfer System Control Unit not in Operation | 131 |
| 82 | Air-Compressor and Solenoid-IN Buttons Depressed, Compressor ON and Solenoid-IN Opened | 132 |
| 83 | Irradiation Flash Light ON, Sample Irradiation in Progress | 132 |
| 84 | Solenoid – OUT Opened, Sample Capsule out of Irradiation Site | 133 |
| 85 | Irradiation Cycle Repeated, Counter Recorded the two Samples for the Cycles | 133 |
| 86 | Air-Compressor and Solenoid-IN Buttons Depressed, Compressor ON and Solenoid-IN Opened (monitored from mobile phone) | 134 |
| 87 | Irradiation Cycle Repeated, Counter Recorded the two Samples for the Cycles (monitored from mobile phone) | 135 |
| 88 | Your AnyDesk and Remote Desk Window for Connectivity | 136 |
| 89 | Window for Remote Desk ID | 137 |

LIST OF ACRONYMS

| | |
|----------|---|
| GHARR-1 | Ghana Research Reactor -1 |
| UCC | University of Cape Coast |
| CRP | Coordinated Research Project |
| TECDOC | Technical Document |
| LED | Light Emitting Diode |
| TRIGA | Training, Research, Isotopes, General Atomics |
| SLOWPOKE | Safe Low-Power Critical Experiment |
| ASCII | Americans Standard Code for Information |
| PIXE | Particle Induced X-Ray Emission |
| ICP-AES | Inductively Coupled Plasma-Atomic Emission Spectrometry |
| ICP-MS | Inductively Coupled Plasma-Mass Spectrometry |
| XRF | X-Ray Fluorescence |
| DC | Direct Current |
| PLC | Programmable Logic Controller |
| ICs | Integrated Circuits |
| MNSR | Miniature Neutron Source Reactor |
| CIAE | China Institute of Atomic Energy |
| IAEA | International Atomic Energy Agency |
| TRIAC | TRIode for Alternating Current |
| NAA | Neutron Activation analysis |
| HEU | Highly Enriched Uranium |
| LEU | Low Enriched Uranium |

CHAPTER ONE

INTRODUCTION

Background of the Study

Ghana's Miniature Neutron Source Reactor (MNSR) also known as Ghana Research Reactor – 1 (GHARR-1) is used mainly for Neutron Activation Analysis (NAA) (Akaho, Maaku, Dodoo-Amoo, & Anim-Sampong, 1999; Akaho et al., 1995). The pneumatic system for MNSR is an auxiliary system of GHARR-1 used to transfer sample capsule in and out of the reactor irradiation sites. The existing controller of GHARR-1 pneumatic system cannot be used effectively for short-lived radionuclide with half-life < 100 seconds. This is due to the fact that the current one-shot irradiation-counting sequence does not achieve optimum activity levels (approaching saturation activity). The advantages of Cyclic Neutron Activation Analysis (CNAA), as compared with conventional activation analysis (a one-shot irradiation-counting sequence), include significant improvements of the detection limits, analytical precision, and accuracy of elements detection, short experimental time and increased number of samples per unit time (Hou, 2000).

In addition, most of the integrated circuits (ICs) which control bidirectional circuits, a TRIode for Alternating Current (TRIAC) which operate the solenoid valves for the passage of compressed air to transfer the samples into the reactor are outmoded or obsolete. These ICs are out of market, (ICs C035 and C036) (Huabai, Gao, Shuping, & Yulun, 1992) therefore, the need for a new controller unit using a Programmable Logic Controller (PLC) for CNAA

application and to maintain continuous operation of the PTS. The original controller circuits have been consequently modified in order to accommodate the different pin configurations of the equivalent ICs, see Figure 1. This modification differs from the current circuit diagram in the maintenance manual for the pneumatic capsule transfer system. The design is becoming out-of-date in comparison with current standards and technology. With ageing of Ghana Atomic Energy Commission (GAEC) staff and the organization losing the old GHARR-1 experienced staff, it has become imperative therefore to redesign the PTS controller using an industrial computer based PLC to ensure proper documentation for future reference and continuous use of the facility. Hence, the present situation poses future maintenance problems. The reactor has one control rod serving as regulating rod as well as safety rod. An alternative means of reactor control is provided using external cadmium materials encapsulated in vials for transfer by the PTS into the inner irradiation sites of the reactor, which ensure reactor sub-criticality in case of rod – stuck accidents. The PTS therefore has to be in operation along the reactor.

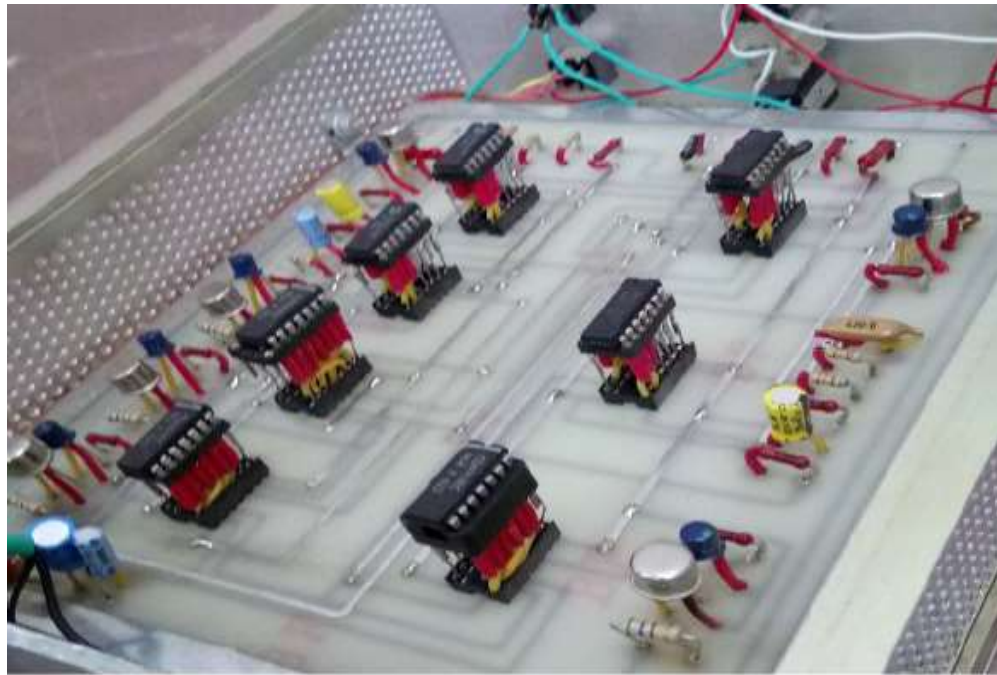


Figure 1: The existing modified PTS controller.

Ghana Research Reactor -1 (GHARR-1)

GHARR-1 is a commercial type of the MNSR designed, manufactured and constructed by China Institute of Atomic Energy (CIAE), Beijing, China. It is designed for use in universities, hospitals and research institutes mainly for neutron activation analysis, education and training, manpower development and commercial activities (Akaho et al., 1995). It is cooled by natural convection and moderated with light water. The reactor was acquired under a tripartite agreement between Ghana, China and International Atomic Energy Agency (IAEA). The reactor was installed in December 1994 and achieved criticality on December 17, 1994. The pneumatic transfer system, normally called “the rabbit system” is an important auxiliary system of the MNSR. The rabbit system is used for the transfer of samples packed in a capsule into the irradiation sites of the reactor. The PTS and its associated controller unit has been in operation for over 24 years

now. The ICs used in designing the control system have become obsolete and out of market. The operating organization of the facility carried out corrective and preventive maintenance on the facility to ensure smooth operation of the reactor. This was done to mitigate obsolescence of components (non-physical ageing), i.e. their becoming out-of-date in comparison with current standards and technology. The management of the facility will inconvenience their clients (as a result of frequent break-down of the system) such as:

- (i) The tertiary institutions for their thesis work
- (ii) The Mines
- (iii) The oil industries
- (iv) Hospitals etc.

In the late 1970s, concerted efforts were made to convert all civilian research reactors around the world from Highly Enriched Uranium (HEU) to Low Enriched Uranium (LEU); any nuclear fuel that has enrichment greater than 20 % is considered HEU.

In the year 2005, the IAEA conceived the conversion of all MNSRs. Feasibility studies for this conversion started in 2006 with all the countries operating MNSR represented. The feasibility studies ended in 2012 with a conclusion that the GHARR - 1 MNSR could be converted from the 90.2 % UAl_4 fuel to a 12.5 % UO_2 fuel. This was later revised to 13.0 % due to certain technicalities. See Table 1 for the comparison of the HEU and LEU- fuelled reactor core specifications (Odoi et al., 2018).

Table 1: Comparison of Highly Enriched Uranium and Low Enriched Uranium-Fuelled Reactor Core Specification

| Parameters | HEU Description | LEU Description |
|---------------------------------|------------------------|-------------------------|
| Reactor Type | Pool –in-tank | Pool-in-tank |
| Rated thermal power | 30 kW | 34 kW |
| Fuel | UAl ₄ | UO ₂ Pellets |
| U-235 enrichment | 90.2% | 13% |
| Core shape | Cylindrical | Cylindrical |
| Core diameter | 23 cm | 23 cm |
| Active core height | 23 cm | 23 cm |
| Fuel element shape | Thin rod | Thin rod |
| Fuel elements in the core | 344 | 335 |
| Control rod | One control rod | One control rod |
| Fuel cladding | Al alloy | Zr-4 alloy |
| Cladding thickness | 0.6 mm | 0.55 mm |
| Fuel meat density | 3.45 g/cm ³ | 10.6 g/cm ³ |
| U-235 weight per fuel pin | 2.87 g | 4.033 g |
| Total U-235 loading in the core | 998.1g | 1355.3 g |
| Reactor cooling mode | Natural convection | Natural convection |

The first MNSR was converted in 2015, in China. Ghana’s MNSR was the first to be converted outside China. The other MNSR operating countries are Iran, Nigeria, Pakistan and Syria. The HEU fuel was removed from the reactor in August, 2016 and returned to China as per contract signed prior to the supply of the reactor to Ghana.

On June 22, 2017 the fresh LEU fuel was received in Ghana via National Nuclear Research Institute-Ghana Atomic Energy Commission. On July 5 assembling of the fuel cage commenced, it was loaded into the reactor on July 12 and the GHARR-1 went critical for the second time on July 13, 2017 at about 13:30 GMT.

The reactor complex contains five (5) major components. These are the reactor assembly, control console, auxiliary systems (including PTS), irradiation system and the pool containing light water. The reactor assembly consists of the reactor vessel which contains the reactor core, beryllium (Be) reflector, small fission chambers for detecting neutron fluxes, 1 central cadmium (Cd) control rod and its drive mechanism, and thermocouples for measuring inlet and outlet temperatures of the coolant. The reactor vessel is a cylindrical aluminium (Al) alloy container, 0.6 m in diameter and 5.6 m high. The container, which is built in two (2) sections, is suspended in a stainless steel-lined water pool surrounded by reinforced concrete.

The reactor core consists of fuel elements, which form a fuel cage. The cage is inside an annular beryllium reflector and rests on a lower beryllium reflector plate. The volume of the vessel is 1.5 m³. The fuel elements are arranged in 10 multi-concentric circle layers at a pitch distance of 10.95 mm. The element cage consists of 2 grid plates, 4 tie rods and a guide tube for the control rod. Screws connect the 2 grid plates and 4 tie rods. There are 5 inner irradiation tubes installed within the beryllium annulus. Five outer irradiation tubes are also installed outside the beryllium annulus (Gao Jijin, 1993) shown in Figures 2 and 3.

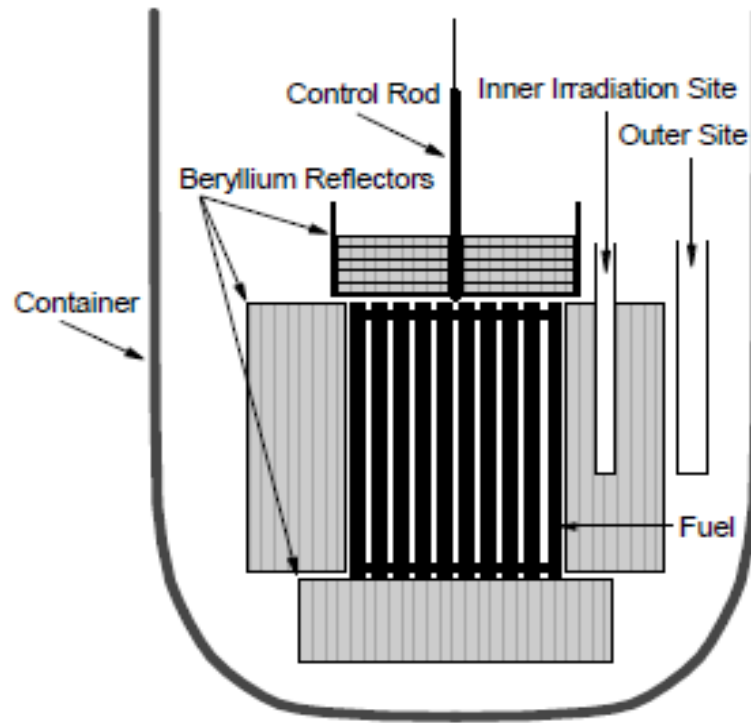


Figure 2: Vertical cross section of GHARR-1 reactor.

Source: (Chilian & Kennedy, 2009)

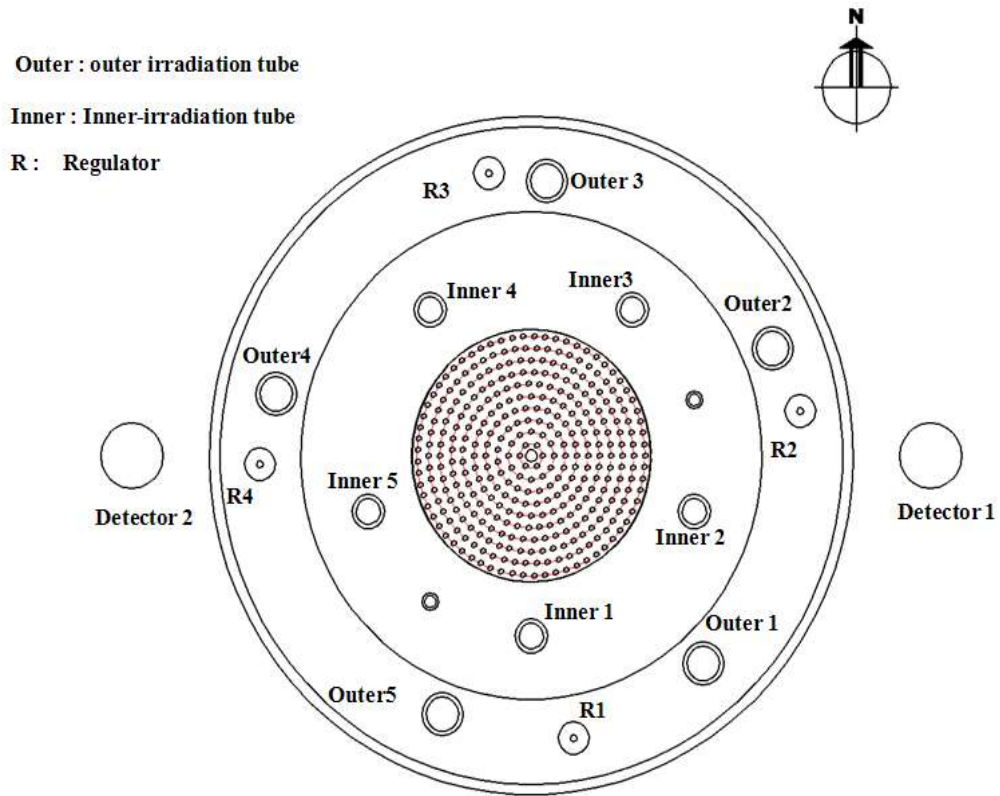


Figure 3: The cross-sectional view of GHARR-1 core.

Source: (Yiguo et al., 2017)

Statement of the Problem

The pneumatic transfer system of GHARR-1 was originally not designed to facilitate cyclic activation analysis.

The existing PTS is required to facilitate the determination of short-lived nuclides by instrumental neutron activation analysis (INAA) technique (Gao Jijin, 1993). Instead, it is not suitable for the determination of very short-lived nuclides (half-lives <100 seconds). Furthermore, maintenance of the control system is becoming increasingly difficult owing to non-availability of old electronic components due to current technological advancement. The existing controller uses integrated

circuits (ICs) which were designed over twenty four (24) years ago and out of market.

Objectives of the Study

To replace the GHARR-1 existing PTS controlling unit by redesigning and constructing a new controlling system with a computer based programmable logic controller (PLC) to facilitate cyclic neutron activation analysis. This will ensure continuous operation of the facility and eliminate the difficulty of getting up-to-date components to replace the outmoded ones in the PTS controller.

Specific Research Objectives

- (i) To develop an integrated system to incorporate the PLC, newly designed power supply and relay bank to enable automatic control of the CNAA.
- (ii) To facilitate rapid and successive transfer of capsules in and out of reactor irradiation sites through a newly designed controlling interface.
- (iii) To validate the effectiveness of the newly constructed PTS controlling unit through simulation.
- (iv) To incorporate a web support system for the Reactor Facility Manager to monitor the operation of PTS remotely from his PC or cell phone.
- (v) To enable remote and automatic control of the air compressor during operation of the PTS using the PLC.
- (vi) To provide a well-documented circuitry for the PTS controller unit to facilitate future maintenance.

Significance of the Study

Incorporation of CNAA will expand the analytical capabilities and also deal with the issue of obsolescence of components for maintenance of PTS.

Knowledge and skills acquired in the use of PLC can be used in training human resource in the following areas

1. Nuclear Power Programme of Ghana.
2. Radiation Technology Centre (RTC)
3. Tertiary Institutions as well as Industries.
4. Applicable to MNSR Member States

Nuclear power programme of Ghana

It is anticipated that Ghana will add Nuclear energy to its energy mix. Nuclear Power Plants deal with various controls which could include PLC. The knowledge acquired would be helpful in training human resource toward the development of the country's Nuclear Power Programme.

Radiation Technology Centre

The PLC could be used to control the ^{60}Co gamma source for radiation processing for the treatment of food and medical supplies (conveyor system).

Tertiary Institutions

A course could be developed in the Tertiary Institutions to pass on knowledge to students and also develop critical manpower and expertise in dealing with PLC.

The MNSR countries can take advantage to upgrade their pneumatic transfer systems to PLC to facilitate NAA programme at their centres. The project would also be applicable to industries where control of motors and other control devices are done.

The study will facilitate the determination of Selenium, Fluorine, and Oxygen in biological materials; Lead, Fluorine, Scandium, and Silver in

environmental Samples; Oxygen, Scandium, Silicon, Aluminum, Silver, Gold, Rhodium, Hafnium, Lead and Uranium in geological and industrial materials. A successful integration of cyclic mode NAA in the one-short conventional system will enable the technique to be applied in biological, environmental, geological, industrial and forensic studies (Hou, 2000).

Delimitations

The scope of the study will cover the removal of the existing pneumatic transfer system controller, design and construct a new controller interface using PLC LOGO with a software (LOGO! Soft Comfort V8.0) to enhance cyclic and conventional modes of neutron activation analysis. The study will design and build eight-channel relay bank to operate the solenoid valves. The relay bank will serve as interface between the PLC unit and solenoids in the system which open and close to allow a compressed-air to pump the samples in the capsules into the reactor for irradiation. A dual regulated power supply (+24 VDC and +12 VDC) will be designed and built to operate the PLC and the relay coils.

A remote and automatic control of the air-compressor through the magnetic starter is designed using the PLC to control its operation during sample irradiation. A casing is designed and constructed to accommodate the various circuits designed and built to constitute a controller unit. Five bulbs are mounted on a board to simulate the operation of the solenoids and the compressor respectively.

A web support system is incorporated for the Reactor Facility Manager to monitor the operation of PTS remotely from his PC or cell phone. Finally, to provide a well-documented circuitry for the PTS to facilitate future maintenance.

Limitations

The application of CNAAs is limited by the number of elements determined, because only some of the elements determined by conventional activation analysis can be determined by this method. In addition, samples become more active after each irradiation and therefore dead time and pile-up effects increase as the number of cycles increases and must be corrected.

Organization of the Study

This thesis is organized into five chapters: Chapter one describes the background of the study with short introduction that presents the problem under study, why the problem is important and how the study relates to previous work. The chapter also gives the practical and theoretical implications of the study and further described the context within which the problem occurs for readers to put the problem in context. It points out existing knowledge gaps to be resolved, that is, what the previous research in the area did or could not resolve. The chapter stated the purpose of the study in broad terms and defines the research objectives. The significance of the study is how the results could be used and the benefits from the results is highlighted. The chapter covers the delimitations which defines the scope of study in the research design and also the limitation of the study.

Chapter two is the literature review which is a recap of what the study is about; provides a summary of the pertinent literature with respect to what is known about this topic of study and the gaps in knowledge that must be closed. It explores the key concepts and theories around which the study is built. This is followed by the chapter three which focuses on the methodology and describes the designed procedures of the circuits used in the study in sufficient details.

Chapter four contains the results from the study which includes the actual design and construction of the controller and associated components designed with emphasis on important observations. The study is concluded in chapter five with the conclusions and suggestions for future study.

Chapter Summary

In chapter one, the background of the study was presented and also the basis for conducting the research. The chapter provides information on statement of problem, relevance and justification of the research, objectives and scope of the research, and concludes with an elaboration of the structure of the study.

CHAPTER TWO

LITERATURE REVIEW

Introduction

This chapter serves to analyse and review the previous works that are related to this study. However, this thesis is focused on the development of facilities and instrumentation in NAA that will vastly improve the detection limits and ultimately, the precision of many typically difficult elements. The theoretical frame and the conceptual base of the study have been declared and the elements addressed.

The Concept of Neutron Activation Analysis

NAA still remains the most used technique in these activation analysis facilities. However, the analytical demands for low detection limits for environmental, geological and biological specimens have made other methods such as Inductively Coupled Plasma-Atomic Emission Spectrometry (ICP-AES) and ICP-Mass Spectrometry (ICP-MS), X-Ray Fluorescence (XRF) and Particle Induced X-Ray Emission (PIXE) very attractive. Furthermore, many of the analytical systems are totally automated to produce results almost instantaneously.

Activation process of nuclides

The most suitable source of neutrons for NAA is a research reactor. There are several application fields in which NAA has a superior position compared to other analytical methods, and there are good prospects in developing countries for long-term growth. Among the activation analysis techniques, NAA is the most common type where neutrons are employed as the bombarding particle to induce radioactivity. Neutrons interact with the target nuclei in the sample by capture

reactions, most commonly (n, γ) reactions whereby a radionuclide (i.e. radioactive isotope) may be formed. A radionuclide has a characteristic half-life and mode of decay. During the decay process a nuclide may emit positrons, alpha, beta and / or gamma-rays or involved in electron capture or internal conversion. The majority (about 90%) of the nuclides formed by the (n, γ) process undergo beta decay which is most often associated with the emission of one or more gamma rays as the product nuclide de-excites to a more stable state (DeSoete, Gijbels, & Hoste, 1972; Laul, 1979) as shown in Figure 4.

Activation analysis has been well documented as a powerful technique for elemental analysis. Its high sensitivity and accuracy, simultaneous multi-element analytical capability, and matrix-free and nondestructive analysis has led to it being widely applied in a variety of research fields, such as biological, environmental, geological, industrial, archaeological, and forensic studies. Of the various kinds of activation analysis, reactor neutron activation has been mostly used, and as many as 70 elements can be easily determined.

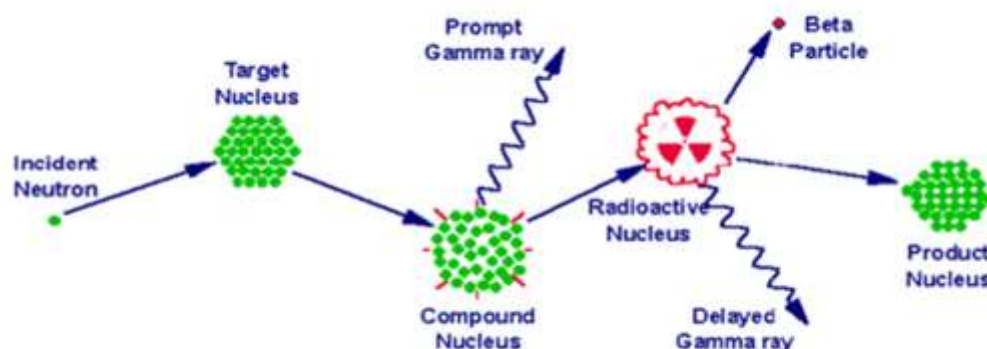


Figure 4: A typical activation process of nuclides.

Source: (De Sooete et al, 1972; Kruger, 1971)

However, for many elements, an analytical period of as long as from one day to several weeks is needed because the nuclides have long half-lives, such as ^{75}Se (120 d), ^{46}Sc (84 d), $^{110\text{m}}\text{Ag}$ (250 d), and ^{181}Hf (45 d). To attain the required sensitivity, a long irradiation, delay, and counting time is necessary. This reduces the competitive capability of the method compared with other analytical techniques, such as inductively coupled plasma mass spectrometry (ICPMS). The use of the short-lived nuclides of elements in preference to their longer lived activation products can significantly reduce the total experimental time, which in turn can reduce the analytical period and increase the number of samples which can be measured per day, and make activation analysis more cost effective and competitive. On the other hand, several elements can be determined by NAA only through the measurement of short-lived nuclide, such as ^{20}F (11 s), ^{19}O (27 s), and $^{207\text{m}}\text{Pb}$ (0.8 s) (Hou, 2000). Therefore, NAA using short-lived nuclides has been attracting more and more attention. The saturation activation of short-lived radionuclides is reached quickly on irradiation, and there is no further increase in activity with time. Similarly, the counting is also limited by the half-life since the activity of a short-lived radionuclide soon decays away and further counting cannot accumulate any more counts.

Invention and early development of PLCs

The growing demand for integrated control meant that relay systems required a rethink. In 1968, Bill Stone from the Hydromatic (the automatic transmission division of General Motors (GM)) issued a brief which outlined the difficulties he was facing in his factory. GM engineers then drafted a design

criteria for a ‘standard machine controller’, which was issued to the following four companies,

- (i) Allen-Bradley, by way of Michigan-based Information Instruments, Inc.
- (ii) Digital Equipment Corporation (DEC)
- (iii) Century Detroit
- (iv) Bedford Associates

The most basic function of a PLC is to receive inputs from status components, which can be from sensors or switches to control the outputs. Some of the basic components of a PLC are input modules, a central processing unit, output modules, and a programming device (Yanik, 2017a) as shown in Figure 5. When an input is activated, some output will also be activated by whatever the machine is told to do. Some advantages to using a PLC over other programming devices are that, the user does not have to rewire anything, the PLC has very little downtime in-between running different programs, the user can program off-line, and PLC's are not time constrained. If the user tells the PLC to perform an output in 10 ms, it will perform the output in 10 ms unlike other programs like LabView which can have a delay in activation (Yanik, 2017b).

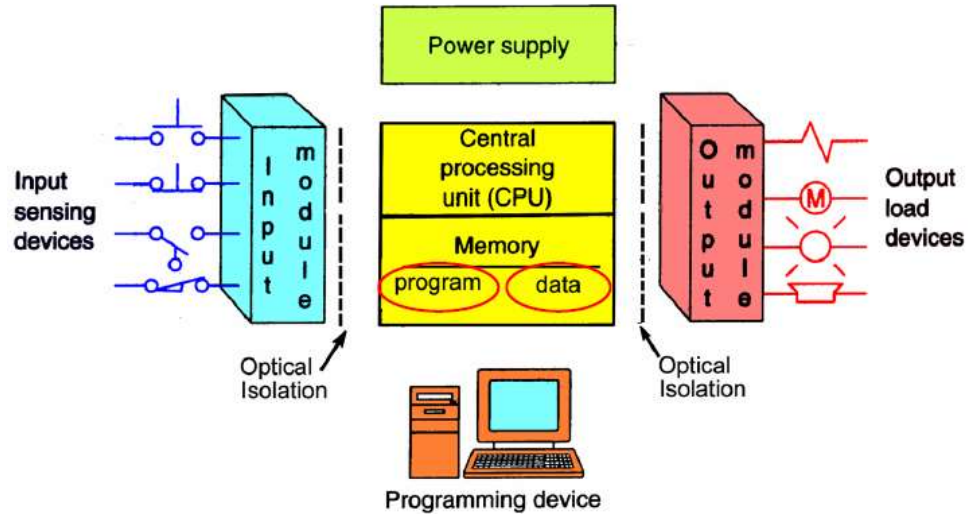


Figure 5: A PLC System.

Source: (Yanik, 2017b)

It was not until 1969 when Bedford Associates met the needs of the brief or proposal to replace the electronics for hard-wired relay systems based on a white paper written by Engineer Edward R. Clark. This was the Modicon 084 which stood for **MOD**ular **DI**gital **CON**troller, an ‘eighty-fourth’ project of Bedford Associates (Laughton & Warne, 2003). This solved dominant algorithms associated with ladder logic. Bedford Associates started a new company dedicated to developing, manufacturing, selling, and servicing this new product. One of the people who worked on that project was Dick Morley, who is considered to be the "Father" of the PLC (Alison Dunn, 2008). In 1970 Allen-Bradley released the Bulletin 1774 PLC. This was their second attempt at producing a motion controller, and the first time the term PLC was used. Later, Rockwell Automation acquired Allen-Bradley although the trading name remained intact. While Allen-Bradley were producing the Bulletin 1774, sales continued to grow for Bedford Associates. In 1975, they built on their initial success with the release of the

Modicon 184. It was designed by Engineer Michael Greenberg and marketer, Lee Rousseau. This was the first PLC designed to meet market needs, and was hugely popular. The Modicon brand was sold in 1977 to Gould Electronics, later acquired by German Company *Allgemeine Elektrizitäts-Gesellschaft* (AEG), and then by French Schneider Electric in 1997, the current owner.

One of the very first 084 models built is now on display at Schneider Electric's facility in North Andover, Massachusetts. It was presented to Modicon by GM, when the unit was retired after nearly twenty years of uninterrupted service. Modicon used the 84 moniker at the end of its product range until the 984 made its appearance. The automotive industry is still one of the largest users of PLCs. Early PLCs were designed to replace relay logic systems. These PLCs were programmed in "ladder logic", which strongly resembles a schematic diagram of relay logic. This program notation was chosen to reduce training demands for the existing technicians. Other early PLCs used a form of instruction list programming, based on a stack-based logic solver. Modern PLCs can be programmed in a variety of ways, from the relay-derived ladder logic to programming languages such as specially adapted dialects of BASIC and C. Another method is state logic, a very high-level programming language designed to program PLCs based on state transition diagrams. The majority of PLC systems today adhere to the IEC 61131/3 control systems programming standard that defines 5 languages: *Ladder Diagram (LD)*, *Structured Text (ST)*, *Function Block Diagram (FBD)*, *Instruction List (IL)* and *Sequential Flow Chart (SFC)* (Bolton, 2009).

Many early PLCs did not have accompanying programming terminals that were capable of graphical representation of the logic, and so the logic was instead represented as a series of logic expressions in some version of *Boolean format*, similar to *Boolean algebra*. As programming terminals evolved, it became more common for ladder logic to be used, for the aforementioned reasons and because it was a familiar format used for electromechanical control panels. Newer formats such as state logic and Function Block (which is similar to the way logic is depicted when using digital integrated logic circuits) exist. Even though PLCs were a vast improvement over relays, there were still limitations. Critically, they were designed for specific applications in the automotive industry. A single PLC can be programmed to replace thousands of relays (Bolton, 2009). Additionally, clean rooms were needed to house the PLC, along with air conditioning and filters. Finally, this was an industry in its infancy, and so PLCs were prone to malfunction. Things have come a long way since those early days, with PLCs being common in most factories. Huge innovations have been made, and many new companies have appeared to meet the needs of the market.

PLC Programming

Early PLCs, up to the mid-1990s, were programmed using proprietary programming panels or special-purpose programming terminals, which often had dedicated function keys representing the various logical elements of PLC programs (Laughton & Warne, 2003). Some proprietary programming terminals displayed the elements of PLC programs as graphic symbols, but plain American Standard Code for Information Interchange (ASCII) character representations of contacts, coils, and wires were common. Programs were stored on cassette tape

cartridges. Facilities for printing and documentation were minimal due to lack of memory capacity. The oldest PLCs used non-volatile magnetic core memory. More recently, PLCs are programmed using application software on personal computers, which now represent the logic in graphic form instead of character symbols. The computer is connected to the PLC through USB, Ethernet, RS-232, RS-485, or RS-422 cabling. The programming software allows entry and editing of the ladder-style logic. In some software packages, it is also possible to view and edit the program in function block diagrams, sequence flow charts and structured text. Generally the software provides functions for debugging and troubleshooting the PLC software, for example, by highlighting portions of the logic to show current status during operation or via simulation. The software will upload and download the PLC program, for backup and restoration purposes. In some models of programmable controller, the program is transferred from a personal computer to the PLC through a programming board which writes the program into a removable chip such as an EPROM.

Cyclic Neutron Activation Analysis

CNAA which is the main focus of this study is a technique that is used to enhance the sensitivity of short-lived nuclides by improving counting statistics. This is done by repetitive irradiation-transfer-counting process of a sample for a suitable number of cycles and the gamma-ray spectra accumulated for analysis. The most commonly used CAA method is CNAA by irradiation with thermal, epithermal, and fast neutrons produced from a nuclear reactor, accelerator, or isotopic neutron source. Preliminary investigations indicated the usefulness of the technique for the determination of 18 elements: O, F, Na, Sc, Ge, Se, Br, Y, Rb,

Rh, Ag, In, Er, Hf, W, Yb, Ir, and Au. However, the term “CAA” was not mentioned. (Caldwell, Mills, Allen, Bell, & Heath, 1966) suggested use of a similar technique as a part of a combination neutron experiment for remote elemental analysis. The term “CAA” was first used by (Givens, Mills, & Caldwell, 1969) when they measured ^{16}N and $^{24\text{m}}\text{Na}$ using a technique similar to that of Anders. A nuclear reactor can supply a very high neutron flux and is most often used for this purpose. At least 20 elements which produce short-lived nuclides (half-life less than 100 seconds) by thermal neutron bombardment, and also more than 10 elements which produce nuclides with half-lives of 100-600 seconds can be determined by thermal and epithermal neutron CAA.

The advantages of CNAA, as compared with conventional activation analysis, include significant improvements of the detection limits, analytical precision, and accuracy of elements detection, short experimental time, increased number of samples per unit time, a capability for the estimation or confirmation of the half-lives of short-lived nuclides and determination of the degree of homogeneity of samples. The CNAA technique was suggested in 1960 by (Anders, 1960, 1961) and the theory of CNAA has been recently described in detail (Kerr & Spyrou, 1978; Spyrou & Kerr, 1979). Cyclic method was first introduced by Andres in 1969 to determine F via ^{16}N (half-life = 7.4 s) with the reaction $^{19}\text{F} (n, \alpha) ^{16}\text{N}$ using a pneumatic transfer system. Later (Chatt et al., 1981; Grass & Westphal, 1977; Spyrou & Kerr, 1979) applied CNAA techniques for trace element analysis using reactor neutron source and fast pneumatic transfer systems. Since then, other workers have determined short-lived nuclides in

diverse samples using this approach (Chatt & DeSilva, 1979; DeSilva & Chatt, 1988).

Instrumental neutron activation analysis (INAA) involving conventional irradiation, decay, and counting periods has been widely applied for multi-element determination in biological and metallurgical samples. Short (<30 s) irradiation, decay, and counting times have been used in recent years for measuring the levels of a few selected elements (Ward & Ryan, 1979; Dams, Billiet, & Hoste, 1975). At least 38 stable elements, however, produce short- (and long-) lived nuclides under thermal neutron bombardment. Many of these short-lived nuclides can be used for sensitive determinations of a number of trace elements in a variety of sample matrices (Tou & Chatt, 1981).

To detect the γ -rays emitted by short-lived (half-life <100 s) nuclides, it is necessary to develop methods based on the principles of cyclic activation analysis. In cyclic INAA (CINAA), a sample irradiated for a short time, is rapidly transferred to a detector for counting, and the entire process is repeated for a number of cycles. Investigation of the cyclic techniques in neutron activation analysis on Da Lat Research Reactor for determination of very short-lived radionuclides in biological materials has been conducted (Doanh, Dung, Thien, Sy, & Dien, 2015).

CNAA method was conducted for determination of Se in food samples. High accuracy and good precision were proved by analyzing certified reference materials (CRMs) of chicken (GBW100 18), rice (GBW10010) and cabbage (GBW10014). The detection limits for the three CRMs reached 0.16, 0.66 and 1.2 ng after 6 cycles at the 161.9 keV c-peak from ^{77}mSe , under a neutron flux of

$9.09 \times 10^{11} \text{ n cm}^{-2} \text{ s}^{-1}$ and the conditions of 30 s irradiation, 2 s decay, 30 s counting and 2 s waiting, significantly lower than those of conventional neutron activation analysis without any cycles, which were 0.94, 3.6 and 4.3 ng, respectively (Zhang, Chai, Qing, & Chen, 2009).

Dalhousie University SLOWPOKE-2 Reactor (DUSR) facility-CANADA

A pseudo-cyclic INAA method, which involved manual transfer of samples, was initially developed for use with the Dalhousie University SLOWPOKE-2 Reactor facility; it was successfully applied to multi element determinations in biological samples (Chatt & DeSilva, 1979). A rapid automated transfer cyclic system has been subsequently designed and installed. The rapid automated transfer cyclic system was designed in collaboration with Atomic Energy of Canada Limited, Commercial Products. The system consists of two main components: a recycle irradiation controller and a switching unit. The recycle irradiation controller contains an irradiation timer, a delay timer, a counting timer, and a recycle counter and the switching unit contains two 2-way diverters and a solenoid valve. The rapid pneumatic transfer cyclic system for use with the SLOWPOKE reactor designed, allows detection of nuclides with half-lives as short as 0.8s. Reliable reproducibility is achieved with a 1 s transfer period from reactor to detector.

CINAA has been successfully applied to the determination of Ag, F, Hf, Pb, Rb, Sc, and Se in a variety of biological and metallurgical matrices. The detection limits ranged from 0.01 to 2.2 ppm for all elements studied except Pb (Hou, 2000).

Atomic Institute, Vienna University of Technology- TRIGA Mark II

A fully automated and fast pneumatic transport system for short-time activation analysis was recently developed (Ismail, 2010). It is equipped with a programmable logic controller, software package, and 12 devices to facilitate optimal analytical procedures. 550 ms were only necessary to transfer the irradiated capsule (diameter: 15 mm, length: 50 mm, weight: 4 gram) to the counting chamber at a distance of 20 meters using pressurized air (0.4 MPa) as a transport gas. The system incorporates a sample changer which can accommodate about 30 samples. A control unit was fabricated to manage irradiation-measurement procedures. The unit is based on a 24 V/4 A power supply (Siemens; LOGO-Power), programmable logic controller (PLC; NAI5-FP0), and a group of interfaces and adapters. A software package was developed to manage communication with the control unit, pneumatic devices, sensors, and the irradiation-counting procedures. The software is a Delphi Code, facilitating several functions through three main interfaces. The first interface is for communicating with the control unit for controlling and testing all sensors and valves manually. The second interface is for performing semiautomatic procedures with manual control of all included units or analytical steps. The third interface facilitates fully automatic operations and communication with a digital gamma spectrometer for starting the measurements. The sample exchanger acts as a decay station and a loading unit for automatically feeding the pre-irradiated samples into the chamber for counting. This group possesses two advantages. The first is the ability to irradiate the sample and then wait for a suitable time for the measurements to optimize the analytical conditions (i.e., background) according

to the half-lives of the investigated nuclides, (Ismail, 2010). The second is the possibility to use the unit as a standalone system for automatically analyzing pre-irradiated samples. This arrangement allows the new system to be used during the working hours for short-time activation analysis and overnight for measuring long-lived nuclides. A 24 V / 4 A power supply (Siemens; LOGO-Power) from Siemens was used.

Atomic Energy Commission of Syria – MNSR Facility

The Syrian Atomic Energy Commission has designed an automatic sample changer for their existing gamma-ray spectrometry system (Sarheel, Nassri, & Hatem, 2018). It was a Coordinated Research Project (CRP) by the IAEA. The sample changer allows the fully automated measurement of up to 64 samples in one run. Syria is one of the five member states operating MNSR facility. A Syrian sample changer was designed to transfer an activated sample from the sample tray to the detector, to measure its radioactivity, and to return it to the tray after a specific measurement time. The design did not incorporate the construction of a new controller unit using PLC for CNAA and automation of the air compressor unit.

Equation of CAA

The principle of CAA has been described by (Givens et al., 1969; Spyrou, 1981). In this method, the sample is irradiated for a short period of time, and after a delay period from the end of irradiation the radiation emitted is counted for a short period of time, then the sample is irradiated again and the entire process repeated for a number of cycles (Figure 6)

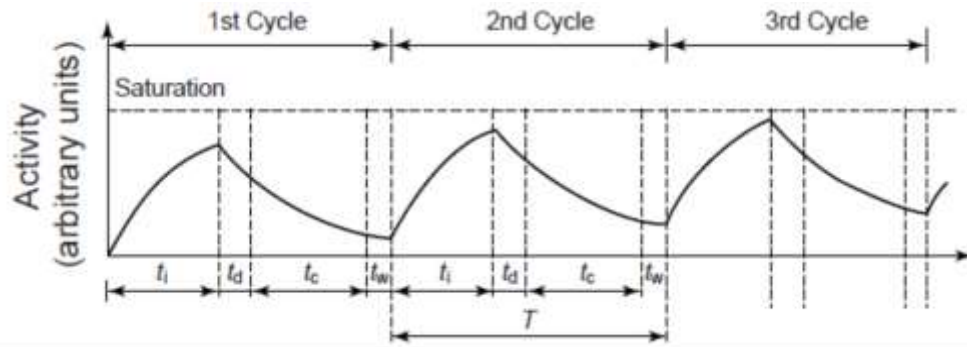


Figure 6: Time parameters of CAA and the variation of the activity of nuclides with time and number of cycles.

Source: (Hou, 2008)

The detected radiations at each counting period are summed and finally a total cumulative detector response is obtained. The cycle period T is given by:

$$T = t_i + t_d + t_c + t_w, \quad (2.1)$$

where t_i is the time of irradiation, t_d is the delay time, t_c is the counting time and t_w is the waiting time. The detector response (or the number of counts) for the first cycle is given by:

$$D_1 = \frac{N\sigma\Phi I\mathcal{E}}{\lambda} (1 - e^{-\lambda t_i}) e^{-\lambda t_d} (1 - e^{-\lambda t_c}), \quad (2.2)$$

where N is number of target nuclei, σ is activation cross-section, Φ is neutron flux, I is the intensity of the radiation of interest, \mathcal{E} is the efficiency of the detector.

In the second counting period, the detector response is the same number of counts due to the second irradiation plus what was left from the first irradiation, and is expressed as:

$$D_2 = D_1 + D_1 e^{-\lambda T} = D_1 (1 + e^{-\lambda T}) \quad (2.3)$$

Similarly, for the n th cycle, which can be expressed as

$$D_n = D_1(1 + e^{-\lambda T} + e^{-2\lambda T} + e^{-3\lambda T} + \dots + e^{-(n-1)\lambda T}). \quad (2.4)$$

Then the total cumulative detector response in all n cycles is given by:

$$\begin{aligned} D_c &= \sum_{i=1}^n D_i \\ &= D_1 \left[\frac{n}{(1 - e^{-\lambda T})} - \frac{e^{-\lambda T}(1 - e^{-n\lambda T})}{(1 - e^{-\lambda T})^2} \right] \\ &= \frac{N\Phi\sigma I\varepsilon}{\lambda} \left[\frac{n}{1 - e^{-\lambda T}} - \frac{e^{-\lambda T}(1 - e^{-n\lambda T})}{(1 - e^{-\lambda T})^2} \right] \times (1 - e^{-\lambda t_d}) e^{-\lambda t_d} (1 - e^{-\lambda t_c}) \quad (2.5) \end{aligned}$$

Equation (2.5) is the basic relationship for CAA.

Dead Time and Pile-up Correction

CAA is usually employed for the determination of short-lived nuclides in a matrix of long-lived activation products. The activity of a sample not only changes considerably during a counting period owing to short-lived nuclide decay, but also increases from cycle to cycle as the matrix activity owing to the accumulation of longer lived products. Consequently, a rapidly changing dead time is encountered in a counting period (Schonfeld, 1966). The basic equation for dead time correction was given by Schonfeld and is expressed as:

$$C = \int_0^{t_c} A_0 e^{-\lambda t} [1 - DT(t)] dt \quad (2.6)$$

where C is the actual acquired net counts in the photopeak of interest, A_0 is the true initial photopeak count rate, and $DT(t)$ is the fractional analyzer dead time at time t . In order to implement this correctly, the variation of fractional dead time during the counting period must be known. By least-squares fitting of the

experimental data (Egan, Kerr & Minski, 1977), found that $DT(t)$ is an exponential function of t , and it can be expressed as:

$$DT(t) = B + Ce^{-kt} \quad (2.7)$$

where B , C , and k are constants. Hence a correction factor (f) for dead time in a counting period can be obtained as:

$$f = \frac{\int_0^{t_c} A_0 e^{-\lambda t} dt}{\int_0^{t_c} A_0 e^{-\lambda t} (1 - B - Ce^{-kt}) dt} \quad (2.8)$$

For cyclic activation with n cycles, the correction factor (F_n) can be expressed as:

$$F_n = \frac{\sum_{n=1}^n \int_0^{t_c} A_0 e^{-\lambda t} dt}{\sum_{n=1}^n \int_0^{t_c} A_0 e^{-\lambda t} (1 - B - Ce^{-kt})_n dt} \quad (2.9)$$

$DT(t)$ not only varies with t in a counting period but also differs from one cycle to another.

It was observed that the correction factor for the dead time, f , is approximately equal to the ratio of the clock time to the live time obtained from the multi-channel analyzer (MCA) clock data in each counting period. Hence, it is usually used to correct for the dead time after each cycle. In this case, it is important to store the g-spectra of each cycle period and correct the counts of the nuclide of interest for dead time before summation of an individual spectrum.

With increasing analyzer dead time, the pulse pile-up loss (also called summing effect or coincidence loss) will become more serious. This can be overcome satisfactorily by introducing a pulser with constant frequency into the

system (Egan, Kerr & Minski, 1977). The ratio of the areas under the pulser peaks, after dead time correction, were measured and the pile-up correction factor was defined as Fp and is expressed as:

$$Fp = \frac{\text{Pulser peak area at } \sim 0.1\% \text{ dead time}}{\text{Pulser peak area at sample dead time}} \quad (2.10)$$

However, pile-up correction, unlike dead-time correction, is implemented on the cumulative spectrum. Wytttenbach (Wytttenbach, 1971) suggested another way to correct the pile-up loss by using the real time (clock time), tc , and the live time of the measurement, Tc given as:

$$Fp = \frac{P}{P_0} = 1 - \frac{2\tau}{\nu} \left(\frac{tc}{Tc} - 1 \right) \quad (2.11)$$

where P_0 is the true photopeak count rate without coincidence losses, P is the actual photopeak count rate including pile up, n is a constant of the detector system, and $\frac{\tau}{\nu}$ can be measured by plotting P/P_0 against tc/Tc and can subsequently be used to correct other spectra. However, it should be considered that actually τ depends on the energy of the γ -ray measured (Alfassi & Tsechansky, Kushelevsky, 1980). In addition, the use of a loss-free counting system with pile-up rejection will avoid this problem (Heydorn & Damsgaard, 1997).

Chapter Summary

The chapter reviewed the invention and the early development of Programmable Logic Controllers (PLCs) including the PLC system (the designed components) and defined the five (5) standard programming languages of PLC. CNAAs which is the main focus of the study was analysed. Institutions of the

Member States operating similar facilities including Safe Low-Power Critical Experiment (SLOWPOKE), Training, Research, Isotope, General Atomics (TRIGA) and MNSR were also reviewed. Therefore, my study is focusing on the design and construction of a new controller interface for the pneumatic sample transfer system of Ghana Research Reactor using Programmable Logic Controller (PLC) to facilitate very short-lived nuclides measurements in cyclic NAA.

CHAPTER THREE

MATERIALS AND METHODS

Introduction

This chapter is about materials and the methodology used in executing the objective of the study. The chapter is focused on designing of various components of the PTS controller unit meant for the CNA A application.

Logo 8 Siemens Programmable Controller Logic (PLC) Specifications

Function block diagram (FBD) is the main programming method used for PLC to control the PTS to operate the cyclic and conventional activation analysis systems. The PLC used for this study is LOGO! Base Module 12/24 RCE Controller, 8 digital inputs and 4 relays (10Amps) outputs (6ED1 052-1MD00-0BA8) from Siemens Industrial Automation Products Ltd. LOGO!Soft Comfort V8.0 is LOGO! programming software used for the study. It runs under Windows (including Windows XP, Windows 7, and Windows 8), Linux, and Mac OS X. It helps to get started with LOGO! and to write, test, print out and archive programs, independent of LOGO!. LOGO! is a universal logic module made by Siemens that integrates:

- (i) Controls
- (ii) Operator and display panel with background lighting
- (iii) Interface for expansion modules
- (iv) Interface for a micro SD card
- (v) Interface for an optional Text Display with Ethernet (TDE) module
- (vi) Pre-configured standard functions, for example, on- and off-delays, pulse relay and softkey

- (vii) Timers
- (viii) Digital and analog flags
- (ix) Inputs and outputs, according to the device type

LOGO! 0BA8 additionally integrates the following components:

- (x) Interfaces for Ethernet communication
- (xi) FE (Functional Earth) terminal for connecting to earth ground
- (xii) One LED for indicating Ethernet communication status

Figure 7 shows the LOGO! Structures for module 0BA8, 12/24RCE used.

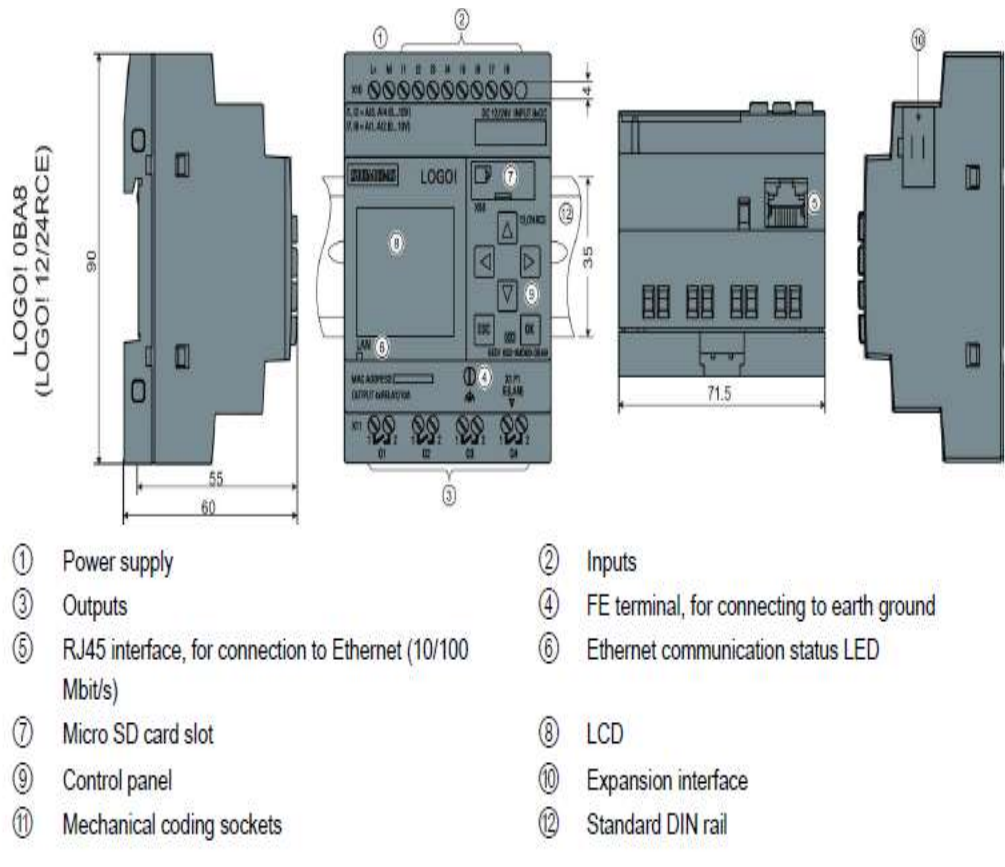


Figure 7: LOGO! Structure for module 0BA8 (LOGO! 12/24VDC RCE).

Source: (Logo & Logo, 2009; Siemens, 2012)

Web server support

LOGO! 0BA8 has a built-in Web server which enables one to operate the LOGO! Base Module or the LOGO! TDE from a traditional PC or a mobile device. In this approach, one can access the LOGO! Base Module using a connected device (conventional PC, tablet or smart phone with Web browsing capabilities) through its IP address (Siemens, 2012).

The Web server allows one to use the mouse pointer or the touch screen, depending on the device one is using, to perform fast and easy operations on the virtualized LOGO! Base Module. LOGO! 0BA8 also provides access security control over the Web server.

The LOGO! Web server supports the following Web browsers:

- (i) Microsoft Internet Explorer with minimum version 8.0
- (ii) Mozilla Firefox with minimum version 11.0
- (iii) Google Chrome with minimum version 16.0
- (iv) Apple Safari with minimum version 5.0
- (v) Opera with minimum version 12.0

The LOGO! Web server supports the following communications devices when one of the above explorers is used:

- (i) Conventional PC
- (ii) Apple iPhone series
- (iii) Apple iPad series
- (iv) Smart phones and tablets with Android system with minimum version Android 2.0

To logon to the web server, one has to follow the following steps below to log on to the desired LOGO! Base Module.

1. Open your Web browser.
2. Enter the IP address of your LOGO! Base Module in the IP address bar.
– LAN (Local Area Network) access:
3. Select an appropriate language from the drop-down menu.
4. Enter the password.

Once logged in, the LOGO! Web server displays all the system information of the LOGO! Base Module including module generation, module type, firmware (FW) version, IP address, and module status.

Network access security

With the enhanced Ethernet function of LOGO! 0BA8 devices, one can access the LOGO!Base Modules through LOGO!Soft Comfort, the Web server, or other compatible devices with Ethernet interfaces. In this case, both Internet and Intranet communication is possible for the LOGO! 0BA8 devices. For Internet communication, accessing the LOGO! Base Module requires a valid user password to ensure network security. One can set or change the password from LOGO!Soft Comfort only. Siemens strongly recommends that one do not put the LOGO! Base Modules device directly on the Internet, but hide them behind a firewall. In addition, make sure one selects TCP port 8080 and block all other ports in the firewall configuration; otherwise, there may be network security risks, for example, data leakage, virus invasion and hacker attack.

Program copy protection

The Copy Protect function provides protection for the circuit programs on micro Secure Digital (SD) cards. A circuit program is protected when you transfer it to a protected memory card.

This additional security feature allows you to bind the circuit program with a specific memory card. If you copy a protected circuit program to another memory card, LOGO! cannot recognize the program and reject loading it after you insert the card.

Basic Components of GHARR-1 Pneumatic System

Pneumatic technology deals with the study of behavior and applications of compressed-air in our daily life in general and manufacturing automation in particular. Pneumatic systems in GHARR-1 uses air as the medium for its operation as shown in Figure 8.

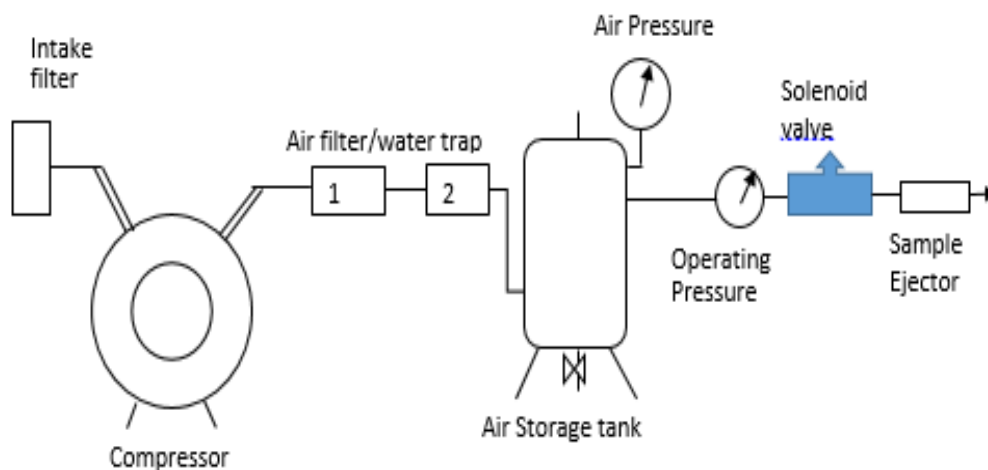


Figure 8: GHARR-1 pneumatic system.

The air is compressed slowly in the compressor. But since the pneumatic system needs continuous supply of air, this compressed-air has been stored in air storage tank or a receiver. The compressed-air is filtrated by two air filters to

remove the impurities and moisture in it and fed to the main pipes of the pneumatic system. The air receiver or the storage tank smoothens the pulsating flow from the compressor. It also helps the air to cool and condense the moisture present. The air receiver is large enough to hold all the air delivered by the compressor. The pressure in the receiver is held higher (between a max. of 0.6 Mega Pascal (MPa) and a minimum of 0.4 Mega Pascal) than the system operating pressure (0.2 Mega Pascal) to compensate pressure loss in the pipes. Also, the large surface area of the receiver helps in dissipating the heat from the compressed-air. The motor operating the compressor cuts-off when the air pressure in the air receiver or storage tank gets to the maximum of 0.6 MPa and starts automatically when the pressure dropped to 0.4 MPa. Compressor is a mechanical device which converts mechanical energy into fluid energy. The compressor increases the air pressure by reducing its volume which also increases the temperature of the compressed-air. The compressor is selected based on the pressure it needs to operate and the delivery volume.

The filter cartridge is made of sintered brass. The schematic of the filter is shown in Figure 9. The thickness of sintered cartridge provides random zigzag passage for the air to flow-in which helps in arresting the solid particles. The air entering the filter swirls around due to the deflector cone. The centrifugal action causes the large contaminants and water vapor to be flung out, which hit the glass bowl and get collected at the bottom. A baffle plate is provided to prevent the turbulent air from splashing the water into the filter cartridge. At the bottom of the filter bowl there is a drain plug which can be opened manually to drain off the settled water and solid particles.

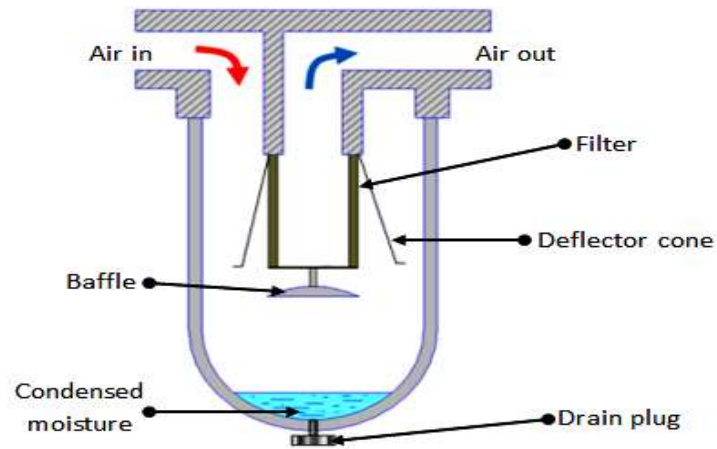


Figure 9: Air filter / water trap.

Source: (Retrieved from: www.Burkert.co.uk).

Solenoid valves

Figure 10 shows the solenoid valves used in GHARR-1 pneumatic transfer system to enhance the compressed-air to transfer sample capsules into the reactor for irradiation. Solenoids are used to automate fluid flow circuits by opening or closing valves by the application of a magnetic current generated when the solenoid coil is energized when an electric current passed through the coil as shown in Figure 10b (Bürkert UK Ltd, 2017) .

*A- Input side B- Diaphragm C- Pressure chamber D- Pressure relief passage
E- Electro Mechanical Solenoid F- Output side.*

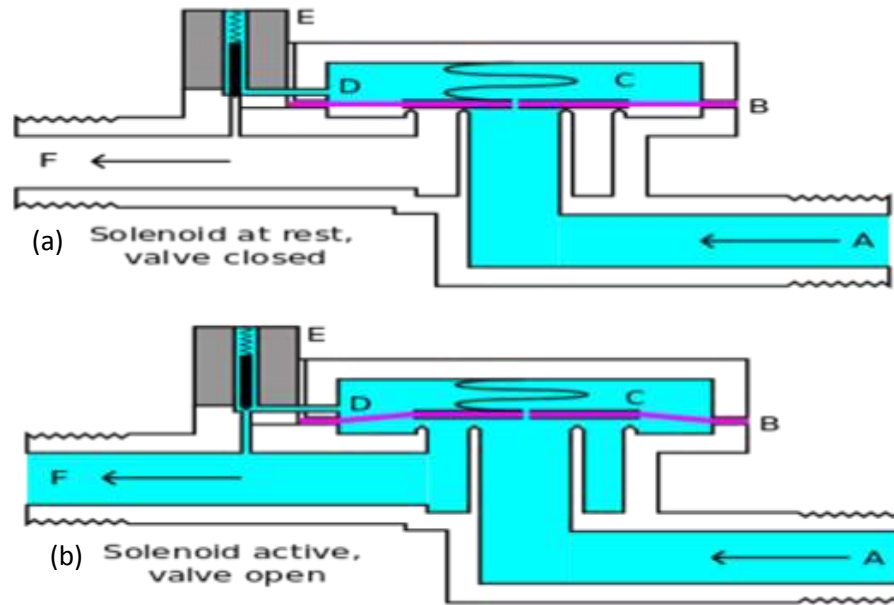


Figure 10: Solenoid valves used in GHARR-1 pneumatic transfer system.

Source: (Retrieved from: www.Burkert.co.uk).

Operation of the Solenoid

The solenoid valve has two main parts: the solenoid and the valve. The solenoid converts electrical energy into mechanical energy which, in turn, opens or closes the valve mechanically. A direct acting valve has only a small flow circuit, shown within section **E** of Figure 10a (this section is mentioned as a pilot valve). A diaphragm piloted valve multiplies this small pilot flow, by using it to control the flow through a much larger orifice. A spring is used to hold the valve opened (normally open) or closed (normally closed) while the valve is not activated. The Figure 10 shows the design of a solenoid valve, controlling the flow of air. Figure 10a is the valve in its closed state. The compressed air under pressure enters at **A**. **B** is an elastic diaphragm and above it is a weak spring pushing it down. The diaphragm has a pinhole through its center which allows a very small amount of air to flow through it. This air fills the cavity **C** on the other

side of the diaphragm so that pressure is equal on both sides of the diaphragm, however the compressed spring supplies a net downward force. The spring is weak and is only able to close the inlet because air pressure is equalized on both sides of the diaphragm.

Once the diaphragm closes the valve, the pressure on the outlet side of its bottom is reduced, and the greater pressure above holds it even more firmly closed. Thus, the spring is irrelevant to holding the valve closed (Bürkert UK Ltd, 2017).

The above works because the small drain passage **D** was blocked by a pin which is the armature of the solenoid **E** and which is pushed down by a spring. If current is passed through the solenoid, the pin is withdrawn via magnetic force see Figure 11, and the compressed air in chamber **C** drains out the passage **D** faster than the pinhole can refill it. The pressure in chamber **C** drops and the incoming pressure lifts the diaphragm, thus opening the main valve. Compressed air now flows directly from **A** to **F**.

When the solenoid is deactivated and the passage **D** is closed, the spring needs very little force to push the diaphragm down and the main valve closes. From this explanation it can be seen that this type of valve relies on a differential of pressure between input and output as the pressure at the input must always be greater than the pressure at the output for it to work. Should the pressure at the output, for any reason, rise above that of the input then the valve would open regardless of the state of the solenoid and pilot valve (Bürkert UK Ltd, 2017).

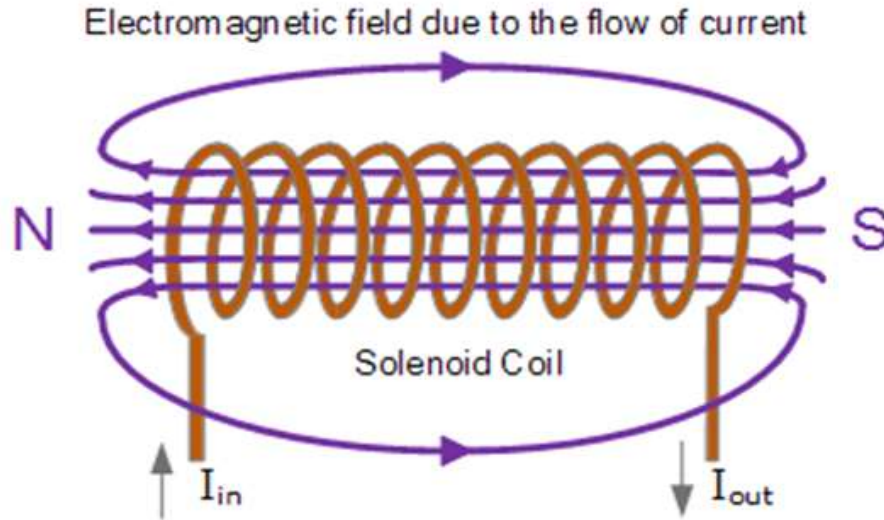


Figure 11: Electromagnetic field circuit.

Source: (Retrieved from: www.Burkert.co.uk)

Linear solenoid's basically consist of an electrical coil wound around a cylindrical tube with a ferro-magnetic actuator or "plunger" that is free to move or slide "IN" and "OUT" of the coils body. Solenoids can be used to electrically open doors and latches, open or close valves, move and operate robotic limbs and mechanisms, and even actuate electrical switches just by energizing its coil (Bürkert UK Ltd, 2017).

When electrical current flows through a conductor it generates a magnetic field, and the direction of this magnetic field with regards to its North and South Poles is determined by the direction of the current flow within the wire. This coil of wire becomes an "Electromagnet" with its own north and south poles exactly the same as that for a permanent type magnet.

Schematic of CNAA of PTS

Figure 12 shows the Schematic diagram of PTS with little modification for CNAA application with regards to my study. Similar facilities have been set up for CNAA in institutions such as the Dalhousie University, Canada (Chatt et al., 1981), MNSR, China Institute of Atomic Energy (Hou & Das, 1997), Atominstitut, Vienna (Ismail, 2010), and University of Missouri, USA. (Joshi & Agrawal, 1995).

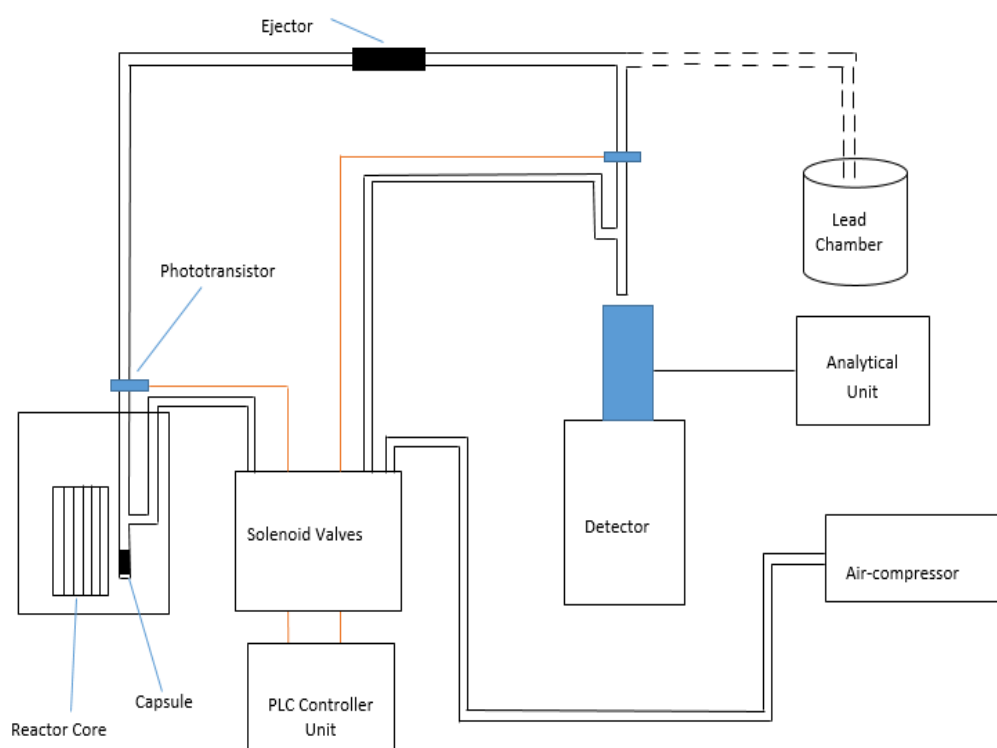


Figure 12: Schematic diagram of PTS with little modification for CNAA.

The system consists of an ejector in which sample capsules are put and air compressor releasing a compressed-air at an operating pressure of 0.2 MPa to transfer the capsule sample into the reactor for irradiation. Phototransistors are fixed at an appropriate locations on top of the reactor and the detector respectively for two purposes; first is to guarantee that the sample capsule has passed a certain

point in the system; if that is not the case, the total process will be interrupted. The second is to start specific processes, such as irradiation timer, decay of sample, and measurements or counting. With the existing PTS, the phototransistor was located on the receiving lead chamber, where the operator picks the sample and places it on the detector, (Tao Huabai, 1992). The control unit designed consists of a PLC, a high current dual voltage regulated power supply and the relay bank to control the solenoid valves (open and close) for the compressed-air to transfer the sample capsules into the reactor for irradiation. The detector is a high purity germanium (HPGe) for detection of photons. The analytical unit is spectrometry system consisting of a high voltage to bias the detector, pre-amplifier to provide an output pulse with an amplitude proportional to the integrated charge output from the detector, main amplifier for amplification and pulse shaping, multi-channel pulse height analyzer sorting successive signal pulses into parallel amplitude channels (Glenn Knoll, 2000). The computer serves as the display of the pulses in the form of spectrums as shown in Figure 13 (Nafaa Reguigui, 2006).

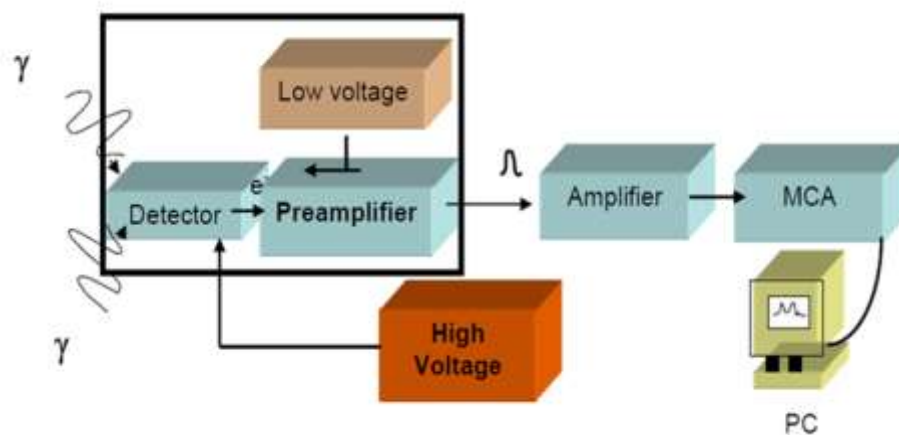


Figure 13: Block diagram of a basic gamma spectrometry system.

Pneumatic transfer loop system

Figure 14 shows the block diagram of the pneumatic transfer loop system.

Numbers 1 to 4 are solenoid valves.

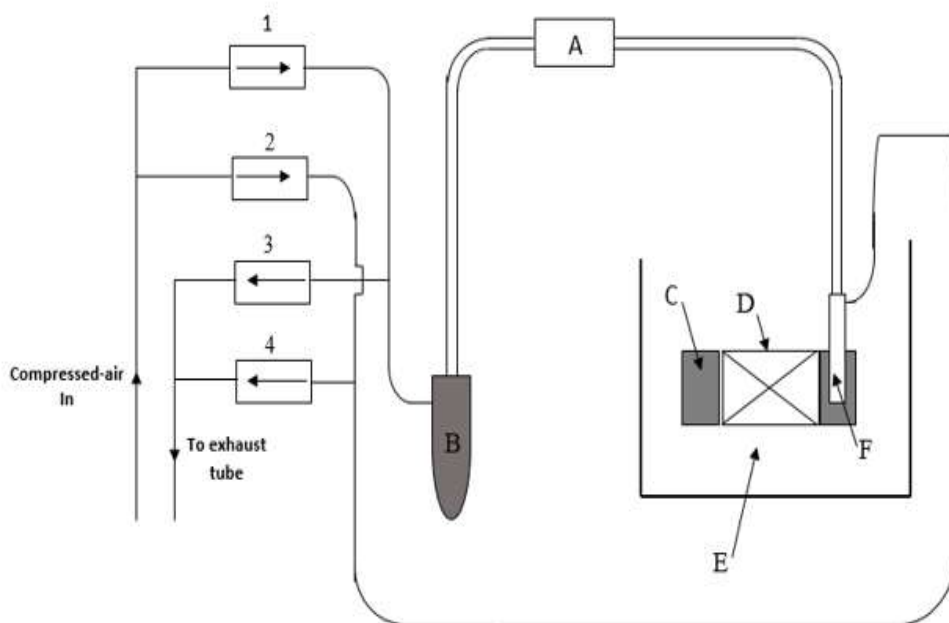


Figure 14: Block diagram of pneumatic transfer loop system.

A - Ejector

B - Detector

C - Beryllium reflector

D - Reactor core

E - Pool

F - Inner irradiation tube

1-4 - Solenoid valves

The irradiation system operates on positive pressure. The entire pneumatic loop is sealed to avoid air leakage. When irradiated samples are returned from the reactor, they are automatically placed on the detector for both conventional and CNAAs where they are allowed to decay and be counted. The main switch for

activating the system is on the reactor control console. This allows the reactor operator to permit insertions into the reactor only for experiments that have been reviewed and approved. Solenoid valve four (4) of the system guarantees that the air that has been irradiated in the irradiation site is directed to the exhaust and not to the receiver station. The exhaust from the system is passed to the exhaust chimney (Huabai et al., 1992). Solenoid valves 1 and 3 operate to transfer the sample into the inner irradiation site while 2 and 4 retrieve the sample from the irradiation site onto either the detector or the lead chamber, see Figure 15.

Proposed PLC controller unit

The illustration of the controller unit to be designed and constructed is shown in Figure 15. The controller unit consists of three main components, high current dual regulated voltage power supply, PLC device and an 8-way relay bank.



Figure 15: Block diagram of the proposed controller unit.

The power supply to be designed and constructed will have a dual voltage of +24 VDC and +12 VDC and could be regulated from its internal reference voltage minimum of 1.25 to a safe maximum voltage of 30 VDC at a safe operating current of 5 Amps. Two high current power transistors, 2N3055 and MJ 2955 are used alongside LM 317 voltage regulator which is capable of supplying (1.5 A) (Texas Instrument, 2014). The +24 VDC operates the PLC and the +12 VDC controls the output switching system to operate the relay bank. The

8-way relay bank has eight +12 VDC relays that is controlled by the PLC output to supply a 220 VAC to operate solenoid valves. Figure 16 shows a block diagram of a complete system flow of the PTS with the controller.

Control flow chart of PTS

From Figure 16, the air-compressor system will be controlled by the PLC controller unit to be designed and constructed. The 220 VAC contactor coil of the compressor will be started and stopped when the irradiation process (the reactor operation) is over.

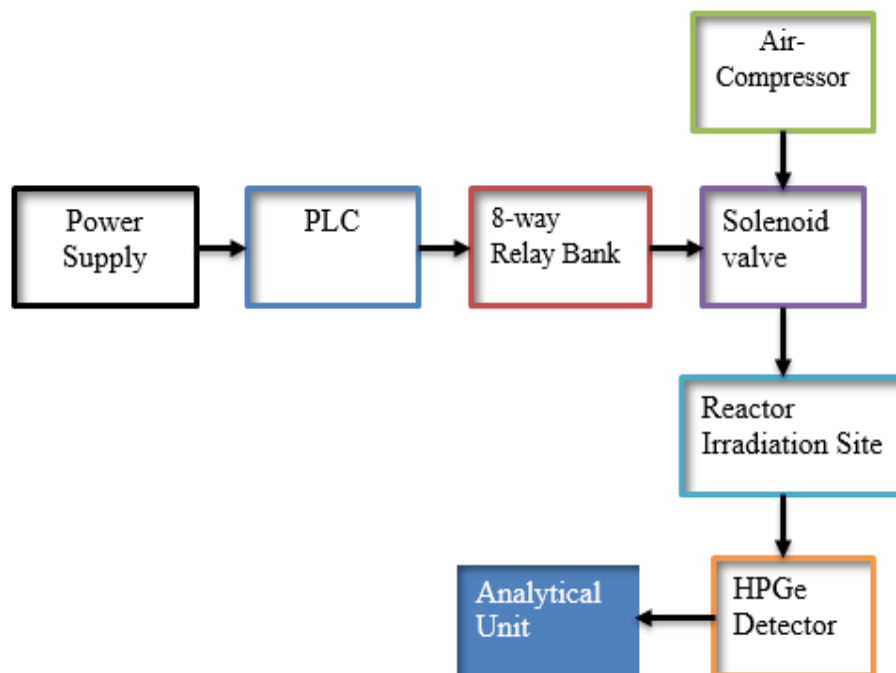


Figure 16: A complete block diagram of PTS.

The PLC will be programmed such that the PTS will not be able to operate until the maximum air pressure is reached (0.6 MPa). The solenoid valves will be opened upon the pressure build-up to allow the compressed-air to move the sample capsule into the irradiation site of the reactor. In the case of the existing

conventional neutron activation analysis (one-shot process), the sample is picked up by the operator from a lead chamber to the HPGe detector for counting. The new design allows the sample to be transferred onto the gamma detector for counting. In the case of cyclic mode, the phototransistors together with timers in the PLC will come into play, see Figure 17.

Control flow chart of a cyclic mode operation with conventional mode option

Figure 17 shows the control flow chart for cyclic mode activation analysis with conventional mode analysis as an option.

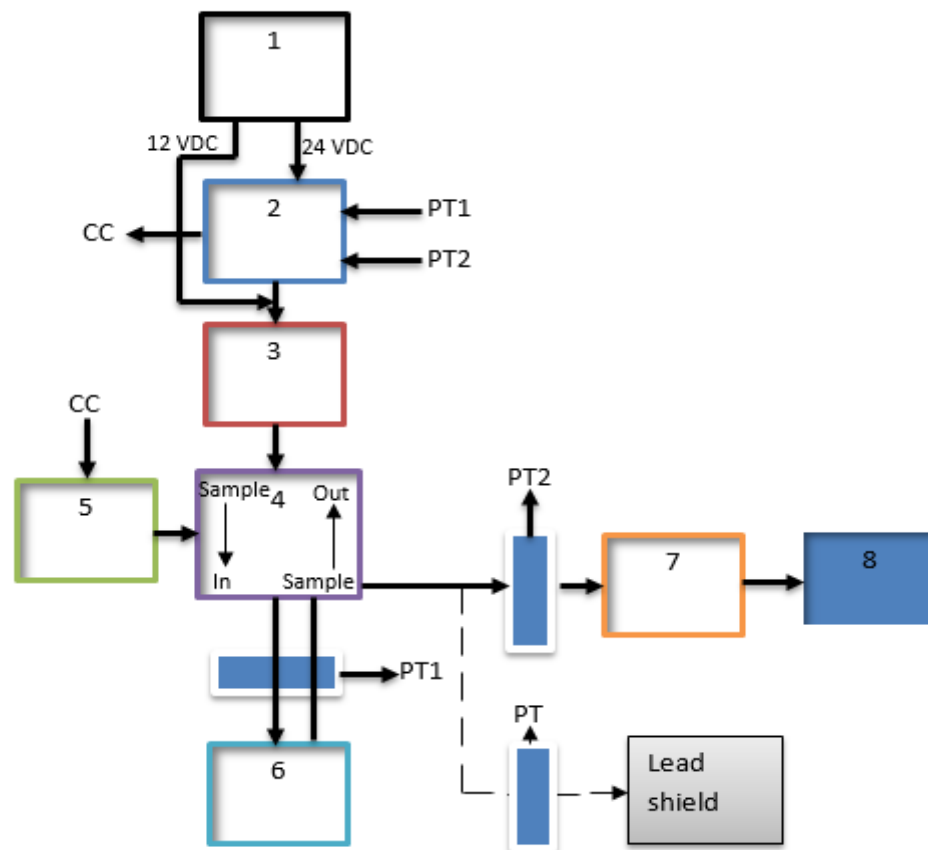


Figure 17: Flow chart for cyclic mode analysis with conventional mode option.

- | | |
|--------------------------------|-----------------------|
| 1. Dual regulated power supply | 2. PLC |
| 3. 8-way relay bank | 4. Solenoid valves |
| 5. Air-compressor | 6. Reactor |
| 7. HPGe Detector | 8. Analytical unit |
| PT Phototransistor | CC Compressor control |

The system will be designed such that when the capsule passes by the phototransistor (PT1) on top of the reactor into the irradiation site, the phototransistor on top of the reactor will change from logic low level to high level, giving out a positive pulse signal to the PLC. Two “sample-in” solenoid valves will close and the irradiation of the capsule will begin per the preset time of an irradiation timer (t_i) in the PLC. When the irradiation time elapses as per the preset, the timer will give a positive pulse signal to open two “solenoid-out” valves, thus the capsule will be transferred by a compressed-air from the irradiation site in the reactor to an HPGe-detector for counting. The design will be such that, when the capsule passes by the phototransistor (PT2) on top of the detector, a decay timer (t_d) will start per the preset for the sample to decay. After the preset value is reached, a positive pulse signal will be sent to a counting timer (t_c) for the sample to be counted or analysed. A positive pulse signal is sent to a delay or waiting timer for the sample to delay for some seconds and the process is repeated per the number of cycle the operator will set.

In the case of the conventional mode analysis, the capsule will be transferred by the compressed-air from the irradiation site in the reactor to the lead chamber per the existing design. When the capsule passes by the phototransistor on top of the receiving lead chamber, the two “sample-out”

solenoid valves close. The operator will allow the sample to decay and pick it to the detector for counting. Per my design, the sample will be transferred onto the detector for counting. The PLC software (soft comfort, V8.0) will be used to design the process to facilitate the cyclic and the conventional modes of analysis.

Block diagram for the proposed PLC power supply

A dual voltage regulated high current power supply (12 / 24 VDC) to be designed and constructed to operate the PLC and the relays in the relay bank are shown in Figure 18.

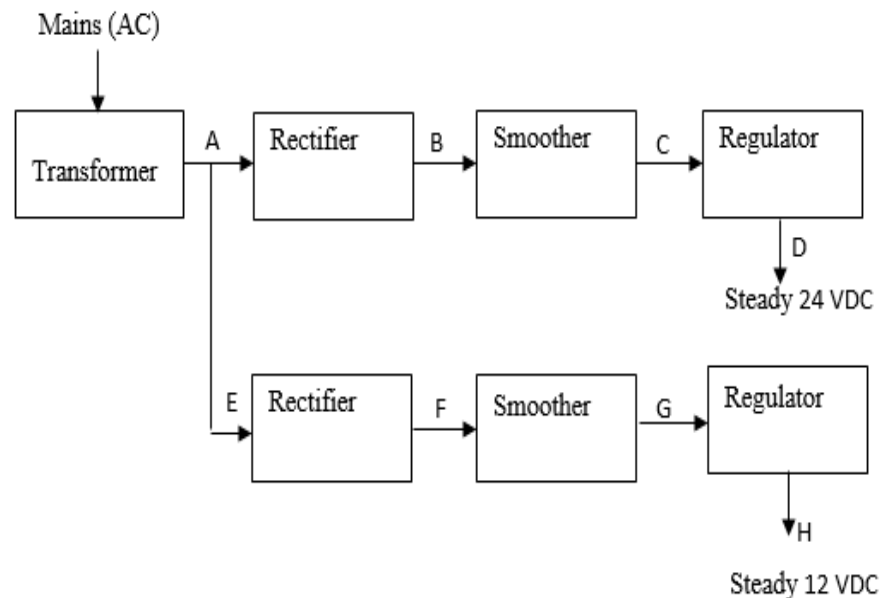


Figure18: Block diagram of a dual regulated voltage power supply.

The diagram consists of a center tapped (15-0-15 CT) transformer to reduce a 240 VAC to 30 VAC and 15 VAC (A & E) respectively. A bridge type rectifier will convert the AC voltage into a pulsating DC voltage (B & F). The smoothing block that consists of a smoothing capacitor to convert the full-

wave rippled output of the rectifier into a more smooth DC output voltage. The regulator block consists of LM317 to regulate the output voltages and keep them constant at the desired level. Potentiometers will help to adjust the output voltages. The 2N3055 transistors along with MJ2955 will be incorporated in the circuits to allow higher currents to flow to the output which is beyond the capability of LM317 (1.5 Amps). The silicon power transistors for general-purpose switching and amplifier application have a maximum collector current of 15 amps and base current of 7 amps, collector-emitter voltage of 60 volts at a power of 115 watts (Onsemi, 2005). The LM317 device is an adjustable three-terminal positive-voltage regulator capable of supplying more than 1.5 Amps over an output-voltage range of 1.25 V to 37 V. It requires only two external resistors to set the output voltage. The device features a typical line regulation of 0.01% and typical load regulation of 0.1%. It includes current limiting, thermal overload protection, and safe operating area protection, see

Figure 18 (Texas Instrument, 2014). Over-current and over-temperature shutdown protects the device against overload or damage from operating in excessive heat. When an overload occurs the device will shut down Darlington NPN output stage or reduce the output current to prevent device damage. The output may be reduced or alternate between on and off until the overload is removed. The device will automatically reset from the overload. The device OUTPUT pin will source current necessary to make OUTPUT pin 1.25 V greater than ADJUST terminal to provide output regulation.

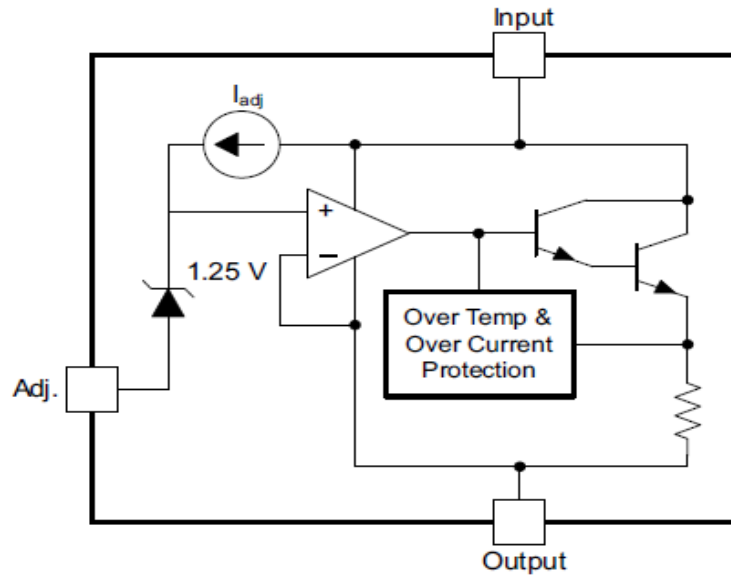


Figure19: IC LM 317 Functional Block Diagram.

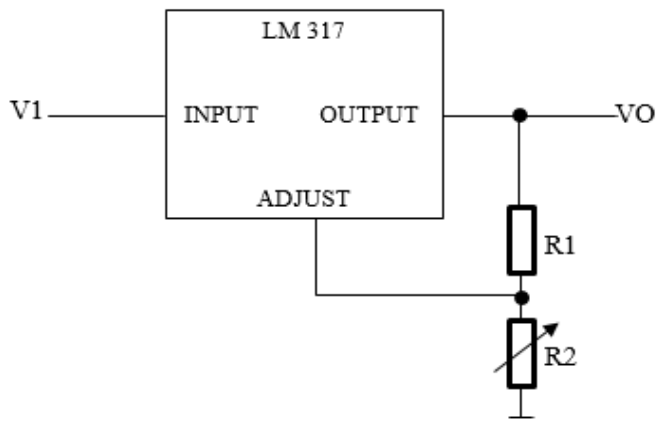


Figure 20: Output voltage regulation diagram.

Since the value of V_{REF} is constant, the value of Resistor 1 (R_1) of Figure 20 determines the amount of current that flows through R_1 and Resistor 2 (R_2). The size of R_2 determines the IR drop from ADJUSTMENT to Ground (GND). Higher values of R_2 translate to higher V_{OUT} . The voltage across the feedback resistors R_1 & R_2 are constant, 1.25V reference voltages, V_{ref} produced between the “output” and “adjustment” terminal. The adjustment terminal current is a constant current of $100\mu A$ (Texas Instrument, 2014). Since the reference voltage

across resistors R1 & R2 are constant, a constant current, 'I' will flow through the resistors resulting in an output voltage of:

$$V_o = V_{REF} \left(1 + \frac{R2}{R1} \right) + I_{ADJ} R2 \quad (3.1)$$

where V_{REF} is the Reference voltage (1.25) and

I_{ADJ} is the Adjustment terminal current (μA)

Power supply characteristics

Power supplies are characterized by number of quantities, some of which are mentioned below:

Output voltage

Rectification efficiency

Output frequency

Peak voltage

Load regulation

Output voltage after rectification

The maximum output voltage from the power supply is given by

$$V_{DC} = 1.414 V_T - 0.8 n \quad (3.2)$$

where V_{DC} is the unloaded voltage B, V_T is the rms output of the transformer A and n is 2 for full wave bridge rectifier circuit, refer to page 53. The 1.414 is the voltage dropped on two diodes during conduction.

$$\text{The primary to secondary turns ratio} = \frac{N_P}{N_S} = \frac{8}{1} = \frac{V_P}{V_S}, V_S = \frac{V_P}{8} = 30V$$

Rectification efficiency

$$\text{After rectification, mean} = V_{rms} - 1.414 \quad (3.3)$$

$$\begin{aligned} \text{Rectification efficiency } \eta &= \frac{P_{OUT}}{P_{IN}} = \frac{I_{dc}^2 R}{I_{rms}^2 R} = \frac{V_{dc}^2 / R}{V_{rms}^2 / R} \\ &= \frac{V_{dc}^2}{V_{rms}^2} \end{aligned} \quad (3.4)$$

$$V_{av}(\text{Mean}) = \frac{2V_{pk-pk}}{\pi} \quad (3.5)$$

$$V_{rms} = \frac{V_{pk-pk}}{\sqrt{2}} \quad (3.6)$$

$$\text{Rectification efficiency } \eta = \frac{V_{dc}^2}{V_{rms}^2} \times 100\% \quad (3.7)$$

The $V_{dc}^2 = \text{mean or } V_{av}$

Output frequency

Alternating current (AC) **frequency** is the number of cycles per second in an AC sine wave. **Frequency** is the rate at which current changes direction per second. It is measured in hertz (Hz), an international unit of measure where 1 hertz is equal to 1 cycle per second.

Output frequency is the frequency after rectification (f_{out}). One cycle is a period (T), and it is 10 ms for 50 Hz. Therefore, frequency $f = 1 / T$ (Hz).

The period of output frequency T^1 is twice the period of input frequency (f_{in}) T.

$$T^1 = \frac{1}{2} T \Rightarrow T = 2T^1$$

$$\frac{1}{f_{in}} = \frac{2 \times 1}{f_{out}} \Rightarrow f_{out} = 2f_{in} = 2 \times 50\text{Hz} = 100\text{Hz} \quad (3.8)$$

So the 100 Hz is the ripple frequency.

Peak voltage calculation

$$\text{Peak voltage (V}_{pk}) = V_{rms} \times 1.414 \quad (3.9)$$

Load regulation

Load regulation, abbreviated LR (also called the load effect), is the change in regulation output voltage when the load current changes from minimum to maximum.

$$LR = V_{NL} - V_{FL} \quad (3.10)$$

where LR is the load regulation, V_{NL} is the load voltage with no load current and V_{FL} is the load voltage with full load current.

Regulation expressed as a percentage by dividing the load regulation by the full-load voltage and multiplying the result by 100 percent.

$$\text{Load Regulation (\%)} = \frac{V_{NL} - V_{FL}}{V_{FL}} \times 100 \% \quad (3.11)$$

Flow chart of an 8-way relay bank

The block diagram of the relay bank shown in Figure 21 consists of eight solid state relays of which two relays (2 and 3) will operate a “sample – in” solenoid valves (to transfer sample into the irradiation site of the reactor) and other two relays (4 and 5) for the “sample-out” solenoid valves (transferring the activated sample from the irradiation site of the reactor to the detector for counting). The objective of designing a relay bank is to protect the PLC from break down as a result of overload, short circuit or power sag and also operate the solenoid valves. The relay bank could easily be repaired or any burnt or damage relays or component replaced. Relay 1 will control the “ON/OFF” operation of

the air-compressor. Relays 6, 7 and 8 serve as reserve components. There will be LED indicators to alert the operator on which action is being performed. The relay coils will be operated by a +12 VDC to control the solenoids from a 220 VAC voltage supply.

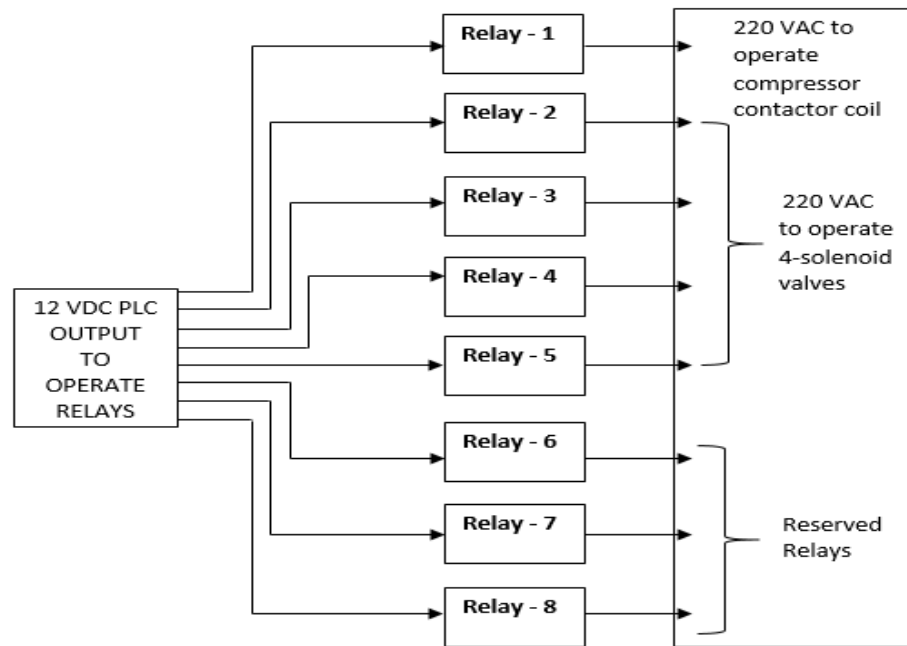


Figure 21: Block diagram of proposed 8-way relay bank.

Common-Emitter Phototransistor

Figure 22 shows the pictorial diagram of the phototransistor for the study.



Figure 22: Pictorial diagram of a phototransistor.

Source: (Electronics Notes, 2018)

Two phototransistors (sensors) are fixed at an appropriate location on top of the reactor and on the detector respectively to register the presence of the sample capsule and activate a timer. The sensors have two functions; the first is to guarantee that the sample has passed a certain point in the system. The second is to start specific processes, such as irradiation time, delay time and measurements etc. When using the sensors, the procedure is controlled by a time period (timeout) which is given to interrupt the process if the sample does not pass the point. A phototransistor is a light-sensitive transistor that converts light energy into electric energy. Phototransistors are similar to photoresistors but produce both current and voltage, while photoresistors only produce current. This is because a phototransistor is made of a bipolar semiconductor and focuses the energy that is passed through it. Photons (light particles) activate phototransistors and are used in virtually all electronic devices that depend on light in some way. A phototransistor generally has an exposed base that amplifies the light that it comes in contact with. This causes a relatively high current to pass through the phototransistor. As the current spreads from the base to the emitter, the current is concentrated and converted into voltage. The phototransistor is bipolar NPN device and is made of three lead components:

(i) The **base** is the lead responsible for activating the transistor. It is the gate controller device for the larger electrical supply. Base current is produced when light strikes the collector base PN junction. The base current is directly proportional to the light intensity. If the size of the base region is doubled, the amount of generated base photocurrent is also doubled.

(ii) The **collector** is the positive lead and the larger electrical supply.

- (iii) The **emitter** is the negative lead and the outlet for the larger electrical supply.

Context Analysis Diagram

The context analysis diagram shown in Figure 31 depicts the PLC software controlling six inputs and four outputs. The inputs are made up of a Compressor start, stop/reset button for compressor unit, sample-in button, sample-in phototransistor, sample-out phototransistor, stop/reset button for sample irradiation. The buttons are all momentary to enable the PLC to control and interrupt the operation of the outputs. The output loads are: a compressor contactor coil, sample-in solenoid valves, sample-out solenoid valves, and sample irradiation flash light / buzzer.

Characteristics of logics used in the PLC FBD program interface

Wiping relay (RS), AND, OR and NOT Boolean logic blocks were used for FBD programming interface. Logic gates are basic building blocks of digital circuits, which are used to implement a Boolean functions. A logical “1” at a specific input is inverted to logical “0” in the circuit program and logical “0” is inverted to logical “1”. Wiping relay (pulse output) timers, on-delay timers, asynchronous pulse generator and up / down counter are also used.

Latching Relays

Figure 23 shows the latching relay that represents a simple binary memory logic.



Figure 23: Latching Relay

The output value depends on the input status and the previous status at the output.

A signal at input S sets the output Q. A signal at input R resets output Q. See

Table 2

Table 2: Logic Table of the Latching Relay

| S | R | Q | Remark |
|---|---|---|------------------|
| 0 | 0 | X | Status unchanged |
| 0 | 1 | 0 | Reset |
| 1 | 0 | 1 | Set |
| 1 | 1 | 0 | Reset |

OR logic function

Figure 24 shows the OR logic block diagram

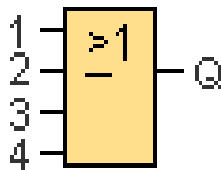


Figure 24: OR logic block.

The output of an OR function is “1” if at least one input is “1” as shown in Table

3.

Table 3: Logic Table of OR Function

| Input 1 | Input 2 | Input 3 | Input 4 | Output |
|---------|---------|---------|---------|--------|
| 0 | 0 | 0 | 0 | 0 |
| 0 | 0 | 0 | 1 | 1 |
| 0 | 0 | 1 | 0 | 1 |
| 0 | 0 | 1 | 1 | 1 |
| 0 | 1 | 0 | 0 | 1 |
| 0 | 1 | 0 | 1 | 1 |
| 0 | 1 | 1 | 0 | 1 |
| 0 | 1 | 1 | 1 | 1 |
| 1 | 0 | 0 | 0 | 1 |
| 1 | 0 | 0 | 1 | 1 |
| 1 | 0 | 1 | 0 | 1 |
| 1 | 0 | 1 | 1 | 1 |
| 1 | 0 | 0 | 0 | 1 |
| 1 | 0 | 0 | 1 | 1 |
| 1 | 0 | 1 | 0 | 1 |
| 1 | 0 | 1 | 1 | 1 |

AND logic function

Figure 25 shows the AND logic block diagram.

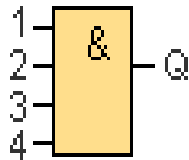


Figure 25: AND logic block

The output of an AND function is only “1” if all inputs are “1” as shown in Table

4.

Table 4: AND Function Logic Table

| Input 1 | Input 2 | Input 3 | Input 4 | Output |
|---------|---------|---------|---------|--------|
| 0 | 0 | 0 | 0 | 0 |
| 0 | 0 | 0 | 1 | 0 |
| 0 | 0 | 1 | 0 | 0 |
| 0 | 0 | 1 | 1 | 0 |
| 0 | 1 | 0 | 0 | 0 |
| 0 | 1 | 0 | 1 | 0 |
| 0 | 1 | 1 | 0 | 0 |
| 0 | 1 | 1 | 1 | 0 |
| 1 | 0 | 0 | 0 | 0 |
| 1 | 0 | 0 | 1 | 0 |
| 1 | 0 | 1 | 0 | 0 |
| 1 | 0 | 1 | 1 | 0 |
| 1 | 0 | 0 | 0 | 0 |
| 1 | 0 | 0 | 1 | 0 |
| 1 | 0 | 1 | 0 | 0 |
| 1 | 0 | 1 | 1 | 0 |
| 1 | 1 | 0 | 0 | 0 |
| 1 | 1 | 0 | 1 | 0 |
| 1 | 1 | 1 | 0 | 0 |
| 1 | 1 | 1 | 1 | 1 |

NOT logic function

NOT logic block diagram is shown in Figure 26.

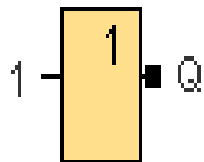


Figure 26: NOT logic block

The output of an NOT function is “1” if the input is “0”. The NOT block inverts the input status. See Table 5.

Table 5: NOT Function Logic Table

| Input 1 | Input |
|---------|-------|
| 0 | 1 |
| 1 | 0 |

Wiping relay (pulse output) timer

Figure 27 shows the output timer used in the Function Block Diagram programming interface.

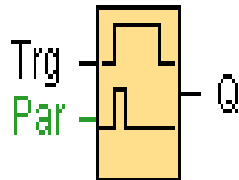


Figure 27: Pulse output timer block

A signal generates an output signal of a considerable length. Input Trigger (**Trg**) triggers the time for the wiping relay with a signal at input Trg. Parameter (**Par**) represents the time after which the output resets (output signal transition “1” to “0”). A pulse at Trg sets the output (Q). The output stays set until the time T has expired and if Trg = “1” for the duration of this time.

A “1” to “0” transition at Trg prior to the expiration of T also resets the output to “0”. The wiping relay (pulse output) timer controls the compressor, pressure build-up time and also the asynchronous pulse generator for the flash light.

On-delay timer.

Figure 28 shows the on-delay timer block.

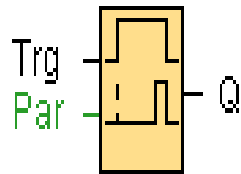


Figure 28: On-delay timer block

The output does not switch on until a configured delay time has expired. The (Trg) input triggers the on-delay time. Parameter T represents the on-delay time after which the output is switched on (output signal transition “0” to “1”). Output Q switches on after a specific time T has expired, provided Trg is still set. The on-delay timer is used to control the irradiation, decay, counting and delay or waiting time.

Asynchronous pulse generator

Figure 29 shows the asynchronous pulse generator block.

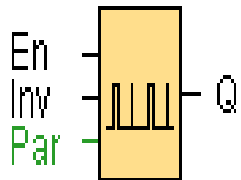


Figure 29: Asynchronous pulse generator block

The pulse shape at the output can be modified by a configurable pulse / pause ratio. The input enable (En) enables / disables the asynchronous pulse generator. The Inv input can be used to invert the output signal of the active asynchronous pulse generator. Parameters T_H and T_L can be used to customized the pulse width (T_H) and the interpulse width (T_L). Output Q is triggered on and off cyclically with the pulse / pause time T_H and T_L , where T_H is Time High and T_L is Time Low. Asynchronous pulse generator is used to operate the irradiation flash light at one (1) seconds T_H and one (1) seconds T_L .

Up / down counter

Figure 30 shows the up / down counter block.

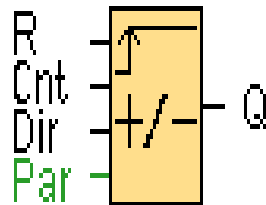


Figure 30: Up / down counter block

An input pulse increments or decrements an interval value, depending on the parameter setting. The output is set or reset when a configured threshold is reached. The direction of count can be changed with a signal at input Dir. The input R resets the output and the internal counter value to the start value with a signal at input R (Reset). The input count (Cnt) function counts the “0” to “1” transitions. It does not count “1” to “0” transition. Input Direction (Dir) determines the direction of count. Dir = “0”: Up and Dir = “1”: Down. Par for parameter setting. The output Q is set and reset according to the actual value at Cnt and the set thresholds.

The counter is used to count samples transferred into the reactor for irradiation.

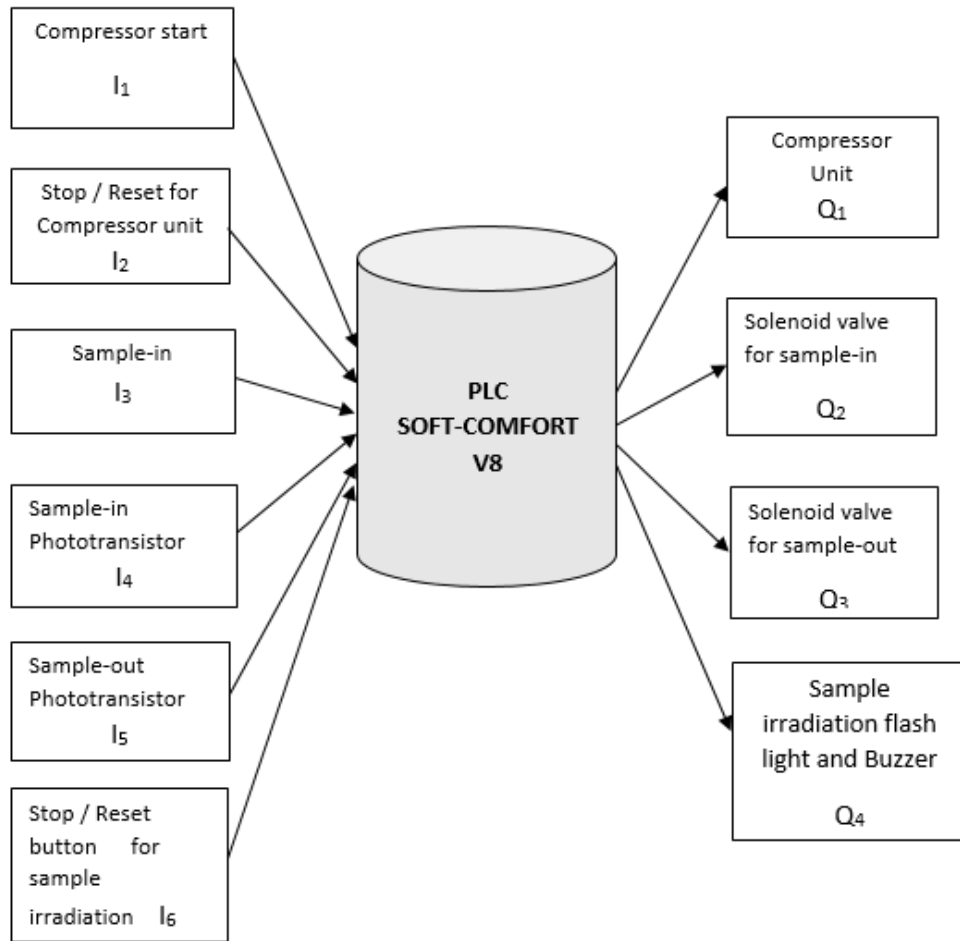


Figure 31: Context analysis diagram.

State Transition Diagram

State transition diagram for sample irradiation application user interface for conventional NAA and cyclic mode operation is shown in Figure 32. The round-head rectangle (oval) boxes represent state and the arrows represent

transition

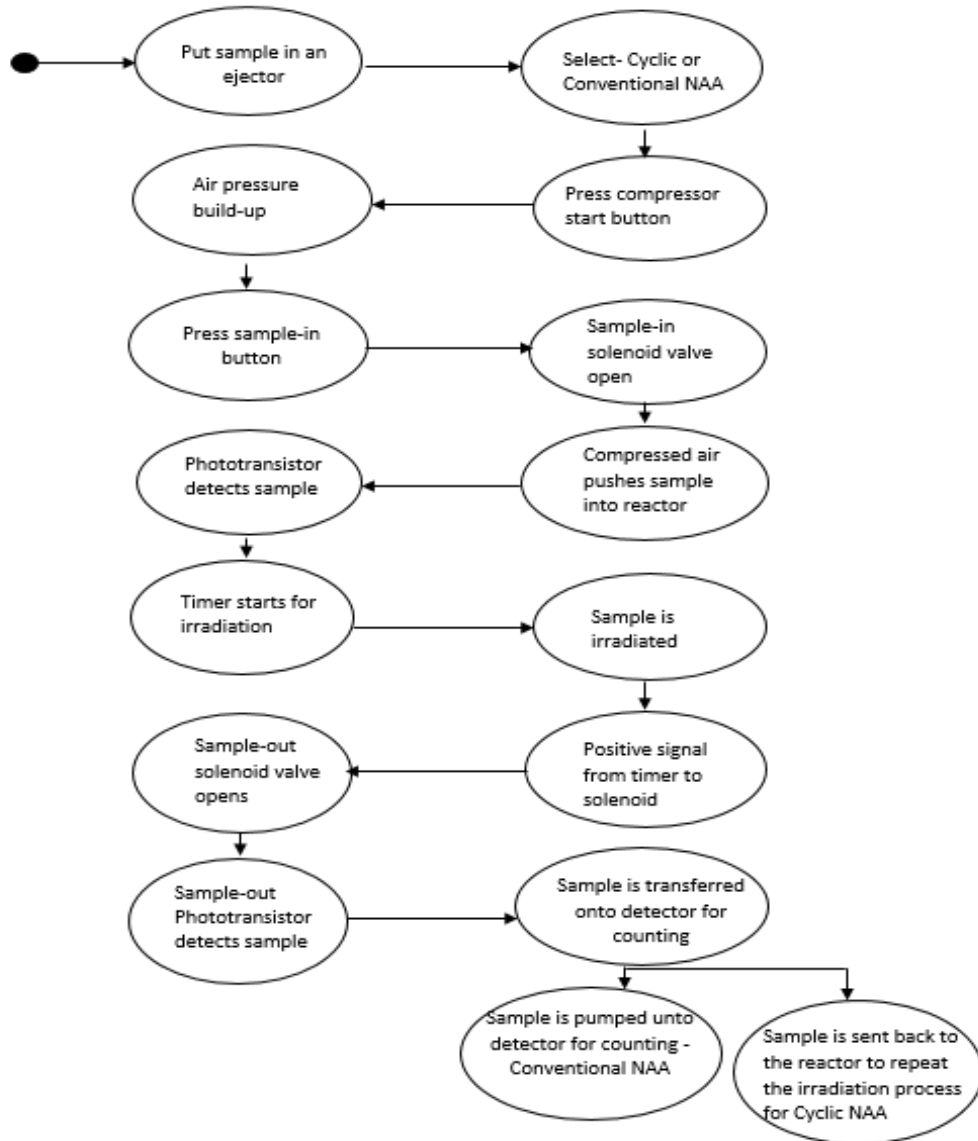


Figure 32: State transition diagram for conventional NAA and cyclic mode operation.

Data flow diagram

Figure 33 is the flow chart showing the Data Flow Diagram (DFD) depicting the flow of information through the irradiation of sample processes. Starting from where a sample capsule is transferred by conventional mode to the reactor for irradiation and the process repeated for optimization in cyclic mode.

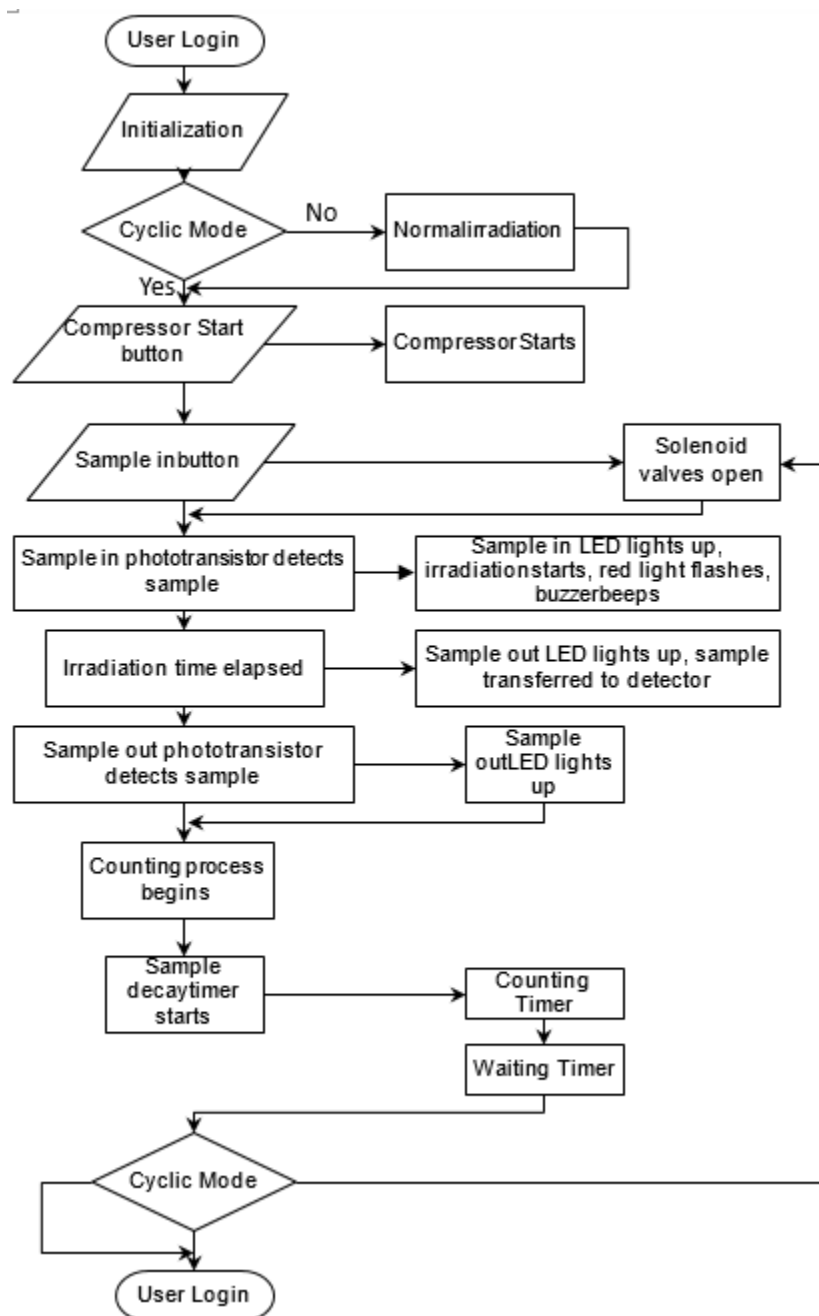


Figure 33: Flow chart for cyclic and conventional modes of analysis.

Data flow diagram is a graphical tool used to describe and analyse the movement of data through a system and normally used as the foundation from which other components are developed. Physical data flow diagrams show the actual implementation and movement of data between the various components in the application.

With any irradiation process, the computer will be connected to the PLC through an Ethernet cable to change or customize the timing set-up on the PLC for particular application. Example: irradiation time, number of cycle to optimize activity, counting time, delay time and waiting time.

Design Requirements for Safety Systems and Components (SSCs)

Engineering Safety Features

According to IAEA documents the design of SSCs of Research Reactors (RRs) follow a certain criteria so not to compromise the safety operations of RRs (IAEA, 2005; IAEA SPECIFIC SAFETY GUIDE No.SSG-39, 2016).

The PTS control unit designed, satisfies the design requirements as follows:

Pre-design appraisal

- i. The PTS control unit designed satisfies the surveillance requirements, as well as decommission and disposal aspects and will not interfere with the Reactor under normal operation.
- ii. Provisions have been made for inspection, periodic testing and maintenance (including simulation of the program) to verify that the engineering safety features continue to function or in a state of readiness to perform the functions and will be reliable and effective upon demand.
- iii. Surveillance test points have been provided as means to measure the AC and DC voltages using externally connected testing devices. POTs have been provided for recalibration of the +12 and +24 DCV power supply.
- iv. Under the design for testability, provision has been made for the PTS control unit to be put under real conditions by exposing the sensors (the phototransistors) of the system to actual process variable rather than simulation.

Safety Considerations for the design of an experiment or modification (IAEA Specific Safety Guide No. SSG-24, 2012).

The design of the controller unit for modification on the existing PTS demonstrate that:

- i. the designed PTS control unit can fulfil the task for which it is intended
- ii. it can be installed and operated without compromising the safety of the Research Reactor
- iii. the unit can be removed or decommissioned without compromising the safety of the RR.

Failure Mode and Effects Analysis for a computer based PLC control unit for PTS

A Failure Mode and Effects Analysis (FMEA) study is conducted to primarily achieve the following:

1. Identify known and potential failure modes,
2. Identify causes and effects of each failure mode,
3. Prioritize the identified failure modes according to the risk priority number (RPN).
4. Provide for problem follow-up and corrective action.

At this report, an FMEA based on the conceptual design of the PTS Control Unit (PTSCU) is presented.

Methodology for FMEA

The methodology used consists firstly of defining a functional block diagram for the Control Unit (CU) device as well as a conceptual full scale for implementation diagram. These diagrams show the main systems and subsystems

associated with the implementation of the PTSCU. Implementing the CU in an operating PTS would not have any effect on other systems. A FMEA has been developed for the major components of the CU in order to identify the most critical components of the system as well as to identify the various failure modes that might affect the effective operation of the CU based on procedures outlined in (MIL-STD-1629A, 1980). FMEA provides valuable descriptive information about the system design and operation, by identifying in a concise manner the failure modes and compensation actions as well as recommend actions to mitigate against these failures.

The failure effect of a component on the CU operation and other systems was the main consideration for the analysis done. In classifying the severity of system failure modes, a numerical code is used which ranks from 1 to 10. A higher number indicates the criticality of the component that must be evaluated for each component failure mode. This index is classified into these main severity levels: none (1), low (2 and 3), medium (4 and 5), high (6 and 7), critical (8 and 9) and catastrophic (10). A description of these indices and their effects is presented in Table 6.

Table 6: Severity Classification and Description used in Failure Mode Effect Analysis

| Effect | System Functionality | Rating |
|---------------|---|---------------|
| Catastrophic | Totally incapacitates the system and fails to satisfy design intent. | 10 |
| | Significantly reduces the effectiveness of the system | 9 |
| Critical | such that it would have little or no benefit and fails to satisfy the design intent | 8 |
| | Significantly reduces the effectiveness of the system such that it would fail to satisfy the design intent. | 7 |
| High | However, the system would still operate and significant benefit would be gained from its operation. | 6 |
| | Reduces the level of redundancy that is built into the system. The effectiveness of the system would not | 5 |
| Medium | be significantly reduced and design intent would still be satisfied. | 4 |
| | Reduces the effectiveness of the system such that it | 3 |
| Low | is outside normal operating limits. However, the design intent would still be satisfied. | 2 |
| None | No effect | 1 |

In Table 7, the likelihood of occurrence of various failure modes is presented and described. The information presented on likelihood of occurrence in the FMEA is mainly based on experience gained from using the various subsystems associated with the CU.

Table 7: Likelihood of Occurrence

| Likelihood of Detection | Criteria: Likelihood of Detection | Rating |
|--------------------------------|--|---------------|
| Uncertain | Uncertain that failure will be detected | 10 |
| Low | Low chance that failure will be detected | 9 |
| | | 8 |
| Moderate | Moderate chance that failure will be detected | 7 |
| | | 6 |
| High | High chance that failure will be detected | 5 |
| | | 4 |
| Very High | Very high chance that failure will be detected | 3 |
| | | 2 |
| Certain | Certain that failure will be detected | 1 |

In Table 8, the likelihood of detecting various failures is presented. This information presented in this section of the FMEA was also based on operational experience in using these subsystems associated with the CU device.

Table 8: Likelihood of Detection of Failures

| Likelihood of Occurrence | Definition Guidance | Criteria: Possible Failure Rates | Rating |
|---------------------------------|----------------------------|---|---------------|
| Certain | Absolute certainty | 100% | 10 |
| High | Very likely to occur | 65% - 99% | 9 |
| | | | 8 |
| Medium | Likely/Possible | 35% - 65% | 7 |
| | | | 6 |
| Low | Unlikely to occur | 5% - 35% | 5 |
| | | | 4 |
| Remote | Very unlikely to occur | 1% - 5% | 3 |
| | | | 2 |
| None | Will not occur | 0% | 1 |

Conceptual Full Scale Device Summary

Figure 34 shows the block diagram of the conceptual full scale implementation of the CU in existing PTS.

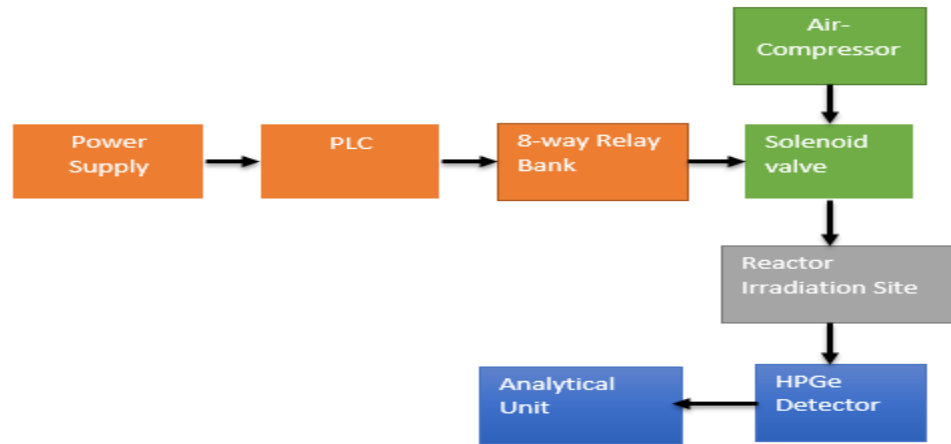


Figure 34: A complete functional block diagram of PTS FMEA.

Figure 35 shows the flow chart for cyclic mode analysis with conventional mode option with the CU incorporated.

Figure 36 is the designed CU to replace the existing control unit

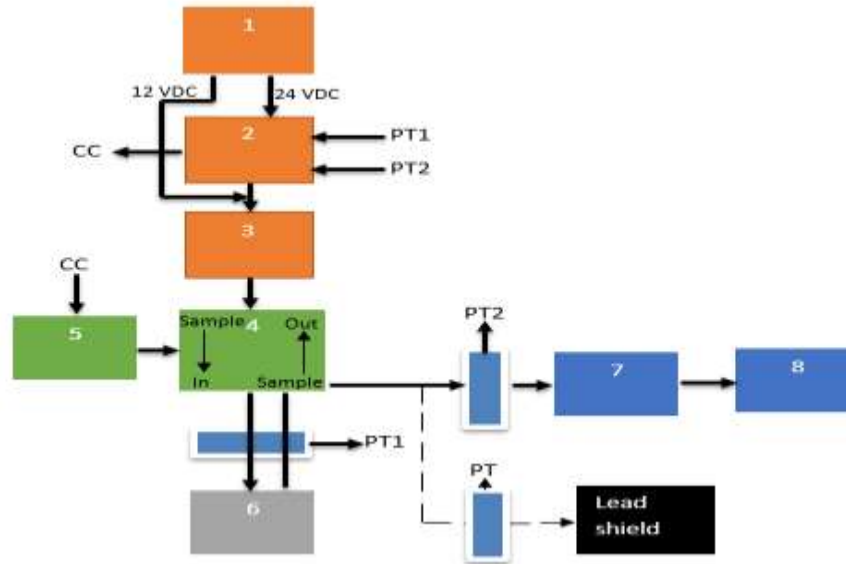


Figure 35: Flow chart for cyclic mode analysis with conventional mode option FMEA



Figure 36: Block diagram of the controller unit FMEA.

| Legend |
|---|
| CU (Electrical and Electronics) |
| Pressurized air (fluid flow side) |
| Neutrons / Gamma Energy |
| Phototransistor side (Sensor) |
| Analytical side (HPGe) detector /computer |
| Sample receiving chamber |

Figure 37: Legend of Figures 34, 35 and 36.

In Figures 35 and 36, the block diagrams of a conceptual full scale integration of the CU with existing PTS is presented. The description of various blocks, their functions as well as likely effects of the CU on other systems has been stated in the thesis.

Details of the FMEA performed for the CU is presented in Table 9. The inputs used in completing the analysis include mainly data of various components in the CU and from manufactures of the components. Figure 37 describe the legend of Figures 34, 35 and 36.

Table 9: Failure Mode and Effects Analysis for PTS Control Unit

| (1) Item No. | (2) Component | (3) Function | (4) Failure mode | (5) Failure cause | Failure Effects | | (8) System failure mode detection | (9) Compensating Action | Risk Analysis | | | | (14) Recommended Action |
|-----------------|-------------------|---|--|---|-------------------------------|--|--|---|---------------------|---------------------|---------------------|---------------------|--|
| | | | | | (6) Local | (7) System | | | (10) S E V | (11) O C C | (12) D E T | (13) R P N | |
| 1 | AC voltage meter | Measures AC voltage | No reading | Damage | Humming | Loss of supply voltage monitoring | Humming | Fuses (Main fuse and F1) to prevent circuit overloads | 3 | 2 | 2 | 12 | Replace voltmeter |
| 2 | Solenoid valves | Open and close to control the passage of a compressed-air | i. Fails to open ii. Fails to close | i. Voltage failure ii. Coils short or burnt iii. control Spring failure | i. Overheating ii. Humming | Sample capsules cannot be transferred into the reactor and back. | Valves not open or close to transfer sample capsules | Fuses (Main fuse, F1 & F2) to prevent circuit overloads | 5 | 2 | 4 | 40 | i. Replace solenoid valve ii. . Periodic inspection and preventative maintenance |
| 3 | Photo-transistors | It switches +24 DCV when detect dark at its base glass surface to control the solenoid valves | i. Permanently ON or OFF ii. Fails to control | i. High radiation of samples ii. Malfunction of LED | Fails to switch | Solenoid valves open and close cannot be controlled | i. Sample capsule into the reactor and back to the detector not being controlled | Fuses (Main fuse and F1) to prevent circuit overloads | 5 | 2 | 3 | 30 | i. Replace phototransistor ii. . Periodic inspection and preventative maintenance |

| | | | | | | | | | | | | | |
|---|-----------------------------|--|--|---|---|---|--|---|---|---|---|----|---|
| 4 | Light Emitting Diodes (LED) | semiconductor device that emits visible light to operate the phototransistor | i. Burnt or ii. Illumination intensity reduced | i. Dropper resistor failure ii. Supply voltage reduced | Fails to turn ON ii. Light flickering | i. The phototransistor or cannot function ii. Solenoid valves cannot be controlled | Intermittent operation of solenoid valves and phototransistors | Fuses (Main fuse, F1 & F2) to prevent circuit overloads | 5 | 2 | 3 | 40 | i. Replace LED ii. . Periodic inspection and preventative maintenance |
| 5 | Switches | Isolate and De-isolate load(s) from the power supply. | i. Fails to open ii. Fails to close | i. contact dirty/corroded ii. Release spring failure | i. Overheating ii. Arcing | i. Intermittent operation of loads ii. Intermittent measurements | i. Loads not operating ii. Abnormal measurements iii. Visual smoke or arcing | None | 7 | 2 | 2 | 28 | i. Replace switch ii. Add or replace with circuit breakers |
| 6 | Fuses | Prevents overcurrent | i. Blows prematurely ii. Fails to blow upon overcurrent | i. Overcurrent ii. Improper fuse selection | i. Blown fuse ii. Arcing across fuse electrodes iii. Fuse burned into place | i. System shut-down ii. System malfunction iii. System power overload | i. visual smoke ii. loads not operating iii. Indication and warning lights OFF | Fuses (F1 & F2) to prevent circuit overloads | 8 | 3 | 1 | 24 | i. Remove the overload, replace fuse with spare. ii. Add suppressor diode against over-voltage |
| 7 | Relays(coils and contacts) | Closes a relay contacts when energized, | i. Coil short circuit or burnt. | i. contact dirty/corroded ii. Release | Overheating | i. Circuit overheating ii. blown fuse | i. Humming ii. visual smoke | Fuses (F1 & F2) to prevent circuit | 5 | 3 | 3 | 45 | Replace relay and any blown fuse(s), |

| | | | | | | | | | | | | | |
|--|--|--|--|----------------|--|--|--|-----------|--|--|--|--|---------------------------|
| | | The contacts engages and disengages the solenoid valves to the circuit | ii. Fails to close (engage) iii. Open (disengage) | spring failure | | iii. Loss of power supply to operate the solenoid valves | iii. loads (solenoid valves) not operating | overloads | | | | | wire(s), or connector(s). |
|--|--|--|--|----------------|--|--|--|-----------|--|--|--|--|---------------------------|

Definitions important for understanding various items in Table 9

1. Item No.

Unique line item for each identified component under review.

2. Component:

Name or description of the item or system function being analyzed.

3. Function:

A concise statement of the function performed by the hardware item shall be listed.

4. Failure Mode:

All predictable failure modes for each indenture level analyzed shall be identified and described. Additional information concerning the context of the failure mode may be included such as:

- i. The mode of operation.
- ii. The time constraints.
- iii. The environmental stresses.
- iv. The operational stresses.

5. Failure Cause:

The most likely causes for each potential failure mode is identified and described. Since a failure mode may have more than one cause, all probable independent causes should be identified and entered.

6. Failure Effects (Local):

Local failure effects identify the impact of the failure mode on the operation and functionality of the system item/equipment under consideration. The purpose of defining the local effects is to provide a basis for evaluating compensating

provisions and for recommending corrective actions. It is possible for the “local” effect to be the failure mode itself.

7. Failure Effects (System):

System level failure effect describes the total impact of the failure mode on the operation, function and status on the system level which the item/equipment is operating.

For example, the local failure effect of a control solenoid valve failing open will have a system effect of transferring sample capsule.

8. System Failure Mode Detection:

Description of how the failure mode is detected by the system or operator shall be determined. Means of detection may be done by methods such as annunciations, operator procedures such as visual inspection or other preventive, predictive and corrective maintenance activities.

9. Compensating Action:

A listing of the compensating action(s) which mitigate the effect of the failure mode on the system shall be documented. The action(s) can be either design related (ex: design redundancy) or operator procedural actions. Any operator procedural actions used as a compensating action shall reference the governing operating manual or procedure utilized by the operator

10. Risk Analysis - Severity (SEV):

A qualitative measure of severity is assigned to each failure mode to represent the worst potential consequences from that failure on the system level.

11. Risk Analysis - Occurrence (OCC):

A qualitative measure of occurrence is assigned to each failure mode to represent the probability of the failure mode and its particular effect over a defined time period.

12. Risk Analysis - Detection (DET):

A qualitative measure of detection is assigned to each failure mode to represent the ability of the design to detect the failure mode *before* the resultant effect reaches a system-level failure

13. Risk Analysis –Risk Priority Number (RPN)

The Risk Priority Number is the product of the Severity (S), Occurrence (O) and Detection (D):

$$RPN = S \times O \times D$$

14. Recommended Action:

Review of the risk attributes requires caution and good judgment. A thorough review of the values of Severity, Occurrence and Detection is required before forming any opinions and deciding if undertaking corrective actions is required.

The following decision options are available:

- i. Implement corrective actions in order to reduce the associated failure mode risk.
- ii. Try to eliminate the failure mode.
- iii. Minimize severity of the failure.
- iv. Reduce the occurrence of the failure mode.
- v. Improve the detection.
- vi. Accept the failure mode risk without change to the design. Documenting the justification for accepting the associated risk is required.

15. Action Taken

If implementation of corrective action(s) is required then document the corrective action changes made to the design which were required to reduce the associated failure mode risk. Any previous corrective actions to the design shall be retained if previous attempts to reduce failure mode risk were attempted.

16. Action Result - Severity (SEV)

The new severity ranking value based on any corrective action taken for the failure mode.

17. Action Result - Occurrence (OCC)

The new likelihood of occurrence ranking value based on the any corrective action taken for the failure mode.

18. Action Result - Detection (DET):

The new likelihood of detection ranking value based on the any corrective action taken for the failure mode.

19. Action Result – RPN:

The new RPN value resulting from any corrective action taken for the failure mode.

List of Components for the 12/24 VDC power supply

Table 10 shows the list of components used to designed and constructed the PTS control unit.

Table 10: List of used Circuit Components

| 24 VDC | | 12 VDC | |
|----------------|--|---------------|-------------------------------------|
| Component ID | Part Number | Component ID | Part Number |
| IC U3 | LM 317 TO-220 | IC U4 | LM 317 TO-220 |
| Transistor Q1 | 2N3055 Metallic | Transistor Q3 | 2N3055 Metallic |
| Transistor Q2 | MJE 2955 | Transistor Q4 | MJE 2955 |
| Resistor R1 | 470 Ohms 0.5Watts | Resistor R9 | 470Ohms 0.5 Watts |
| Resistor R2 | 33 Ohms 5 Watts | Resistor R10 | 33 Ohms 5 Watts |
| Resistor R3 | 4.7 K 0.5 Watts | Resistor R11 | 4.7 Ohms 0.5 Watts |
| Resistor R4 | 10 K Potentiometer | Resistor R12 | 5 K Potentiometer |
| Resistor R5 | 3 K 0.5 Watts | Resistor R13 | 2.61 K 0.5 Watts |
| Resistor R6 | 120 Ohms 0.5 Watts | Resistor R14 | 120Ohms 0.5 Watts |
| Resistor R7 | 2.31 K 0.5 Watts | Resistor R15 | 1.1 K 0.5 Watts |
| Resistor R8 | 1 K 0.5Watts | Resistor R16 | 715 Ohms 0.5 Watts |
| Capacitor C1 | 4700 μ F / 50 V Electrolytic | Capacitor C5 | 3300 μ F / 63 V Electrolytic |
| Capacitor C2 | 10 μ F / 50 V Electrolytic | Capacitor C6 | 10 μ F / 50 V Electrolytic |
| Capacitor C3 | 470 μ F / 50 V Electrolytic | Capacitor C7 | 470 μ F / 50 V Electrolytic |
| Capacitor C4 | 104 Ceramic | Capacitor C8 | 104 Ceramic |
| Diode D1 | IN4007 | Diode D2 | IN4007 |
| Rectifier BR1 | | Rectifier BR2 | |
| Transformer U1 | 15-0-15 Center Tapped 2 Amps Step Down Transformer | | |

Chapter Summary

This chapter comprises of various components, methods and connections to the design and construction of a high current dual voltage regulated power supply, relay bank that control and supply an alternating Voltage (220 VAC) to operate the solenoid valves. The chapter also provided a flowchart, state transition diagram and a context analysis diagrams depicting the flow of steps and PLC software interfacing the inputs to the outputs variables.

The GHARR-1 pneumatic system with its associated compressed-air unit, phototransistors with the PLC controller unit to effect the cyclic mode analysis was described. The main components like the air filter / water trap in the compressed air system and the solenoid valve were also described. Failure mode and effects analysis (FMEA) was conducted on the controller unit and the results reported. Some equations have been provided to correct the effect of dead time and pile-up effect as result of increase of number of irradiation cycles, see pages 29.

CHAPTER FOUR

RESULTS AND DISCUSSION

Introduction

This chapter presents the schematic diagrams showing the connected symbols used to show the functional relationships of the parts of electrical / electronic and mechanical component and the components of the PTS control unit. The chapter also provides the characteristic response curves of the designed power supply and the simulation results of the integrated designed sub-systems of the controller unit.

Designed Circuits

Direct – on – Line Starter connection for the air compressor control system

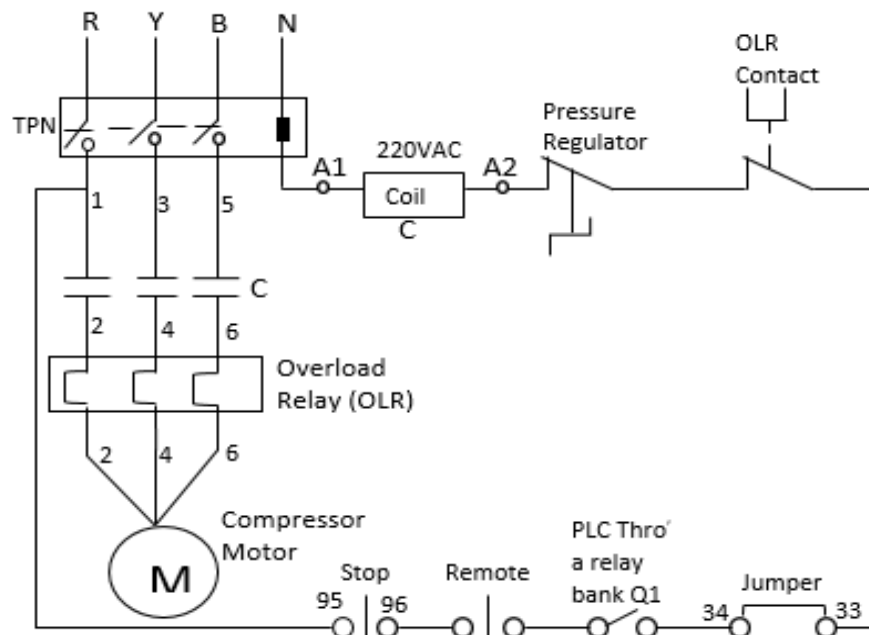


Figure 38: Schematic diagram for a remote control of air compressor system by PLC.

Figure 38 shows the automatic connection for the air compressor system. The circuit consisting of a three-phase and neutral (TPN) isolator connected to a compressor motor through magnetic contactors and an overload relays (OLR). The contactor coil is connected to a 220 VAC and in series to a pressure regulator and an overload relay contact, see Figure 38. The air pressure is regulated between 0.4 MPa and 0.6 MPa. That is, when the air pressure falls to 0.4 MPa the compressor starts automatically to build up pressure to 0.6 MPa and cuts off. The output Q1 of the PLC module Figure 40 is connected to a relay (on a relay bank) that is energized to close a contact in between the remote stop-push-button and the start-push-button which is jumped up to enable the system to be controlled by the PLC through a timer. In the event of any emergency, the remote stop-button could be pressed manually to de-energise the coil and isolate power from the compressor motor. There is a stop/reset button on the controller unit designed and built with the help of the LOGO! SOFT COMFORT V8 software of the PLC to control the operation.

Figure 39 shows the existing remote connection for the air-compressor without the PLC. The stop-buttons are connected through a link to the starts-buttons which are connected in parallel and series to the contactor coil. The remote stop and start buttons are connected closed to the PTS. The other two buttons are located in the air compressor room which is a distant from the PTS.

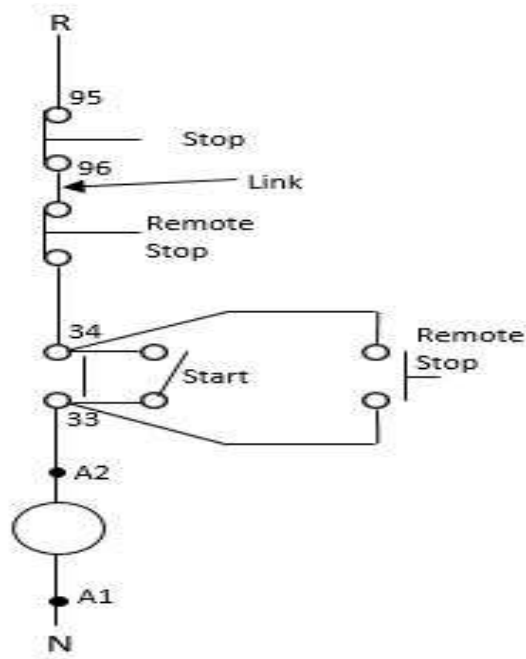


Figure 39: Schematic diagrams of the existing PTS air-compressor connection.

The PLC connections

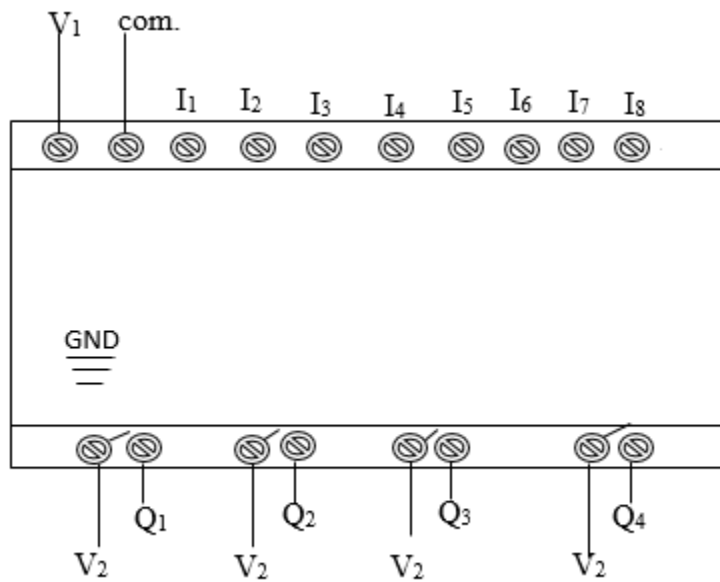


Figure 40: Input and output connections of PLC.

A +24 VDC is connected to input V_1 and common (com.) to operate the relays and electronics in the PLC module. I_1 to I_8 are the input terminals. I_1 to I_6 are for analog parameters while I_7 and I_8 are for digital parameters inputs as shown in Figure 40. A +12 VDC (V_2) is connected to the output contacts Q_1 - Q_4 to operate the relay bank and further control the solenoid valves.

Dual Voltage Regulated High Current Power Supply (1.25-30V/5A)

Figure 41 shows the High Current Dual Voltage regulated power supply (12 / 24 VDC) designed to operate the PLC and the relays in the relay bank. A center tapped (15-0-15 CT) transformer U_1 converts the 240 VAC to 30 VAC and 15 VAC respectively and rectified by a separate full-wave rectifier (bridge type) D_1 and D_2 . The output of the rectifiers are filtered (smoothing) by capacitors C_1 and C_4 .

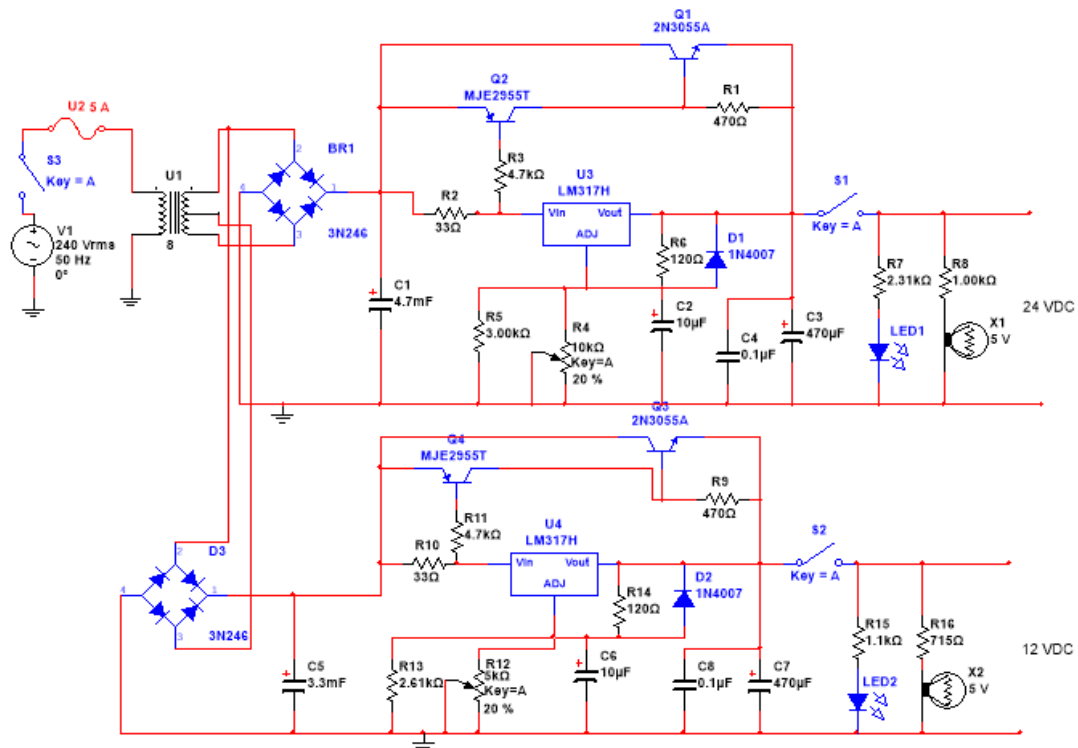


Figure 41: Dual Voltage Regulated Power Supply – (+12 / +24 VDC).

Figure 41 shows the designed dual voltage regulated high current power supply to operate the PLC. With the help of voltage dividers created by the resistors R4 and R12 and series resistors R6 and R14, R4 and R13 voltages at the Adjust (Adj.) pin of LM317 are controlled. These help LM317 to regulate the output voltages and keep them constant at the desired level. R4 and R12 are potentiometers which help to adjust the output voltages. The 2N3055 transistors (Q1 and Q3) along with MJ2955 (Q2 and Q4) in the circuits allow higher currents to flow to the output which is beyond the capability of LM317 (1.5 Amps). 2N3055 and MJ 2955 are complimentary silicon power transistors designed for general-purpose switching and amplifier applications. The transistors are packaged in a To-3 case style, have a maximum collector current of 15 amps and base current of 7 amps, collector-emitter voltage of 60 volts at a power of 115 watts.

The operating and storage junction temperature ranges between -65 to + 200 °C (Onsemi, 2005). The two transistors are mounted on an aluminum heat sink with a mica insulator used to electrically isolate the transistor case from the heat-sink. In combination, LM317 controls the output voltage and the NPN-PNP transistor pair allows most of the current to flow from Input to Output. The LM317 device is an adjustable three-terminal positive-voltage regulator capable of supplying more than 1.5 A over an output-voltage range of 1.25 V to 30 V. It requires only two external resistors to set the output voltage. The device features a typical line regulation of 0.01% and typical load regulation of 0.1%. It includes current limiting, thermal overload protection, and safe operating area protection, see Figure 16 (Texas Instrument, 2014). Over-current and over-temperature

shutdown protects the device against overload or damage from operating in excessive heat.

When an overload occurs the device will shut down Darlington NPN output stage or reduce the output current to prevent device damage. The output may be reduced or alternate between on and off until the overload is removed. The device will automatically reset from the overload. The device OUTPUT pin will source current necessary to make OUTPUT pin 1.25 V greater than ADJUST terminal to provide output regulation. The function of capacitors C2 and C6 is to improve ripple rejection and prevent amplification of the ripple as the output voltage is adjusted higher. The diodes D1 and D2 provide a low-impedance discharge path to prevent the capacitor from discharging into the output of the regulator. The LEDs are connected to indicate the presence of the output voltages. The +24 VDC is connected to the inputs of the PLC while the +12 VDC is connected to the relay bank through the outputs of the PLC. Switches S₁ and S₂ connect and disconnect the output +24 VDC and +12 VDC respectively.

Power supply response curves

Peak-to-peak (pk-pk) voltage response curves for V_{RMS} (30 VAC / 15 VAC)

Figure 42 shows the peak-to-peak voltage response curve for a 30 Vrms sine wave that appeared across the ends of secondary full coil of the transformer used. The x-axis has time-base scale of 10 ms per division and y-axis has 10 V per division. The pk-pk voltage is 42.9 VAC at 50 Hz. From the graph, the Vrms voltage is $42.9 / 1.414 = 30.3$ VAC.

Figure 43 shows a pk-pk of the half coil of the secondary coil of the transformer that gives out 15 Vrms sine wave at 50 Hz. The x and y axis are of

the same scale as the 30 Vrms. The pk-pk voltage is 21.4 VAC. The Vrms voltage is calculated as peak voltage divided by 1.414 and is equal 15.1 VAC. Refer to page 55 equation 3.6.

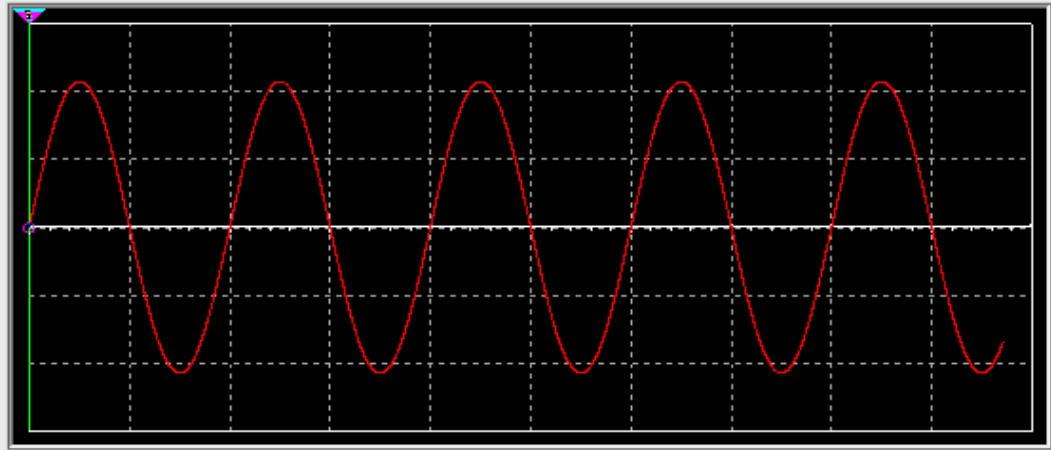


Figure 42: Peak voltage response curve of transformer output V_T for 30 Vrms.

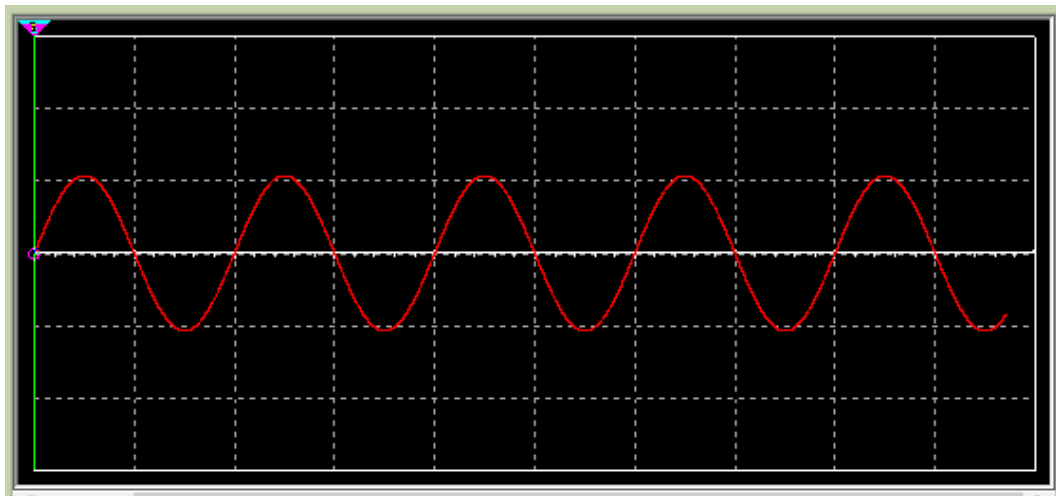


Figure 43: Peak voltage response curve of transformer output V_T for 15 Vrms.

Response curve after rectification

Figures 44 and 45 show the response curves after rectification. Rectification is done with diodes. This act as one-way valves for electric current. From the graphs, the frequency before rectification was 50 Hz. After the

rectification, the frequency becomes twice (100 Hz) as before due to the drops on two diodes at the half cycle of conduction. Refer to page 55 subsection equation 3.8. The pk-pk voltage is 42.8 VDC at a mean of 27.2 VDC. Figure 45 gives pk-pk voltage of 21.3 VDC at a mean of 13.5 VDC. The x-axis scale is 10 ms per division and y-axis scale is 20 V per division for both figures.

This show that the rectification efficiencies (RE) for both figures were good. The maximum RE for a bridge rectifier is about 81.2 % (“Frequency Modulation – Physics and Radio-Electronics,” n.d.). The RE for Figures 44 and 45 are 82 % and 81.1 % respectively. Refer to page 55 equation 3.7.

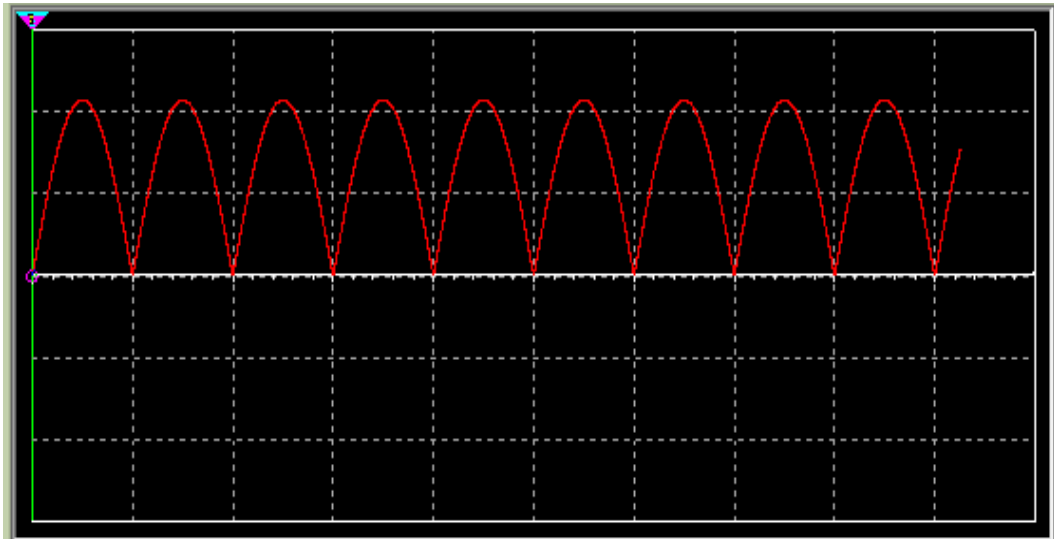


Figure 44: Response after rectification for +24 VDC circuit.

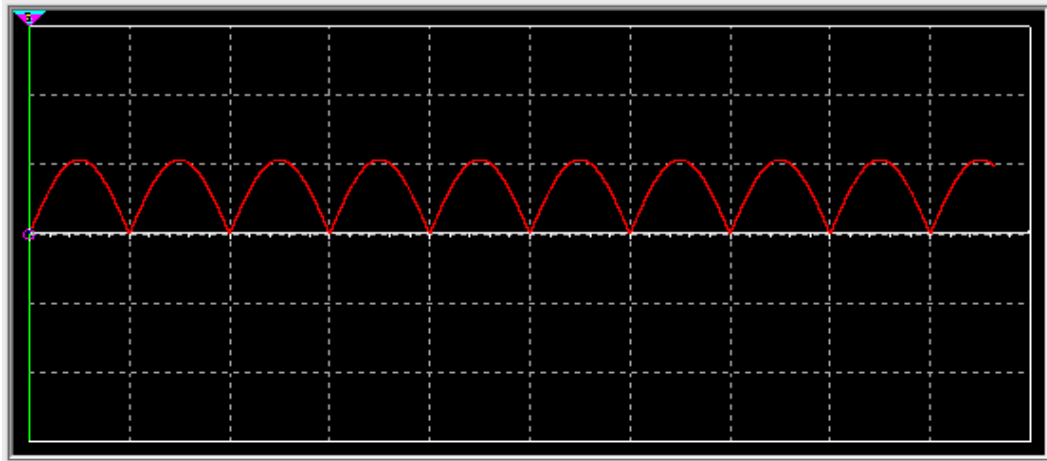


Figure 45: Response curve after rectification for + 12 VDC circuit.

Smoothing capacitor response

The smoothing capacitor reduces the AC component. The effect of this is to increase the average voltage, and provide current when the output voltage drops. Figures 46 and 47 show the response curves after smoothing by capacitors

C1 and C5, see page 90. The scale for x-axis is 10 ms per division for both figures and 20 V and 10 V per the y-axis scale for Figure 47 and Figure 48 respectively. From the graphs, a mean of 40.9 VDC and 19.6 were recorded for the +24 VDC and +12 VDC circuits respectively.

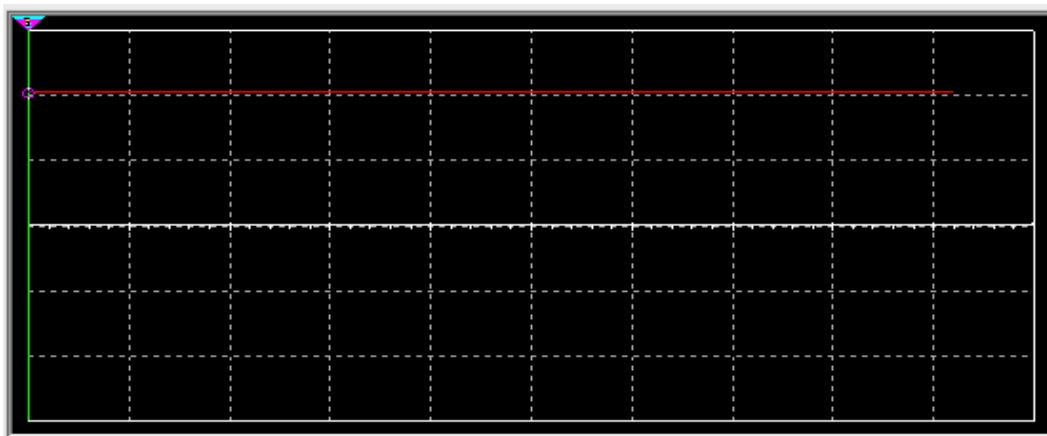


Figure 46: Smoothing by capacitor C₁ and before the regulator for + 24 VDC.

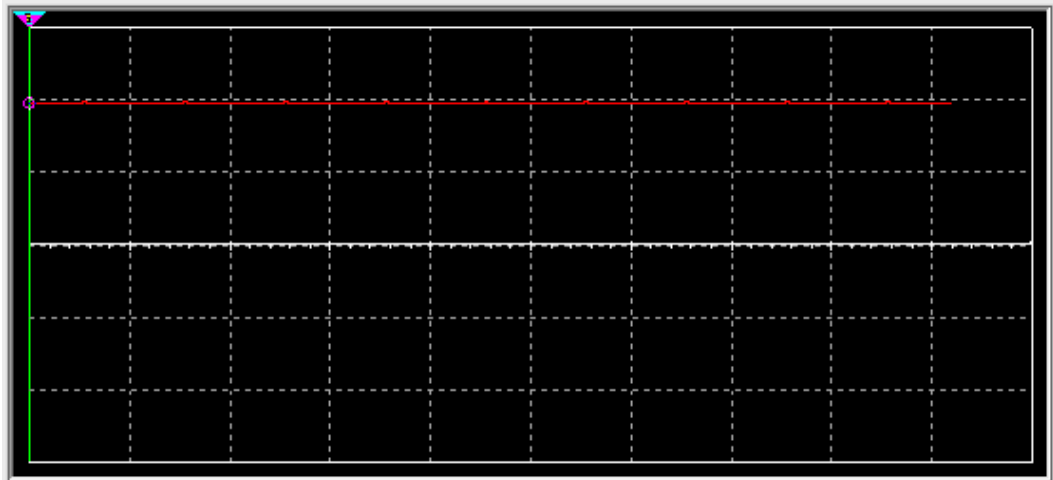


Figure 47: Smoothing by capacitor C_5 and before the regulator for +12 VDC.

Regulated output voltage curves

Figures 48 and 49 show the regulated output voltages. The two figures have the same x and y scale values of 10 ms per division and 10 V per division respectively. The graphs depicts a mean voltage values of 24.2 VDC and 12.2 VDC respectively for Figures 48.and Figure 49

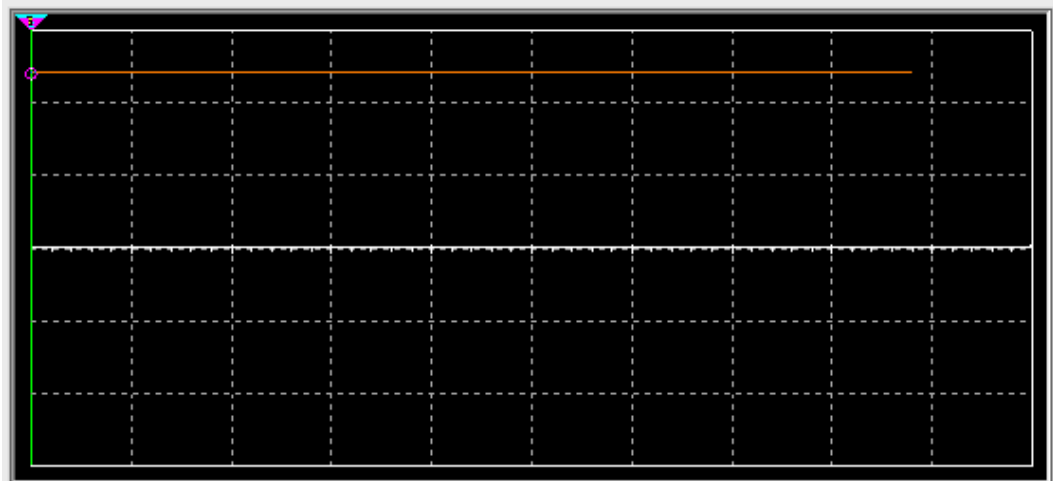


Figure 48: Regulated output voltage for +24 VDC.

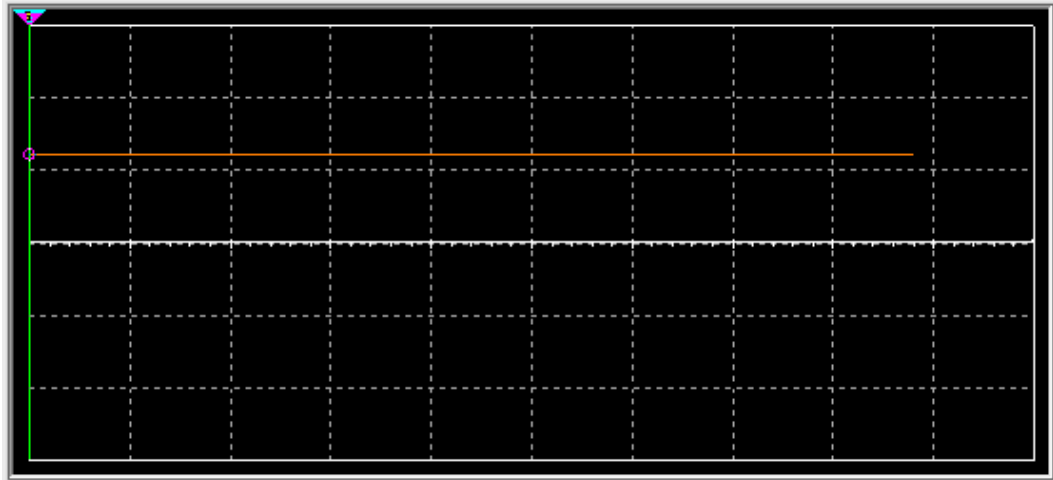


Figure 49: Regulated output voltage for +12 VDC.

Normal conventional NAA operation

There are two controllers in the existing control system, one for inner site irradiation (using smaller capsules) and other one for outer site irradiation (using bigger sample capsules). There are two circuits in each controller, sample-in and sample-out circuits. 220 AC voltage is applied across two solenoid valves which opens and a compressed-air pumps the sample either into or out of the reactor using another two solenoid valves. The old controller uses a metal TRIAC (KS3-8 87.7) with Gate, Anode and Cathode to control the solenoid valves (Huabai et al., 1992). The old controller module will be removed and replaced with the industrial PLC and TRIAC replaced with a relay bank. Four outputs of the PLC of +12 VDC power is sourced from a dual Voltage regulated high current power supply to operate a relay bank, see Figure 41.

Relay Bank for the PLC output loads

Figure 50 shows an 8-way relay bank designed to operate the solenoid valves. A 220 VAC is connected across the solenoid valve (S) through the Solid State Relay (SSR) contacts to operate it using the Soft Comfort V8.0 of LOGO! Siemens software. A compressed-air pump the sample capsule in and out of the reactor per the objective of the project. A +12 VDC from the output of the PLC Q1 (Figure 51) is connected to operate a SSR1 (Figure 50) for a 220 VAC to be connected across compressor contactor coil to be energized and start the compressor. The output Q2 of the PLC controls the SSR2 and SS3 to operate the solenoid valves S_1 and S_3 , and pumped the sample capsule into the reactor for irradiation. For experimental purposes, five energy saving bulbs at 220 VAC are used to represent the solenoid valves and the compressor contact coil. A timer provided by the software is used to control the period of sample irradiation in the reactor and out of the reactor. SSR4 and SSR5 and S_2 and S_4 respectively operate when +12 VDC from Q3 of the PLC is connected, the capsule in the irradiation site is pumped out of the reactor after the set period of irradiation. Q4 connects directly to an irradiation flash light and buzzer.

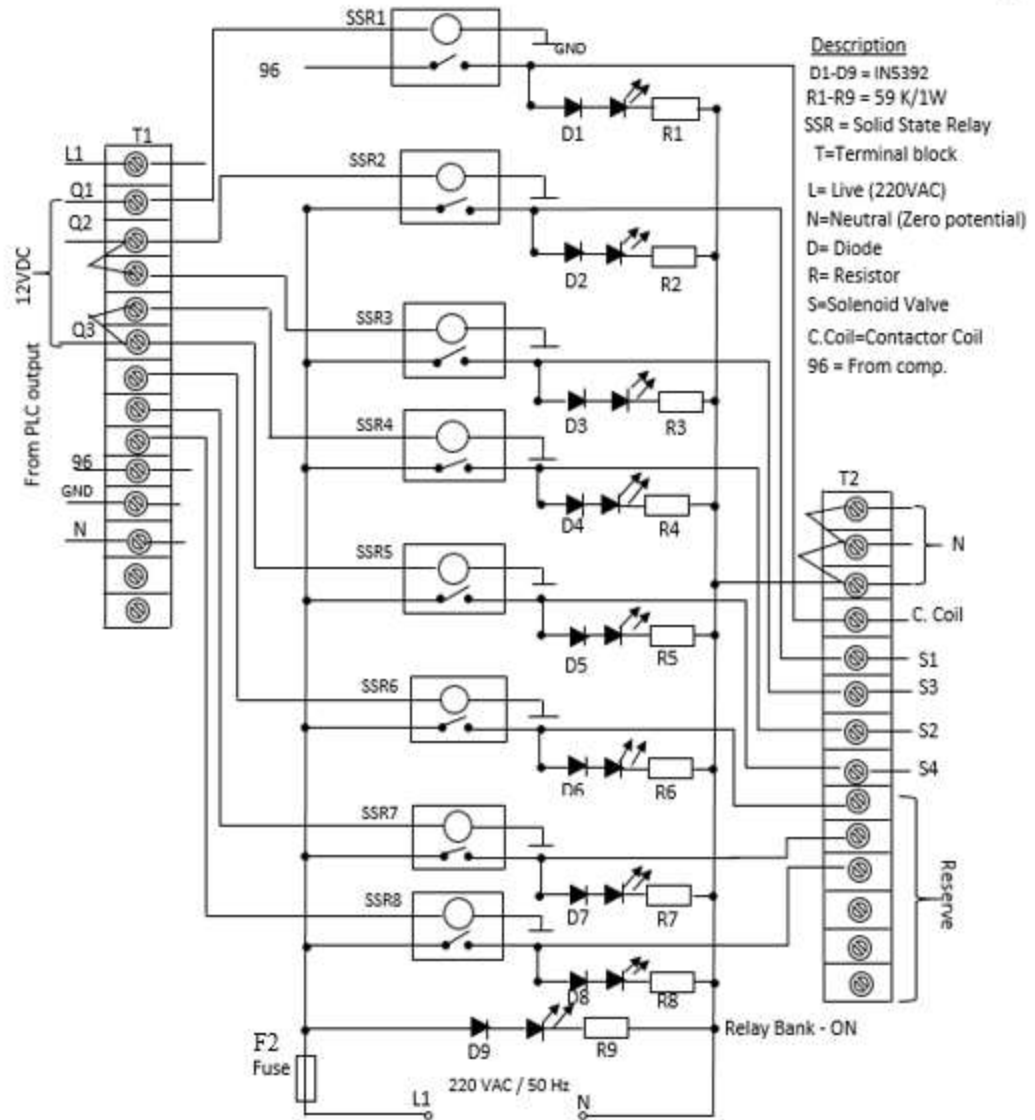


Figure 50: Eight (8)-way relay bank.

CNA A operational mode

In the CNA A mode, the detector is moved in close proximity to the sample capsule transfer room, about 15 meters from the sample irradiation site. The polyethylene pipes that connect the capsule out (receiving lead chamber) will be removed and replaced with different polyethylene pipes to the detector. The pipe is arranged such that the counting geometry of the detector is obtained. The PLC is programmed to facilitate the process of repeating the cycles of the capsule

from the reactor irradiation site to the detector and back using a timer provided by the PLC software, see Figure 51

Function block diagrams (FBD) programming language

CNA mode program designed

The working principle of the cyclic mode activation program is shown in Figure 51 and operates as follows: the PLC software program is designed to control the air compressor during sample irradiation through a timer B018. When a momentary switch I_1 start-button is pressed, timers B018 and B008 will start working per the preset time allotted to the timers. The timer B008 has a special function of ensuring that the operating pressure of the air compressor is built-up to 0.6 MPa, after which the sample-in start-button could be operated. The air-compressor contactor coil Q_1 is energized by a 220 VAC, enabling a 3-phase 415 VAC to be connected across the compressor motor, see Figure 38. The timer B018 starts to count as per the pre-set value and stops when irradiation period is over. The momentary button I_2 could be pressed to interrupt the operation when a problem is detected and resets later to resume operation.

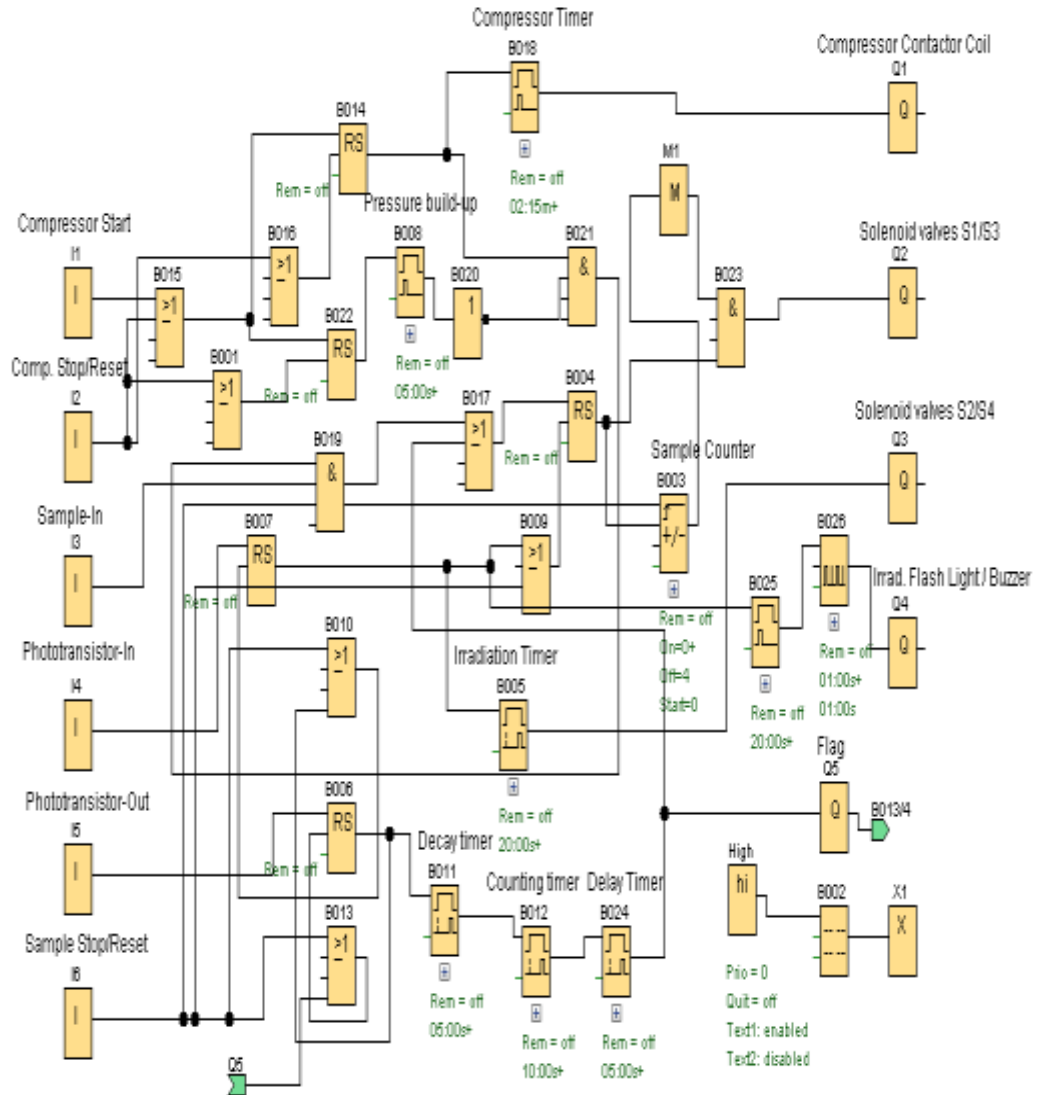


Figure 51: The designed cyclic mode activation program.

The cyclic mode operation works when a start-up-button I₃ (a momentary switch) is pressed, the output of an OR Gate (B017) changes from low level to high level making the output of Latch Set /Reset Gate high to activate (open) the ”Sample-in “solenoids valves S₁ and S₃ (Q₂). A sample capsule is then transferred into the reactor by a compressed-air. Sample counter (B003) records or count the number of sample capsule transferred per cycles of irradiation respectively. When the sample capsule passes by the phototransistor I₄ on top of the reactor, a

positive signal is sent to an irradiation timer (B005) to start counting as per the pre-set value. The timer gives out a positive pulse signal to control the sample-out solenoid valves S_2 and S_4 (Q3) to open for the compressed-air to transfer the irradiated capsule out of the reactor to a HPGe detector for analysis when the irradiation time reaches the pre-set value. The capsule passed by the sample-out phototransistor I_5 sending a positive signal to a decay timer (B011) for the sample in the capsule to decay before counting starts on the detector per the settings. A counting timer (B012) starts as the counting begins. After the pre-set value for counting, a positive pulse signal is sent to a delay timer (B024) to wait for a period before the capsule is sent back to the reactor to repeat the process.

Thus, the sample capsule is irradiated for a short period of time, and after a delay period from the end of irradiation, the radiation emitted is counted for a short period of time, then the sample is irradiated again and the entire process is repeated for a number of cycles. The cycle is set per the sample counter, i.e., the counter is set at four (4) for three (3) cycles of sample irradiation.

The conventional NAA system as shown in Figure 52 has the same operation as the cyclic, the only difference is that the sample cycle is not repeated. It is one-shot process of operation.

Conventional mode program design

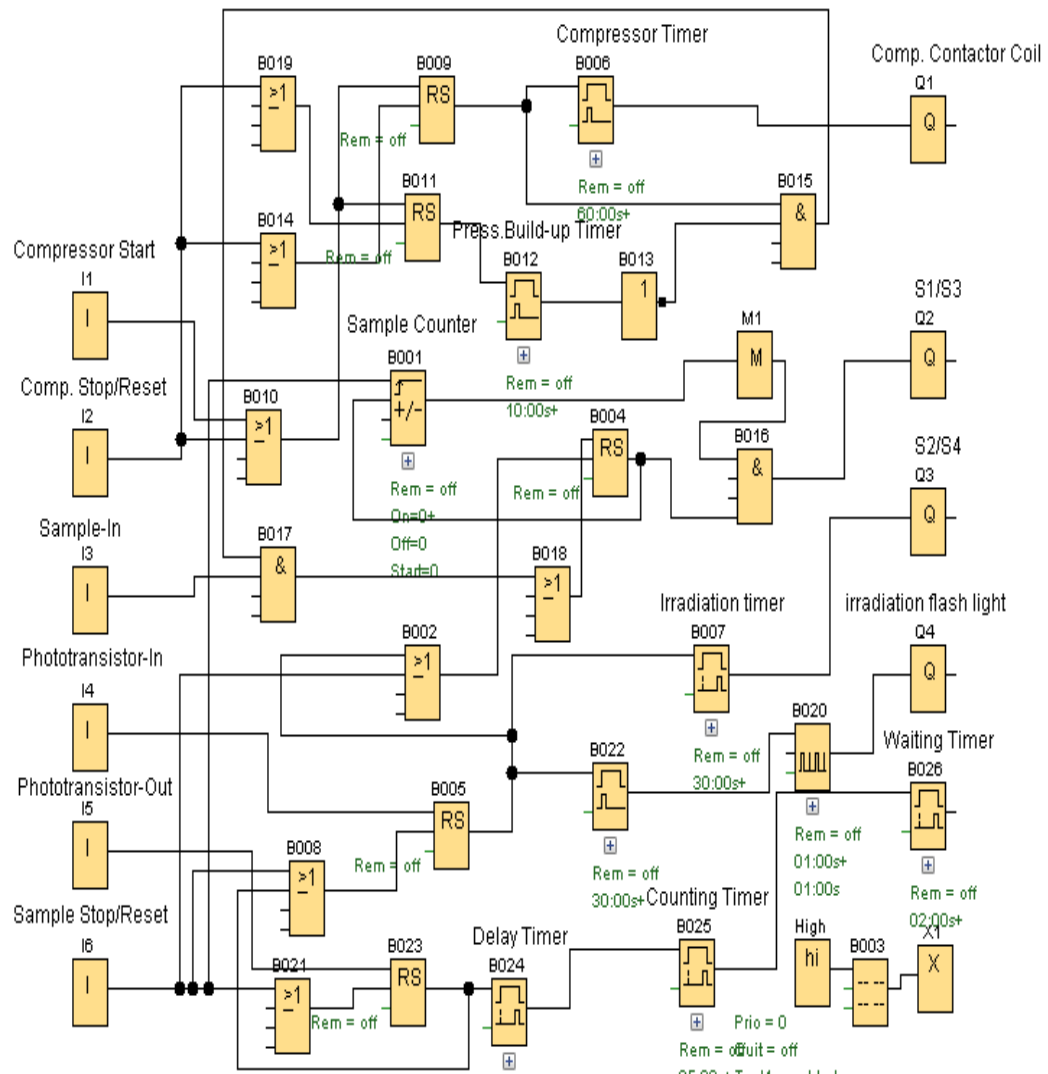


Figure 52: Designed conventional mode activation program.

The irradiation timer B007 starts to count down as per the pre-set value and stops when irradiation period is over. The flash light flashes while the buzzer beeps when the irradiation is in progress. The momentary button I₂ could be pressed to interrupt the operation when a problem is detected and reset later to resume operation. The delay timer B024 (td), counting timer B025 (ti) and waiting timer B026 (tw) come into play when the phototransistor-out on top of the HPGe detector detects the sample.

Common-emitter phototransistor circuit designed

Figure 53 shows a common-emitter phototransistor circuit.

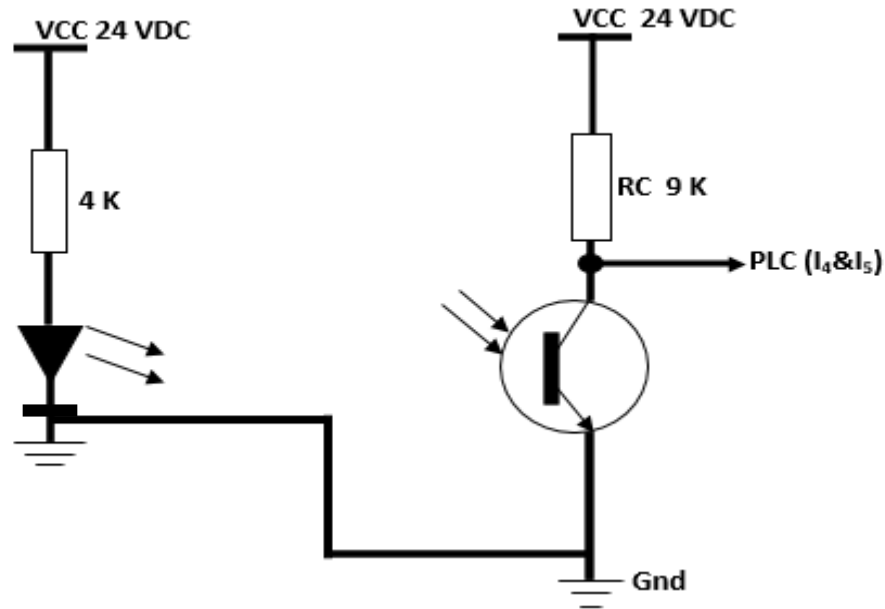


Figure 53: Common-emitter Phototransistor circuit.

Two phototransistors (sensors) are fixed at an appropriate location on top of the reactor and the detector respectively to register the presence of the sample capsule and activate a timer. The phototransistor generally has an exposed base that amplifies the light that it comes in contact with. This causes a relatively high current to pass through the phototransistor. As the current spreads from the base to the emitter, the current is concentrated and converted into voltage.

The collector is taken to the supply voltage of +24 VDC via a collector load resistor (RC), and the output is taken from the collector connection on the phototransistor to the PLC inputs I₄ and I₅ respectively. The circuit generates an output that moves from a high voltage state to a low voltage state when light is detected, and moves from low voltage state to a high voltage state when the sample (dark) is detected (Electronics Notes, 2018). The circuit actually acts as

an amplifier. The current generated by the light affects the base region. This is amplified by the current gain of the transistor in the normal way. The current through a phototransistor is directly proportional to the intensity of the incident light. A light-emitting diode (LED) is connected to a +24 VDC voltage supply through a 4 kilo ohms resistor and produces light to operate the phototransistor.

There's another important consideration for phototransistors which does not apply to photodiodes: they can be used in either active mode or in switch mode. In active mode, the transistor is an analog element with a linear output that is proportional to the intensity of the light. In switch mode the transistor acts as a digital element, and is either in a cutoff (off) or a saturated (on) state. For a given light source illumination level, the output of a phototransistor is defined by the area of the exposed collector-base junction and the dc current gain of the transistor. The collector-base junction of the phototransistor functions as a photodiode generating a photocurrent which is fed into the base of the transistor section. This photocurrent (I_P) then gets amplified by the dc current gain of the transistor. For the case where no external base drive current is applied:

$$I_C = h_{FE} (I_P)$$

where:

I_C = collector current

h = DC current gain

I_P = photocurrent

Series resistor calculation for LED

Using Ohm's Law to calculate a suitable value for the resistor.

$$R = \frac{V_s - V_f}{I(mA)} \quad (4.1)$$

where V_s is the power supply voltage, V_f is the LED forward voltage or the voltage drop across the LED and I is the desire current of the LED. For the purpose of my design, I chose 5.5 mA at an operating voltage of 2 V to reduce the brightness of the LED and power $P = IV$ of the resistor to extend the life span of the LED. See Figure 54

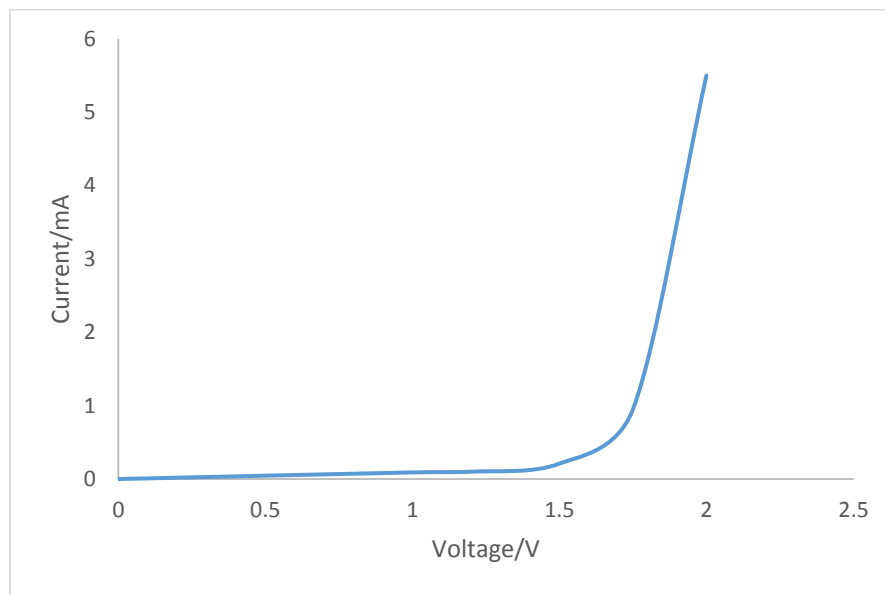


Figure 54: I-V characteristic for the LED

Phototransistor characteristics for common emitter

At the *saturation point*, the maximum possible collector current for the circuit at Figure 54 is

$$I_{C(Sat)} = \frac{V_{CC}}{R_C} \quad (4.2)$$

Where I_C is collector current, V_{CC} is the supply voltage and R_C is collector resistance. The *cutoff point* tells the maximum possible collector – emitter voltage for the circuit. The maximum possible collector- emitter voltage is 24 V, the value

of the collector supply voltage. There is internal open between the collector and the emitter by visualizing the transistor of Figure 53. Since there is no current through the collector resistor for this open condition, all the 24 V from the collector supply will appear at the collector terminal to the PLC input switch, see Figure 53. So the cutoff voltage is

$$V_{CE(\text{cut})} = V_{CC} \quad (4.3)$$

From Figure 55, the saturation collector current ($I_{C(\text{Sat})}$) is 2.7 mA.

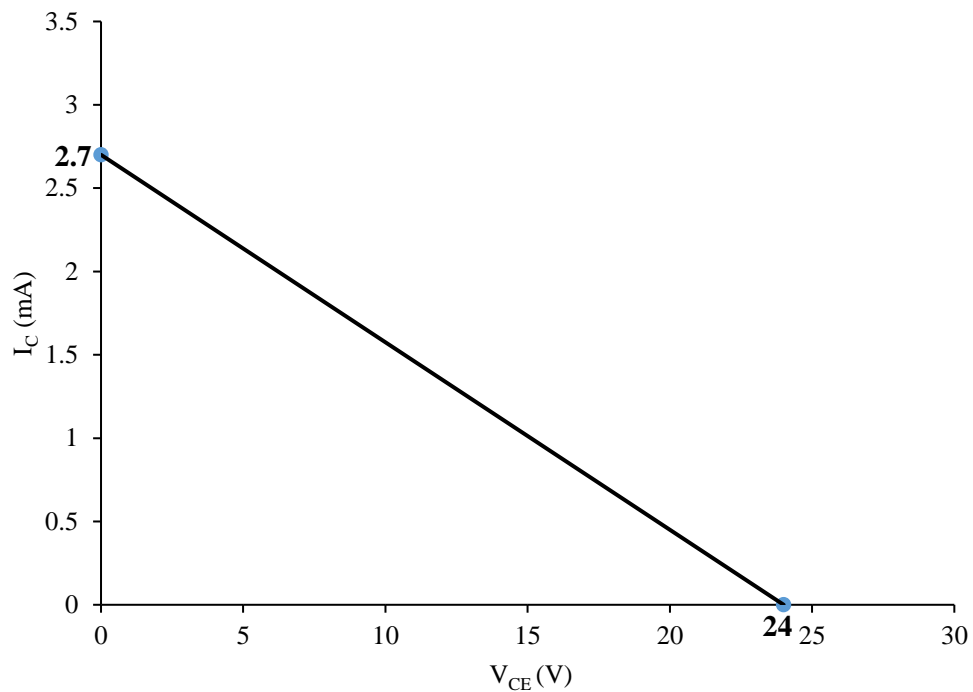


Figure 55: Load line for $I_{C(\text{Sat})} / V_{CE}$

Advantages of phototransistors include:

- (i) Higher current production than photodiodes.
- (ii) Production of a voltage, unlike photoresistors, and works with most visible or near infrared light sources including neon bulbs, fluorescent bulbs, incandescent bulbs, lasers, flames, and sunlight.

- (iii) Fast-acting with nearly instantaneous output.
- (iv) Relatively inexpensive, simple, and small.

Disadvantages of phototransistors include:

- (i) Limited voltage handling capability (silicon cannot handle over 1,000 volts)
- (ii) Electrons do not move as freely as they do in electron tubes.
- (iii) Vulnerable to electrical surges and electromagnetic energy.

Integration of various components of the controller unit

Figure 56 shows a schematic diagram of the PTS with the controller unit. The wiring starts from the dual voltage regulated high current power supply through the PLC, terminal block (T₁) to relay bank. The relay bank connects through the terminal block (T₂) and (T₃) to the solenoid valves. I₁ to I₆ are the input switches used and Q₁ to Q₃ are the outputs of the PLC used to control five (5) relays on the relay bank. Q₄ connects directly to an irradiation flash light and buzzer.

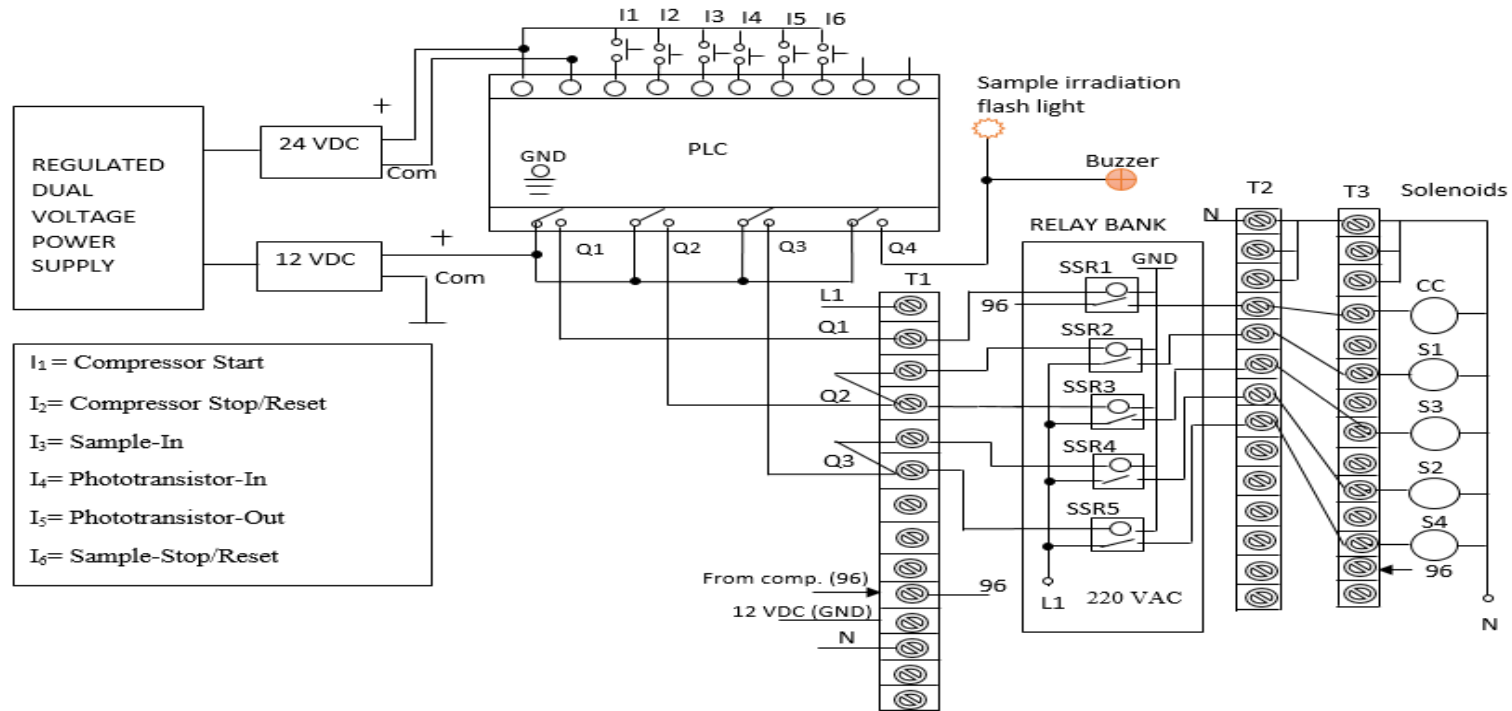


Figure 56: Schematic diagram of PTS Controller.

Controller unit casing design

AutoCAD was used to design the casing for the PTS CU. **AutoCAD** is a 2-D and 3-D computer-aided drafting software application used in architecture, construction, and manufacturing to assist in the preparation of blueprints and other engineering plans. Figures 57 and 58 show the side view one (1) and side view two (2) of the PTS CU. The casing have the following dimensions: the length is 33.2 cm and the height 17.19 cm. Figures 59 and 60 show the front and the back views respectively. The front view is made up of main supply voltage meter, DC power supply points and switches, interface slot, control switches, indication lights, irradiation flash light, fuse point and main switch. The back view is made up of a cable slot, cable connector, 220 VAC points, 13 Amps socket outlet and power cable slot. Figure 61 is the top cover which carries the PLC.

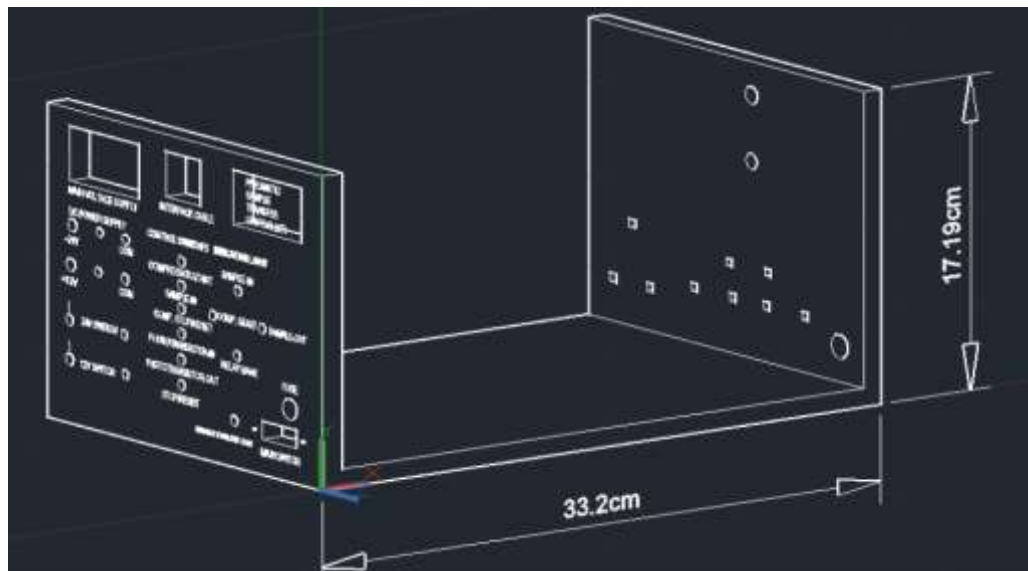


Figure 57: Side view 1 of the PTS PLC controller casing.

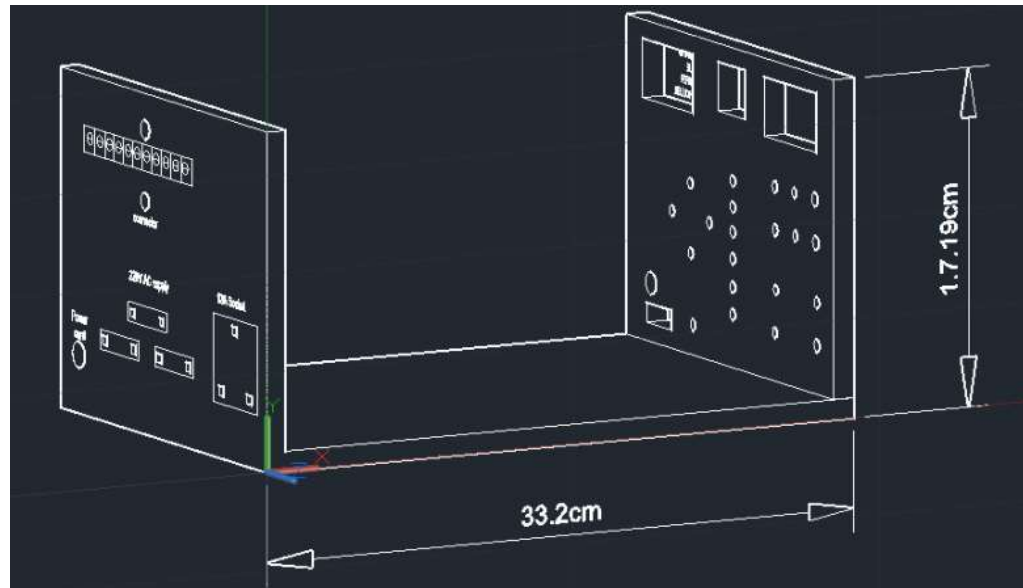


Figure 58: Side view 2 of the PTS PLC controller casing.

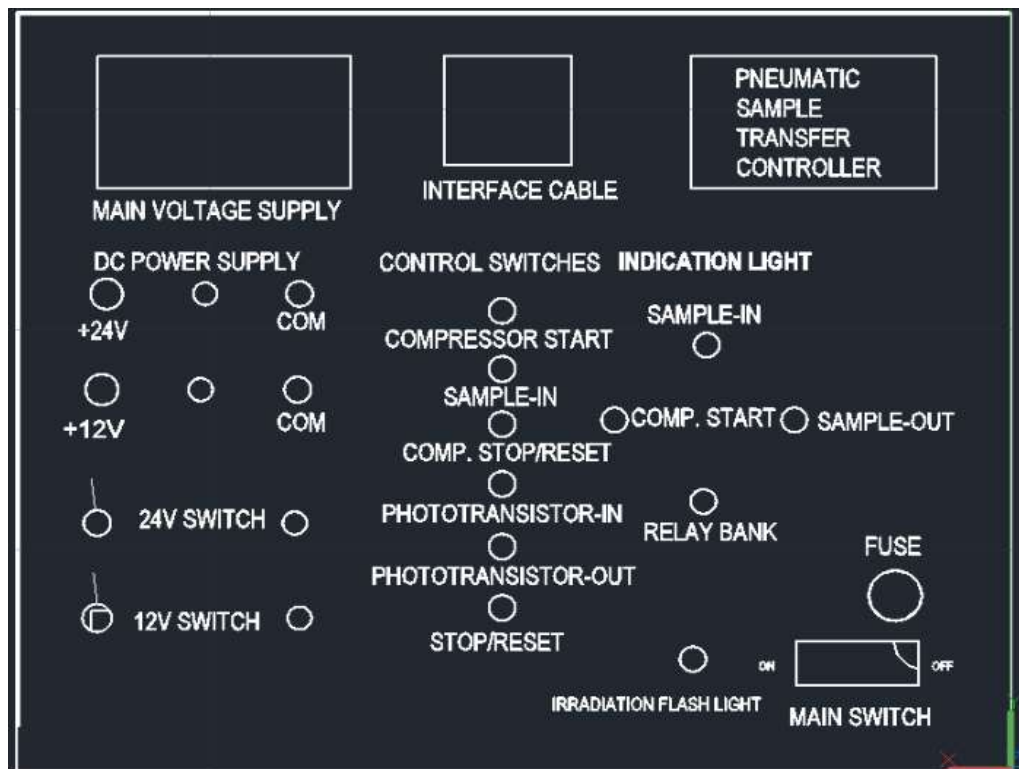


Figure 59: The front view of the PTS PLC controller casing.

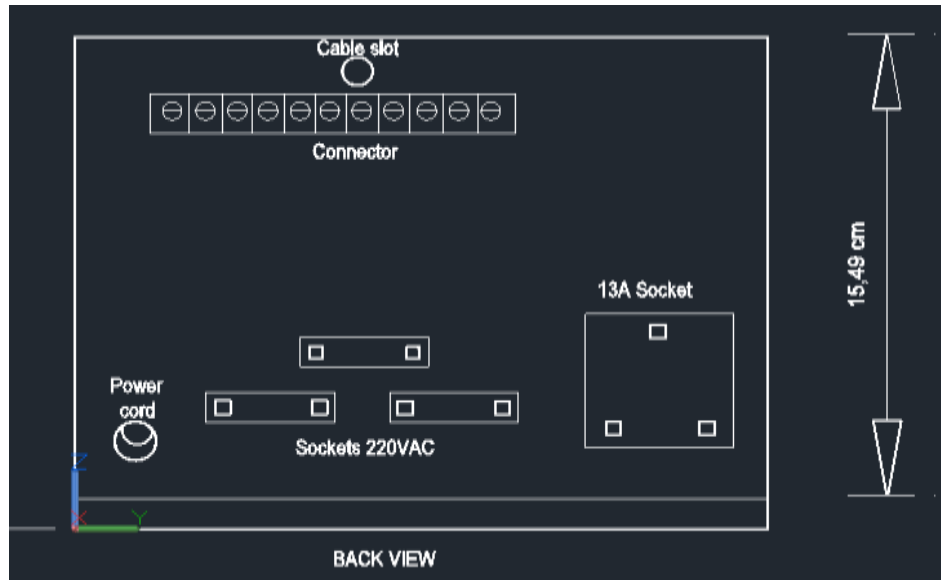


Figure 60: Back view of the PTS PLC controller casing.

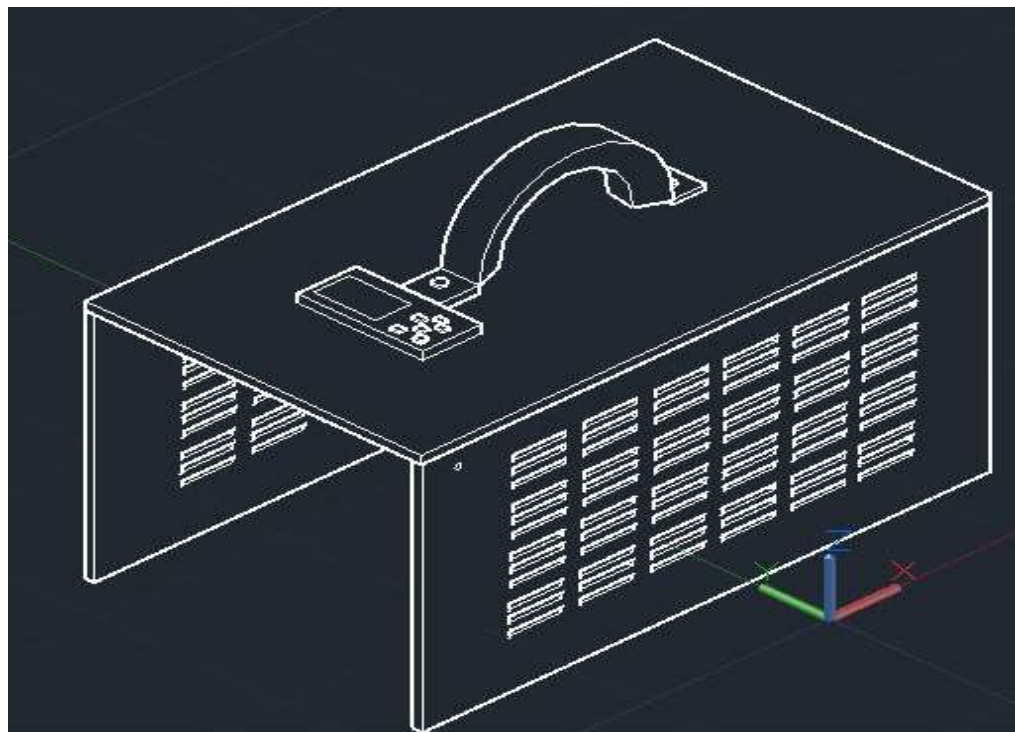


Figure 61: Top cover of the PTS PLC controller casing.

Construction of controller unit

The construction of the PTS controller unit is presented. Various designed circuits have been integrated to communicate effectively with each other electrically. The dual high current voltage regulated power supply, the eight (8)-way SSR bank and the programmed PLC enclosed in a well-designed casing, phototransistor sensor, control knobs and indication LEDs.

Internal features of the PTS controller unit

Figure 62 shows the construction of the PTS controller unit with its internal features. The features consist of a dual voltage regulated power supply and 8-way relay bank modules with the control knobs and indication light circuits.

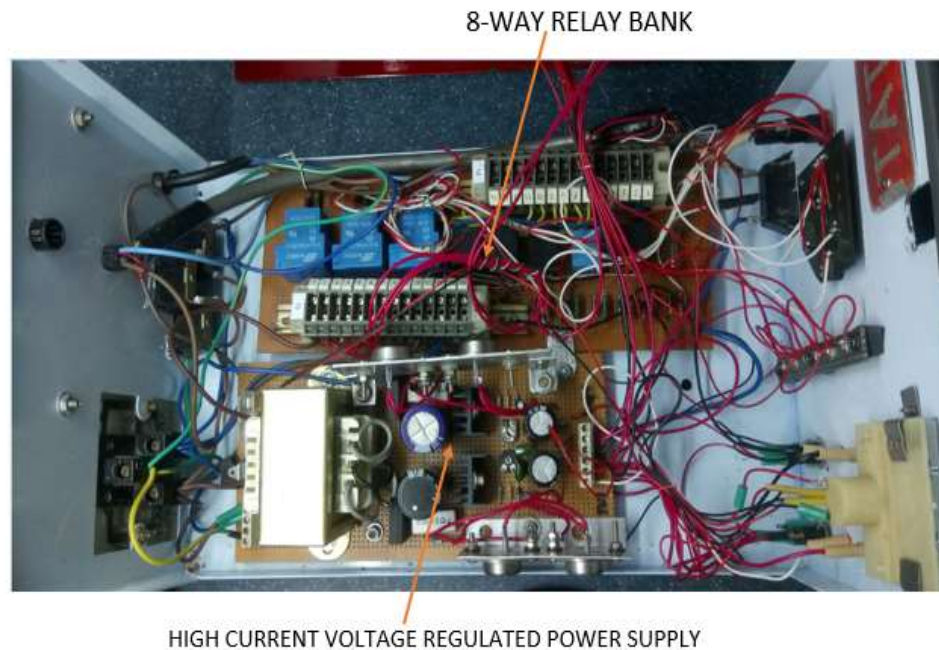


Figure 62: Constructed PTS controller unit.

Front view of the constructed PTS controller unit

Figure 63 shows the front view of the PTS controller unit. The front view comprised of the DC power supply surveillance test points, control switches and indication lights. There are six control knobs, four indication lights, Ethernet communication port, fuse, main switch, main AC voltage meter and irradiation flash light.

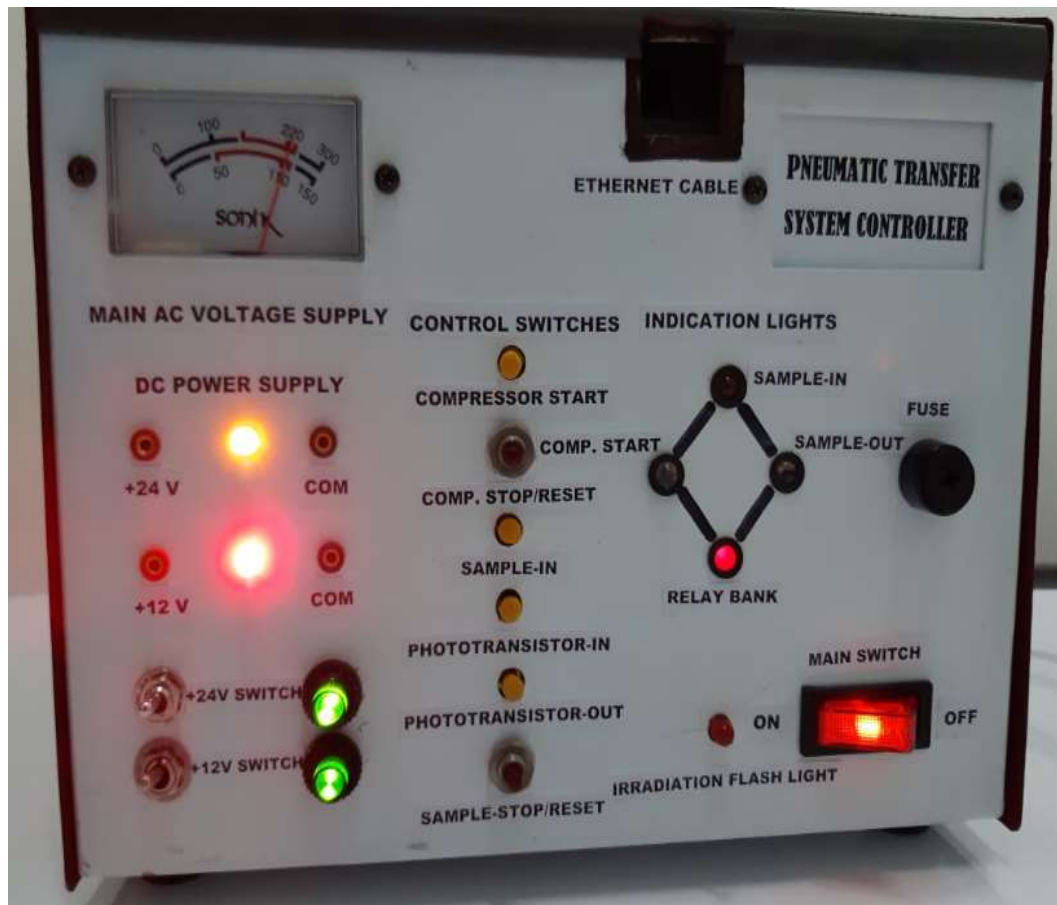


Figure 63: Front view of PTS controller unit.

Complete designed and constructed PTS Controller

Figure 64 shows the PTS controller unit with the Siemens LOGO PLC.



Figure 64: Designed and constructed PTS controller.

PTS controller with bulbs for simulation

Figure 65 shows the PTS controller unit with six bulbs representing the compressor and the solenoid valves for simulation



Figure 65: PTS controller with bulbs to simulate the solenoid valves.

Phototransistor control unit

Figure 66 shows the phototransistor control unit with a sample capsule. The unit consists of a phototransistor and Light Emitting Diode (LED).

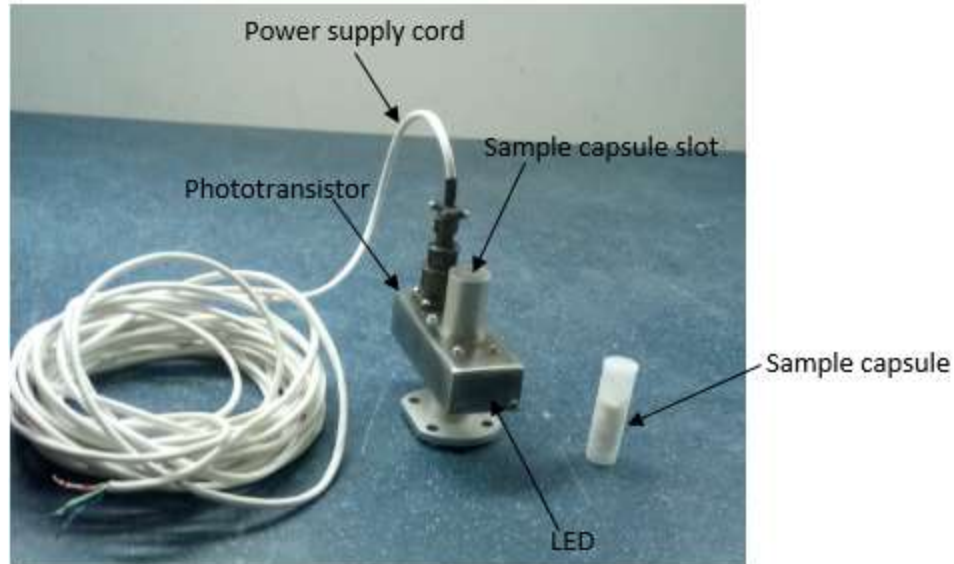


Figure 66: Phototransistor control unit with sample capsule.

Results and Discussions

The computer simulation and experimental test of the PTS controller unit help to understand the operation of the device. The results in the study have therefore been presented in terms of computer simulation and experimental test. Simply put, it demonstrates how the Function Block Diagram (FBD) programming method along with the LOGO!Soft Comfort version 8 software to control opening and closing of the solenoid valves for the CNAA and the conventional application.

Simulation of PTS controller designed program

The design consists of six inputs ($I_1 - I_6$) and four outputs ($Q_1 - Q_4$). Compressor start-button (I_1) is depressed and the compressor contactor coil energized. Timer B006 is set to keep the compressor (Q_1) running till the operation of the reactor is over, see Figure 67. Solenoid valves (S_1/S_3) are activated when a sample-IN button (I_3) is depressed. The pressure build-up timer

B012 enables the air pressure to get to the required level before the sample-IN button could be operated. The Phototransistor-IN on top of the reactor detects the sample and closes the output Q₂ of solenoid valves S₁ and S₃. The output Q₄ in Figure 68 flashes up with associated beeps from a buzzer to indicate that sample irradiation is in progress. Irradiation timer B007 starts per the preset time. The output Q₃ in Figure 69 is energized to indicate that solenoid valves S₂ and S₄ are opened and the compressed-air transferred the activated sample capsule onto the gamma detector for counting after the irradiation. Phototransistor-OUT on top of the gamma detector detect the sample and closes output Q₃ of solenoid valves S₂ and S₄. Delay timer (t_d) B024, counting timer (t_c) B025 and waiting timer (t_w) B026 start in that sequence, see Figure 70. Figure 71 shows that the irradiation cycle repeats and solenoid valves S₁ and S₃ open (second cycle). M₁ is a flag to ensure connectivity.

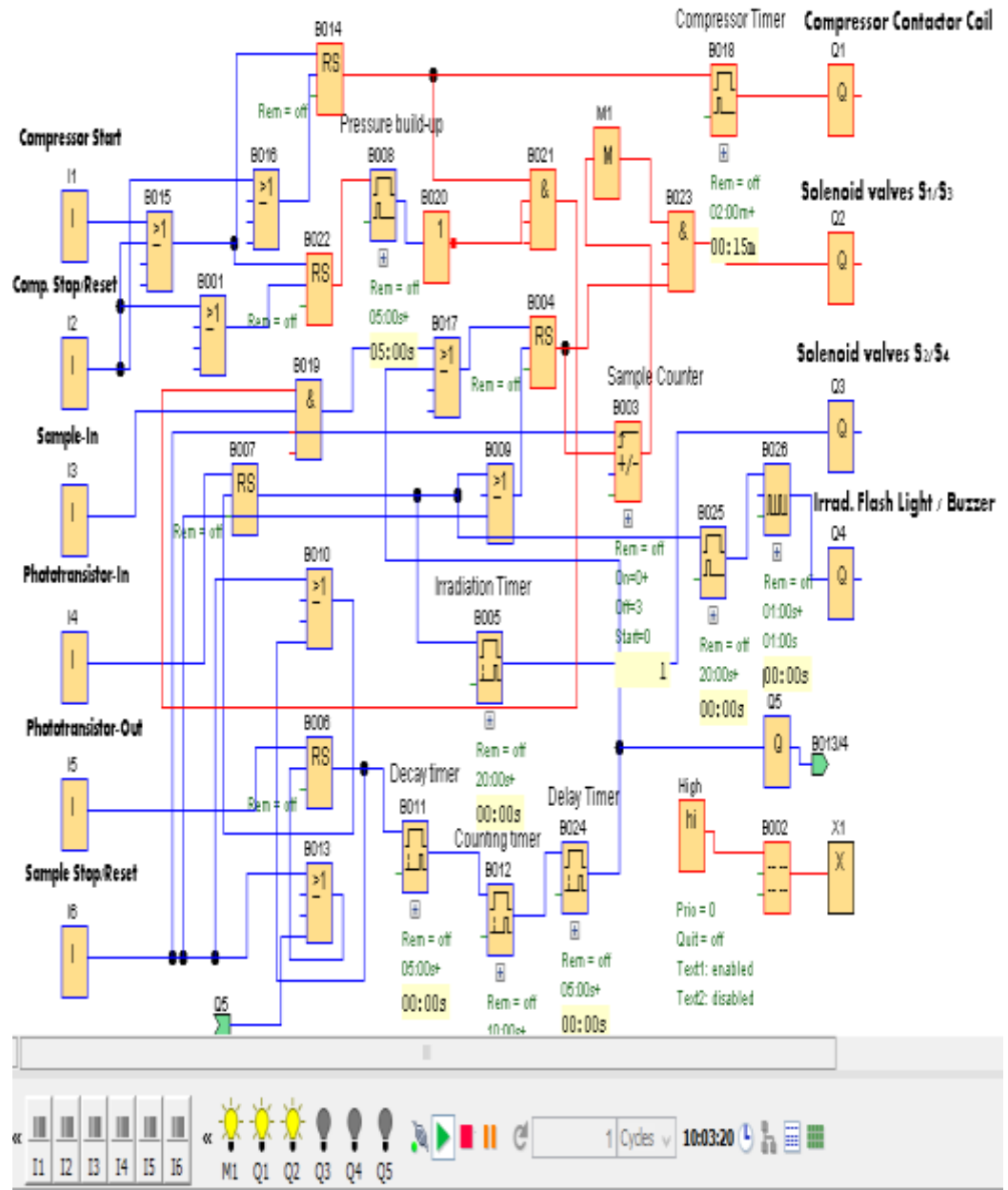


Figure 67: Compressor contactor coil and solenoid valves energized.

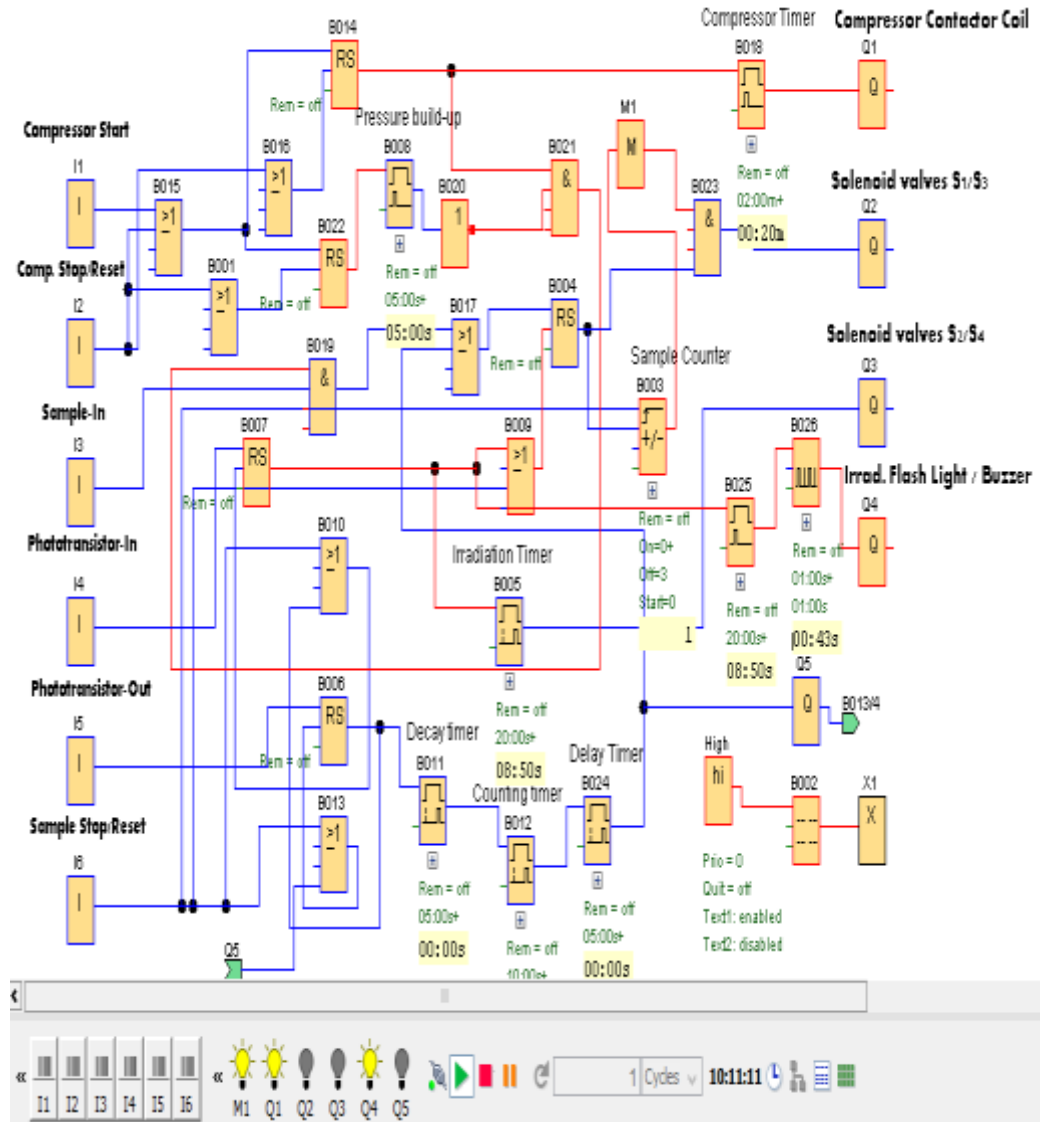


Figure 68: Irradiation process; light flashes and buzzer beeps.

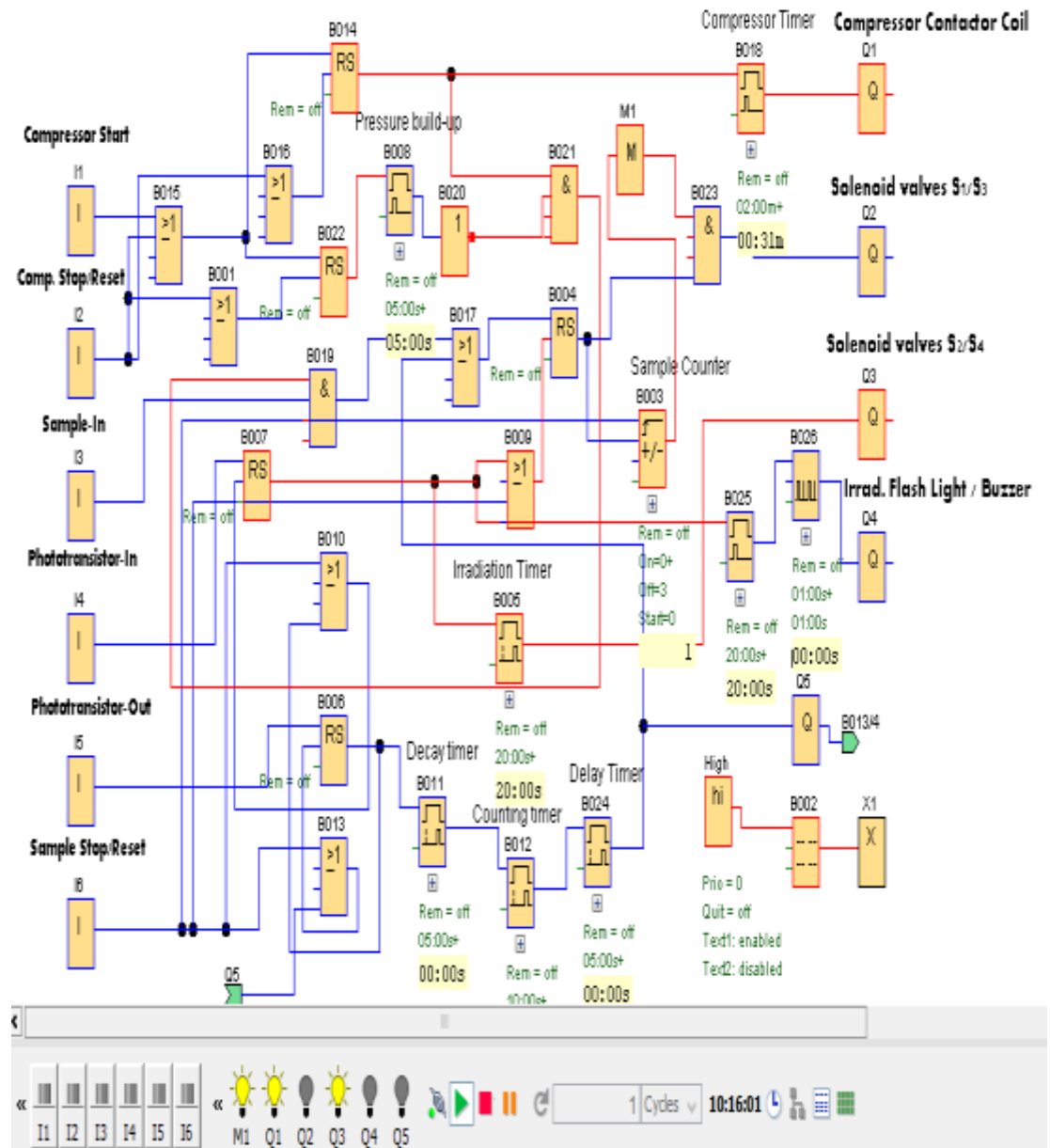


Figure 69: Solenoid valves S₂ and S₄ energized, sample out of irradiation site.

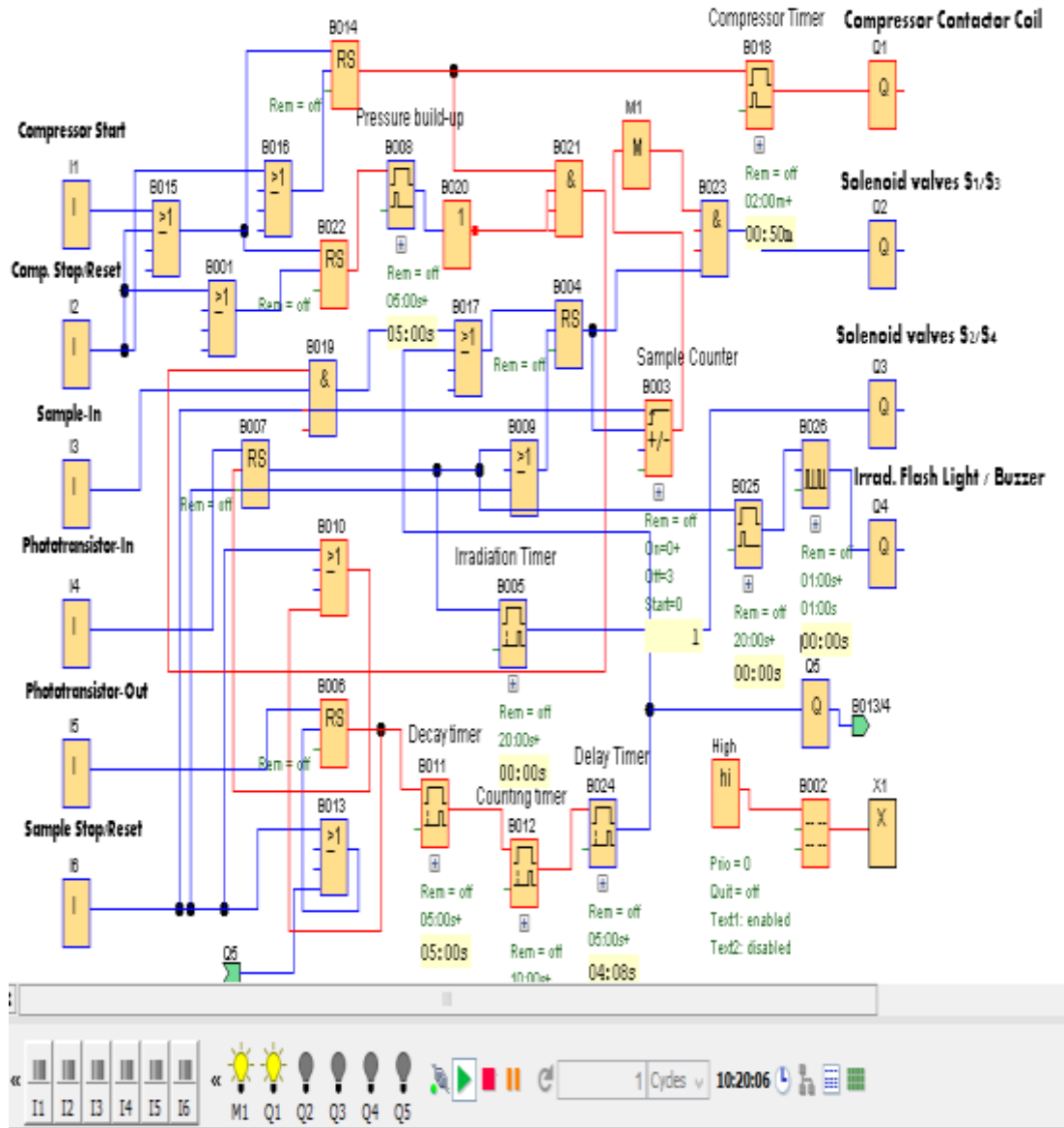


Figure 70: Counting of samples.

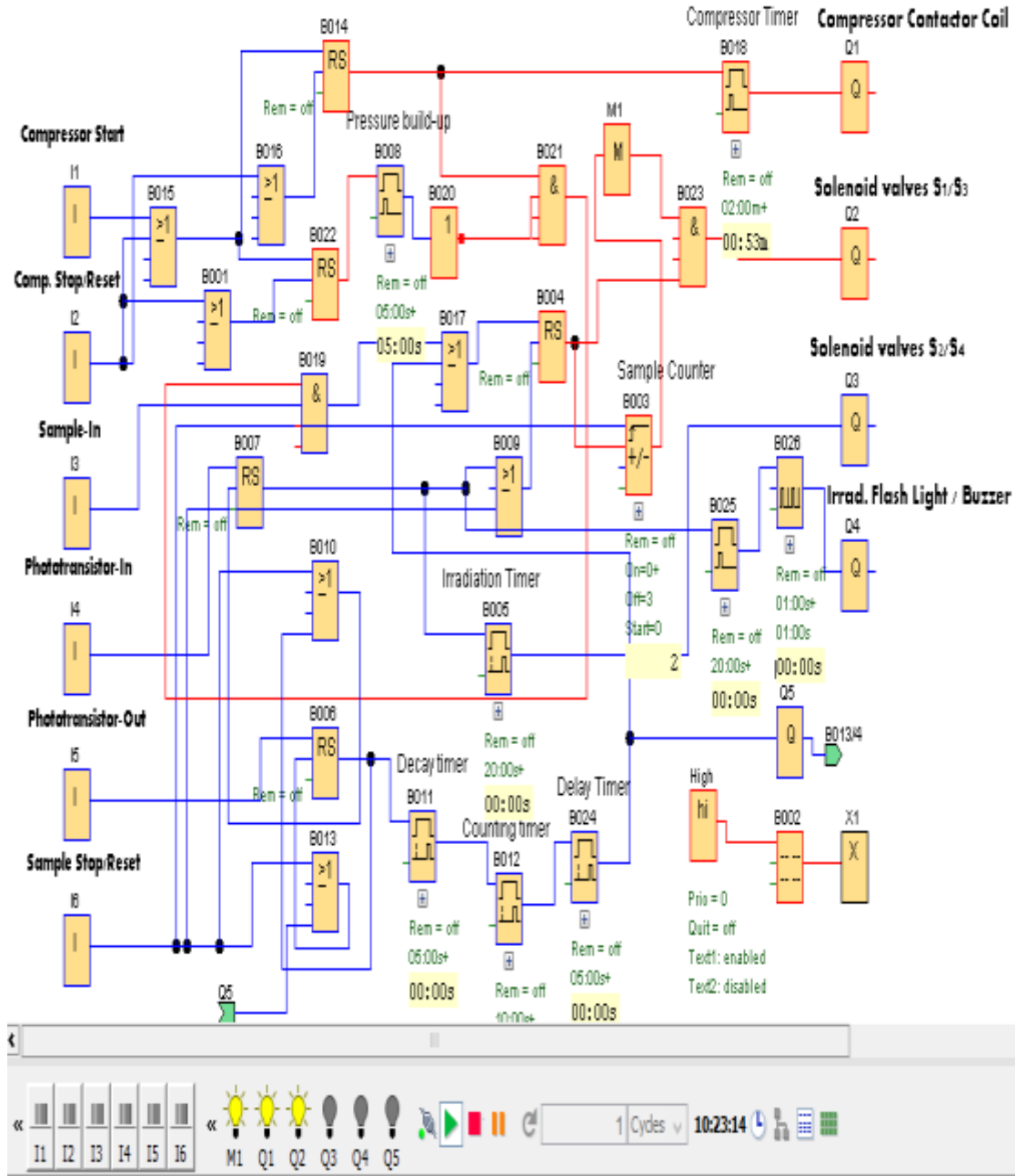


Figure 71: Irradiation cycle repeats and solenoid valves S₁ and S₃ open (Second cycle)

Experimental Test Results

The constructed PTS controller unit was plugged into a 220 VAC socket to test how the controller unit performs in relation to the objective of the study. The red LED on the controller unit shown in Figure.72, indicates that the relay bank is powered. The compressor start-button is depressed and the contactor coil bulb lights up to indicate that 220 VAC is connected across contactor coil of the compressor unit. The contactors are closed and the compressor motor received 415 VAC, 3PH supply to start the compressor unit.

The compressor – start indication light on the controller comes ON to alert the operator that the compressor is in operation. Bulbs for S_1 and S_3 of Figure. 73 light-up to indicate that the solenoid valves are opened for the compressed-air to transfer sample into the irradiation site of the reactor. The yellow LED on the controller alerts the operator that the sample is pumped into the irradiation site of the reactor. When the phototransistor detects the sample capsule either on top of the reactor or on top of the detector, it switches out +24 VDC as shown in Figure 74. When the capsule is on top of the reactor, the +24 VDC signal pulse de-activate (close) the sample-IN solenoid valves S_1 and S_3 per the PLC program software and irradiation begins. In the case of the phototransistor on top of the detector, the +24 VDC starts the counting timers.

The two bulbs are switched-OFF to indicate that the solenoid valves are closed and the sample irradiation is in progress. The irradiation red LED flashes up together with a beep from a buzzer to alert the operator that irradiation is in progress, see Figure 75. The set-up in Figure. 76, illustrates the sample capsule

out of the reach of the phototransistor detection. The phototransistor outputs 0.00 VDC, because the LED is direct on the phototransistor base. No sample is transferred through the sample capsule slot. The phototransistor does not switch, the output remains 000 volts, see Figure 77 Bulbs for S₂ and S₄ of Figure. 78 are 'ON' to indicate that sample-out solenoid valves are opened to transfer the irradiation sample onto the High Purity Germanium (HPGe) detector for counting. The green LED on the controller alerts the operator that the irradiated sample is transferred from the reactor onto the detector. Bulbs for S₁ and S₃ of Figure. 79 are 'ON' to show the repetition of the irradiation cycle. The compressor bulb will go 'OFF' only when the irradiation is over as per the program of the PLC.

Compressor contactor coil energized



Figure 72: Contactor coil energized, compressor starts.

Sample-IN solenoid valves open, bulbs “ON”



Figure 73: SAMPLE-IN button depressed, Solenoid valves S₁ and S₃ open.

Sample – IN phototransistor switched

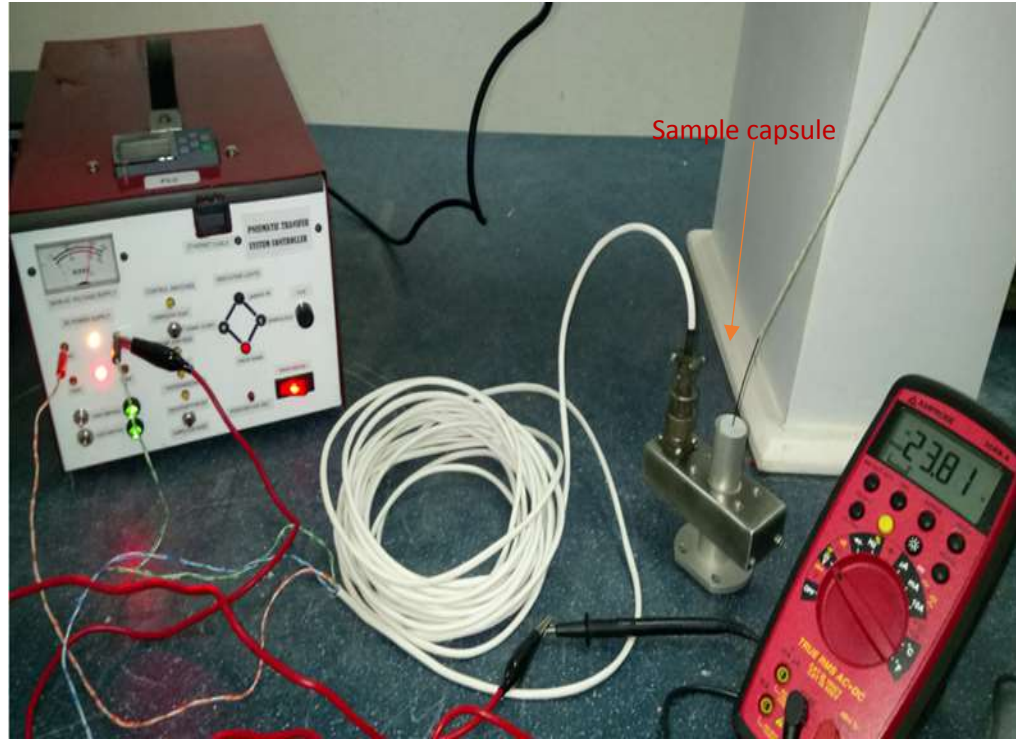


Figure 74: Phototransistor detects sample capsule, output +24 VDC.

Sample-IN bulbs go “OFF”, irradiation starts



Figure 75: Solenoid valves S₁ and S₃ close; sample irradiation starts with flash light / beeps of buzzer.

Sample capsule is out of phototransistor detection limit



Figure 76: Sample capsule moved out the reach of phototransistor

Illumination intensity of LED in sample capsule slot



Figure77: Illumination of LED in the sample slot.

Irradiated sample transferred onto detector for counting



Figure 78: Irradiated sample transferred to detector.

Irradiation cycle repeat, Sample-IN bulbs “ON”



Figure 79: Irradiation cycle is repeated.

Web server support for remote access

LOGO! 0BA8 has a built-in Web server which enables one to operate the LOGO! Base Module from a traditional PC or a mobile device. In this approach, one can access the LOGO! Base Module using a connected device (conventional

PC, tablet or smart phone with Web browsing capabilities) through its IP address. To logon to the web server; refer to page 34. Once logged in, the LOGO! Web server displays all the system information of the LOGO! Base Module including module generation, module type, firmware version and IP address. With regards to network security risk and hacker attacks, refer to page 35.

Unshielded Twisted – Pair (UTP), Registered Jack (RJ-45) with 10/100 Mbit/s speed was used as an interface cable to communicate between the web server and the PLC through the Ethernet communication port. To Log on to the network, go to google and enter the IP address on your computer or mobile phone as shown in Figure 80. The LOGO IP address and the server should be the same (192.168.0.1) after enabling the Transmission Control Protocol (TCP) 8080 from your Local Area Network (LAN). From Figure 83, the text message set in the LOGO! soft comfort software program (using Function Block Diagram programming language) appeared on the screen. The compressor is switched-on by the PLC to operate per the preset time for irradiation. Time is allotted for the build-up of the compressed-air after which the solenoids are activated to open for the sample capsule to be transferred into the irradiation site of the reactor, see Figure 84. Irradiation light flashes to alert the operator that irradiation is in progress, see Figure 83 After the irradiation, the solenoid-OUT valves open and the sample capsule is transferred onto an HPGe detector for analysis, see Figure 86. The sample counter in the program count two (2) to indicate second cycle of the irradiation process, see Figure 85. Figures 86 and 87 are mobile phone monitoring.



Figure 80: Log on to display the information to be monitored.

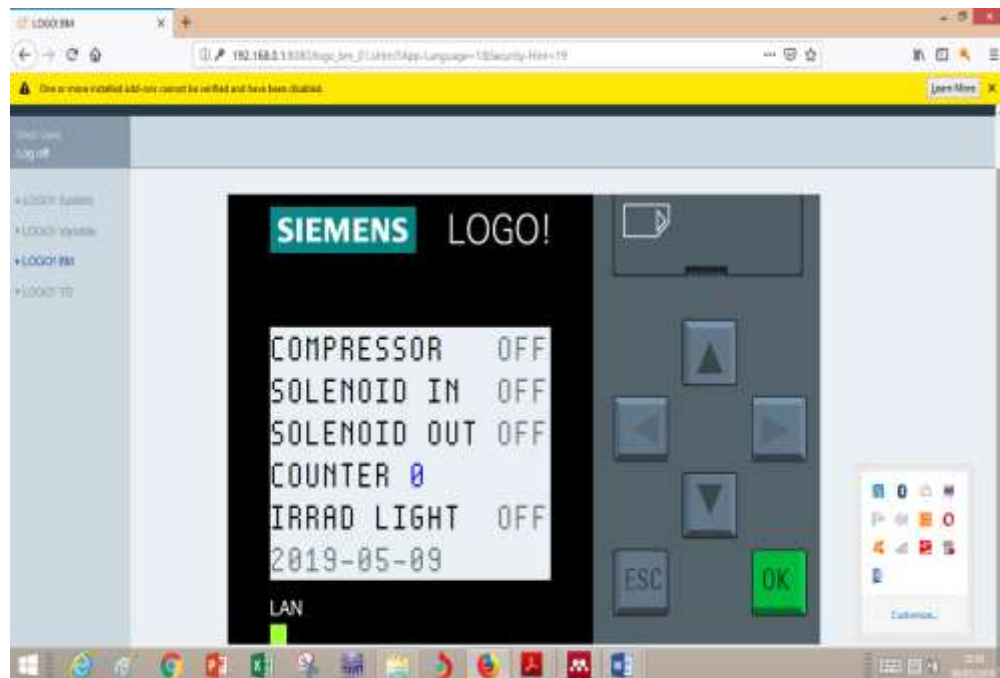


Figure 81 The PTS control unit not in operation.

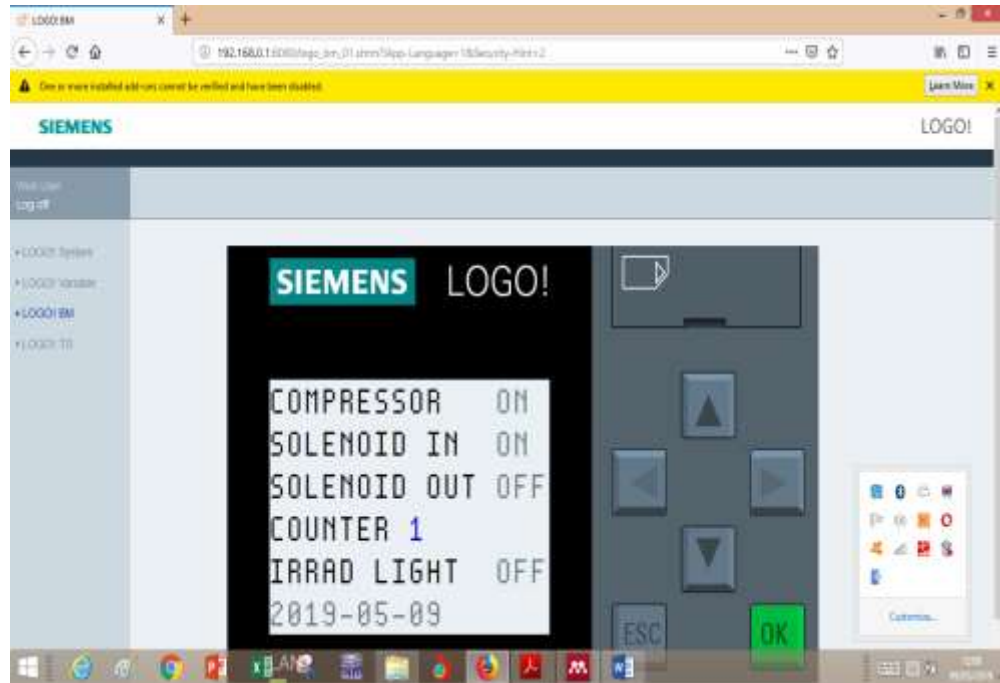


Figure 82: Air-compressor and solenoid-IN buttons depressed, compressor ON and solenoid-IN opened.

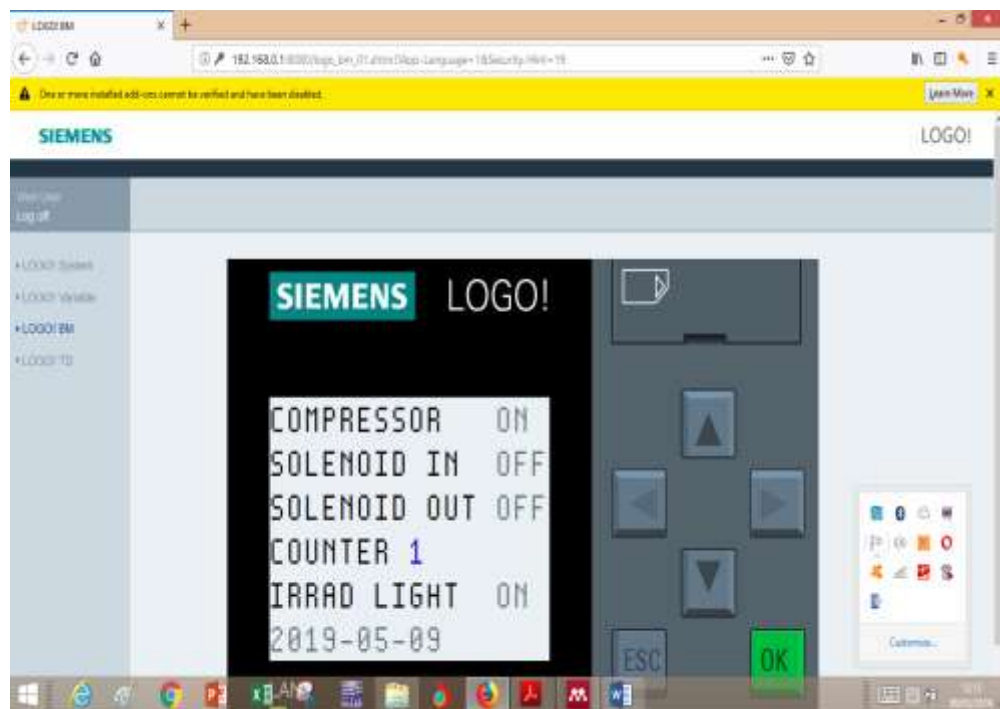


Figure 83: Irradiation flash light ON, sample irradiation in progress.

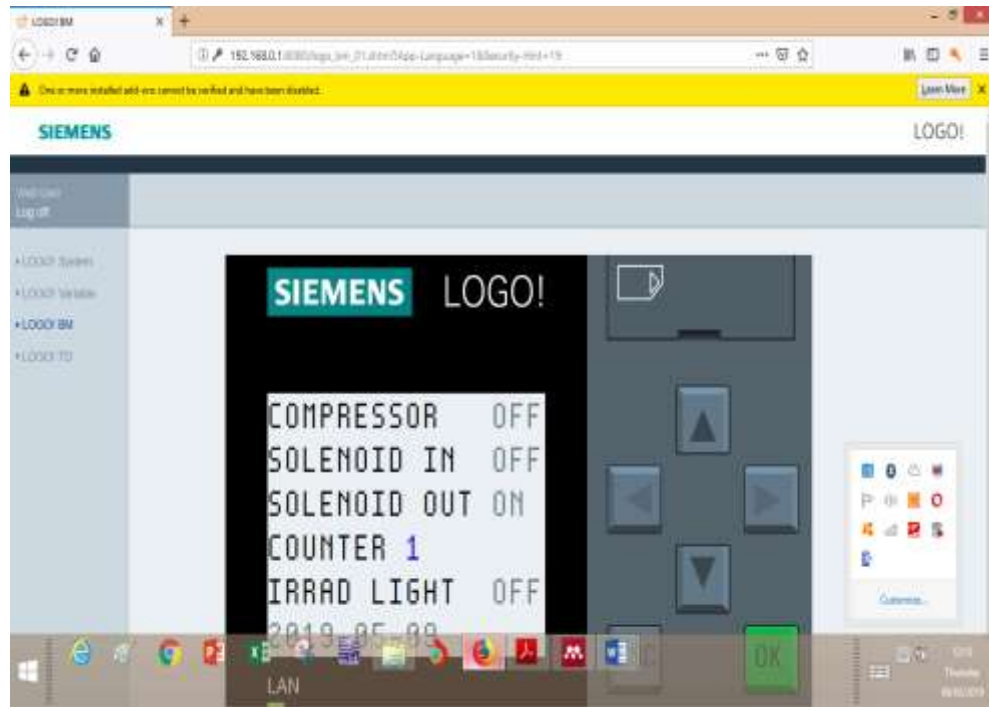


Figure 84: Solenoid – OUT opened, sample capsule out of irradiation site.

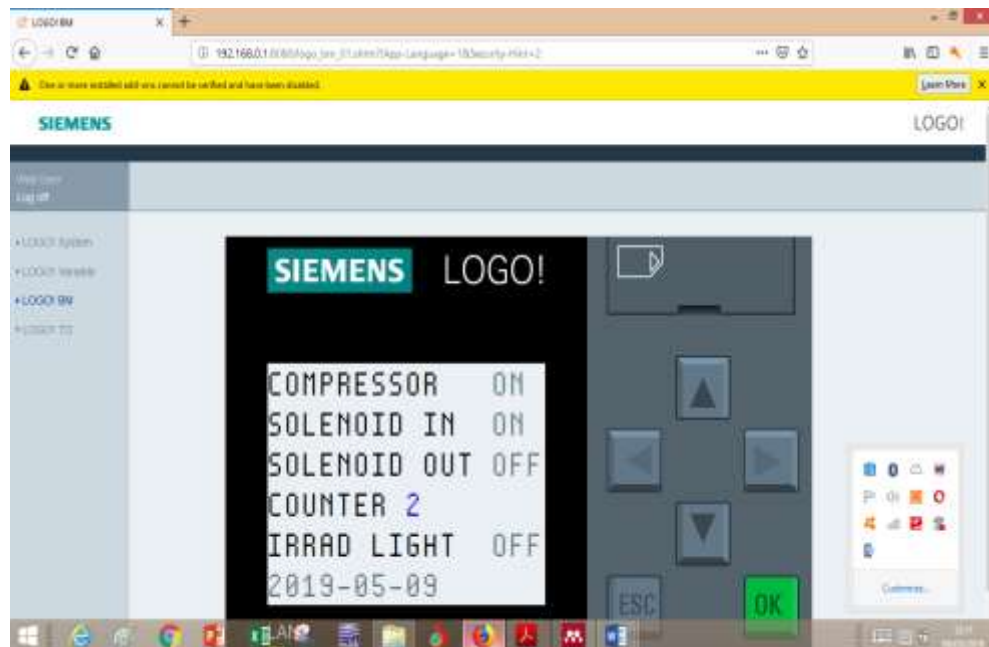


Figure 85: Irradiation cycle repeated, counter recorded the two samples for the cycles.



Figure 86: Air-compressor and solenoid-IN buttons depressed, compressor ON and solenoid-IN opened (monitored from mobile phone).



Figure 87: Irradiation cycle repeated, counter recorded the two samples for the cycles (monitored from mobile phone).

AnyDesk Remote Desktop Software

AnyDesk is software that allows computers to be remotely controlled. Common applications scenarios include a network administrator who wants to manage one or several computers from his / her own computer in order to install updates or adjust system settings, or an employee who would like to access his / her work computer at the office from home. To monitor or control, two computers are needed; the host and a client computers. A client computer that does the controlling, such as the client's laptop, and a host computer that could be

controlled using the client's PC. After the download is complete, run the program file on both computers (host and client) by double-clicking on it on each device. A program interface contains two central fields, (This Desk and Remote Desk) as shown in Figure 90 below for controlling computers remotely. For the client to access the host computer, the client's Any Desk ID is put in the space provided by Remote Desk of the host, see Figure 91 and click "connect" to link up the two computers. A remote control request now appears on the host computer, the monitor of the remote host computer will appear on the client's monitor (AnyDesk, 2017).



Figure 88: Your AnyDesk and Remote Desk window for connectivity

Source: (AnyDesk, 2017)

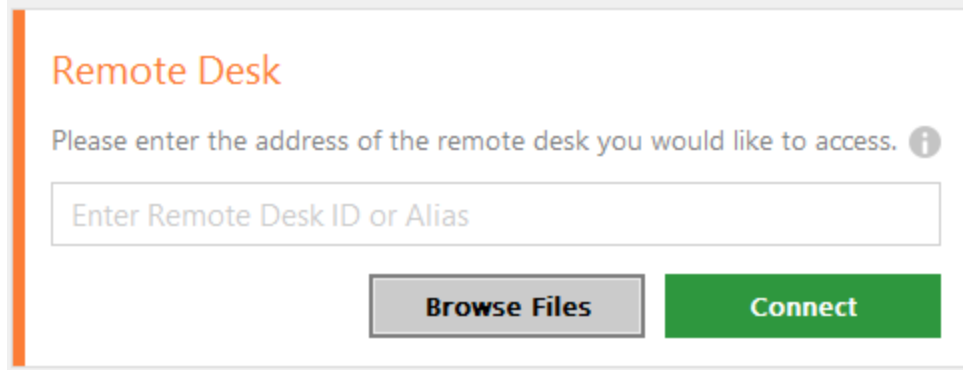


Figure 89: Window for Remote Desk ID.

Source: (AnyDesk, 2017)

The client can now control all actions on the remote host computer using the mouse and keyboard, as if he/she is right in front of the host computer. The client computer can access the host computer from anywhere in the world where there is an internet. Table 11 shows the comparison of the existing and the new PTS control units.

Table 11: Comparison of the Control Units

| New Control Unit | Existing Control Unit |
|---------------------------|-----------------------|
| Programmable | None |
| Component on local market | None |
| Cyclic | One-shot |
| Surveillance test points | None |
| Option for simulation | None |
| Mobile | None |
| Web server support | None |

Chapter Summary

The chapter provided the designed and construction of the various circuits put together to form the PTS controller, their individual functions as well as the PLC controller unit. Multisim Power Pro Edition Version 12 was used to design and simulate the power supply. The rectification efficiency of the power supply for the 24 VDC and 12 VDC were 82%. And 81.1% respectively. Multisim is the schematic capture and simulation application of National Instruments Circuit Design Suite, a suite of Electronics Design Automation (EDA) tools that assists one in carrying out the major steps in the circuit design flow. Multisim is designed for schematic entry, simulation, and exporting to downstage steps, such as PCB layout. Functional Block Diagram programming method along with the LOGO!Soft Comfort version 8 software was used to simulate and experimentally tested the controller of its validity.

The results of the designed and constructed controller unit of PTS to facilitate a cyclic and conventional modes using PLC was found to be measured up to the objective of the study.

CHAPTER FIVE

SUMMARY, CONCLUSIONS AND RECOMMENDATIONS

Overview

The focused of the thesis was on the design and construction of a controller unit for GHARR-1 PTS; using computer based PLC to aid CNAAs application. The controller is to ensure that samples are irradiated, decayed, counted, then irradiated again, and this process is repeated for a number of cycles, the spectra from each counting being summed to give a final total spectrum. The cycle period T is then given by Equation: $T = t_i + t_d + t_c + t_w$, where t_i is the time of irradiation, t_d is the delay or decay time, i.e. the time between the end of irradiation and the start of counting, which is usually the time required to transfer the sample from the irradiation position to the counting station, or to transfer the irradiation source to the sample station, t_c is the counting time, and t_w is the waiting time, i.e. the time between the end of counting and the start of irradiation.

The designed controller unit was programmed such that the pressure of the compressed-air is built-up to the required MPa before a sample could be transferred into the reactor for irradiation. The PLC LOGO! Comfort software version 8 was used together with the FBD programming language method to control the solenoid valves through the designed relay bank. The dual regulated voltage power supply (+24/+12 VDC) was designed and built to operate the PLC and a relay bank which was also designed and built to facilitate the switching of the solenoid valves.

A web support system was incorporated for the Reactor Facility Manager to monitor the operation of PTS remotely from his / her PC or cell phone. For the purpose of monitoring and to count the number of cycles a sample is repeated, a counter was incorporated in the design. The existing PTS was partially modified for the purpose of the CNAA application, see Figure 12. The phototransistor on the receiving chamber was relocated to the detector unit. This arrangement will help to reduce greatly the dose exposure to the operator in case of the conventional NAA, by transferring the activated sample capsule directly from the irradiation site onto the detector for counting.

FMEA study was finally conducted on the control unit to achieve the following:

Identify known and potential failure modes,

Identify causes and effects of each failure mode,

Prioritize the identified failure modes according to the Risk Priority Number (RPN). Frequency of occurrence, severity and detection, and

Provide for problem follow-up and corrective action.

Summary

PTS control interface to facilitate CNAA application in GHARR-1 and further eliminate the difficulty in getting old electronic components for maintenance of the PTS, has been successfully designed and constructed. The controller designed and constructed was simulated using 220 AC volts electric bulbs to represent the solenoid valves and momentary switches for the phototransistors. The phototransistors detect the samples, send positive signal to trigger a timer for irradiation and counting.

Cyclic mode of operation is achieved by the LOGO! Comfort software V8 which provided timers, counters, momentary switches and other logic parameters to control the sample movement. The 8-way relay bank designed and built which serves as an interface between the PLC and the solenoid valves to control the opening and closing of the valves as programmed worked perfectly. The PLC worked as customized per the program to transferred sample per the input action, to control the output. The output voltages of the high voltage were stable to operate the output loads due to the high current of the transistors incorporated into the circuit.

The Web support enables the Reactor Manager to monitor the operation of the PTS facility, and to have an idea of samples irradiated in his / her absence through the simulation and the AnyDesk software support, see Figures 80, 81, 82, through to 87.

Conclusions

Based on the findings of the study, it has proven that the computer based PLC control unit for PTS is capable of facilitating both cyclic and conventional NAA application for GHARR-1 per the simulation results. This approach would ensure the facility's maintainability in the future since the components used were purchased locally on the Ghanaian market and are available for replacement in the case of damage or malfunction.

FMEA conducted for the conceptual CU design to be possibly integrated with the existing PTS has provided recommended actions to be incorporated into the design if the need arise. It is expected that when the recommended actions are

implemented, the RPN will reduce to a significant level to facilitate successful implementation of the modification.

In general, the implementation of the CU in an existing PTS is not expected to pose any significant risks in view of the outlined compensation actions and recommended actions. The study would serve as a valuable tool for subsequent analysis to be conducted in the future. The compensation actions analysis have brought up the idea of incorporating additional components to enhance the compensation actions, like electrical circuit breaker and suppressing diodes to augment the functions of the fuse against any power surge. Per the possible failure rates, the likelihood of occurrence is between low and medium. That is unlikely / likely / possible for failure to occur.

Appendices A, B and C provide a complete maintenance procedures for the pneumatic transfer system control unit.

Recommendations

With the GHARR-1 Centre's decision to go commercial, it is appropriate and proper to adopt and implement the computer based PLC control unit locally designed and built to ensure continuous operation to meet the demands of the customers. Implementation of CNAA at GHARR-1 to expand analytical capabilities.

The findings, knowledge and skills acquired from the study are expected to be useful to the following stakeholders:

- (i) Ghana Atomic Energy Commission (GAEC),
- (ii) National Nuclear Research Institute,

- (iii) Nuclear Regulatory Authority of Ghana,
- (iv) University of Cape Coast
- (v) School of Nuclear and Allied Science, University of Ghana regarding its implementation of M.Sc.in PROCESS CONTROL AND INSTRUMENTATION program .
- (vi) Other Tertiary Institutions and industries using control system.

To keep the PTS in regular operation, effort should be made to adopt the designed PLC controller to avoid losing more customers as a result of frequent breakdowns.

Successful integration of cyclic mode NAA into the one-short conventional system will enable the technique to be applied in Biological, environmental, geological, industrial and forensic studies; (Hou, 2000).

Sample changer should be the next area of study to ensure fully automatic counting system after the implementation of the PLC control system; sponsorship is therefore needed.

REFERENCES

- Akaho, E. H., Maaku, B., Dodoo-Amoo, D. N., & Anim-Sampong, S. (1999). Steady-state Operational Characteristics of Ghana Research Reactor-1. *Journal of Applied Science and Technology (JAST)*, 4, 15–23.
- Akaho, E. H. K., Anim-Sampong, S., Dodoo-Amoo, D. N. A., Maaku, B. T., Emi-Reynolds, G., Osae, E. K., Bamford, S. A. (1995). *Safety Analysis Report for Ghana Research Reactor – 1*. G.A.E.C, Accra-Ghana.
- Alfassi, Z., Tsechansky, A., Kushelevsky, A. (1980). On the Correction of the Self Coincidence in Gamma Ray Spectra Dependence of Resolution Time on Energy'. *Radioanal. Chem.*, 55, 135–139.
- Alison Dunn. (2008). The father of invention: Dick Morley looks back on the 40th anniversary of the PLC | Manufacturing AUTOMATION. Retrieved May 10, 2019, from <https://www.automationmag.com/features/the-father-of-invention-dick-morley-looks-back-on-the-40th-anniversary-of-the-plc.html>.
- Anders, O. U. (1960). Determination of Fluorine by Neutron Activation. *Analytical Chemistry*, 32(10), 1368–1369.
<https://doi.org/10.1021/ac60166a048>
- Anders, O. U. (1961). Use of Very-Short-Lived Isotopes in Activation Analysis. *Analytical Chemistry*, 33(12), 1706–1709.
<https://doi.org/10.1021/ac60180a025>
- AnyDesk. (2017). *AnyDesk User Manual.pdf*, philandro software GmbH.
<https://doi.org/https://download.anydesk.com/docs/AnyDesk-UserManual.pdf>

- Bolton, W. (William). (2009). *Programmable logic controllers*. Newnes Publication (Elsevier Ltd), 5th Edition, Burlington, MA 01803, USA.
Retrieved from: www.amazon.com/Programmable-logic-Controller-William-Bolton/dp/1856177513.
- Bürkert UK Ltd. (2017). Bürkert Fluid Control Systems. Retrieved June 26, 2019, from <http://bit.ly/Burkert>.
- Caldwell, R. L., Mills, W. R., Allen, L. S., Bell, P. R., & Heath, R. L. (1966). Combination Neutron Experiment for Remote Analysis. *Science*, 152(3721), 457–465. <https://doi.org/10.1126/science.152.3721.457>
- Chatt, A., & DeSilva, K. . (1979). Pseudo-cyclic Neutron Activation Analysis of Ag, F, Rb, Sc and Se in Biological Samples?. *Trans. Am. Nucl. Soc.*, 32, 185–186.
- Chatt, A., DeSilva, K., Holzbecher, J., Stuart, D., Tout, R., & Ryan, D. (1981). Cyclic Neutron Activation Analysis of Biological and Metallurgical Samples?. *Can. J. Chem.*, 1660–1664.
- Chilian, C., & Kennedy, G. (2009). *A strategy for managing ageing components of a slowpoke reactor*. Department of Engineering Physics,. Canada.
- Dams, R., Billiet, J., & Hoste, J. (1975). Neutron Activation Analysis of F, Sc, Se, Ag and Hf in Aerosols Using Short-Lived Isotopes. *International Journal of Environmental Analytical Chemistry*, 4(2), 141–153.
<https://doi.org/10.1080/03067317508071110>
- DeSilva, K. ., & & Chatt, A. (1988). A method to improve precision and detection limits for determination of trace elements through short-lived nuclides. *J.*

Trace & Microprobe Techniques, 1, 307.

DeSoete, D., Gijbels, R., & Hoste, J. (1972). *Neutron Activation Analysis*. New York.

Doanh, H. Van, Dung, H. M., Thien, T. Q., Sy, N. T., & Dien, N. N. (2015, August 1). *Investigation of the cyclic techniques in neutron activation analysis on Da Lat research reactor for determination of short-lived radionuclides in biological materials*. Retrieved from https://inis.iaea.org/search/search.aspx?orig_q=RN:47073045

Egan, A., Kerr, S.A. Minski, M. J. (1977). *Determination of Selenium in Biological Materials Using ^{77}mSe and Cyclic Activation Analysis*’, Retrieved May 13, 2019, from 1977 website: [https://books.google.com.gh/books?id=UkhXAAAAYAAJ&q=Egan,+A.,+Kerr,+S.A.+Minski,+M.J.,+\(1977\).+‘Determination+of+Selenium+in+Biological+Materials+Using+ \$^{77}\text{mSe}\$ +and+Cyclic+Activation+Analysis’,+Radiochem.+Radioanal.&dq=Egan,+A.,+Kerr,+S.A.+Mi](https://books.google.com.gh/books?id=UkhXAAAAYAAJ&q=Egan,+A.,+Kerr,+S.A.+Minski,+M.J.,+(1977).+‘Determination+of+Selenium+in+Biological+Materials+Using+^{77}mSe+and+Cyclic+Activation+Analysis’,+Radiochem.+Radioanal.&dq=Egan,+A.,+Kerr,+S.A.+Mi)

Frequency Modulation – Physics and Radio-Electronics. (n.d.). Retrieved June 26, 2019, from <http://www.physics-and-radio-electronics.com/blog/frequency-modulation/>

Gao Jijin. (1993). *General Description of Ghana Miniature Neutron Source Reactor. Training Manual*. Beijing, China.

Givens, W., Mills, W., & Caldwell, R. L. (1969). *Cyclic Activation Analysis*’, in. *Proceedings of International Conference on Modern Trends in Activation Analysis*, 139–147. Washington, DC: National Bureau of Standards,.

- Glenn, F. K. (2000). *Radiation Detection and Measurement*. Retrieved from [http://users.lngs.infn.it/~dimarco/Radiation Detection and Measurement, 3rd ed - Glenn F.pdf](http://users.lngs.infn.it/~dimarco/Radiation%20Detection%20and%20Measurement,3rd%20ed-Glenn%20F.pdf)
- Grass, F., Westphal, G. (1977). Multi-elemental activation analysis of short-lived nuclear states. *Nucl. Instr. And Meth.*, 140(1), 97-108.
- Heydorn, K., & Damsgaard, E. (1997). Validation of a Loss-free Counting System for Neutron Activation Analysis with Short-lived Indicators'. *Radioanal. Nucl. Chem.*, 215(2), 157–160.
- Hou, X. (2000). *Cyclic Activation Analysis*. Encyclopedia of Analytical Chemistry, R.A. Meyers (Ed.). John Wiley & Sons Ltd, Chichester. Pp. 12447-12459
- Hou, X. (2008). Cyclic Activation Analysis. In *Encyclopedia of Analytical Chemistry*. <https://doi.org/10.1002/9780470027318.a6-204.pub2>
- Hou, X., & Das, H. A. (1997). Accuracy, precision and sensitivity in cyclic INAA with short-lived radionuclides. *Journal of Radioanalytical and Nuclear Chemistry*, 223(1–2), 67–72. <https://doi.org/10.1007/BF02223365>
- Huabai, T., Gao, J., Shuping, C., & Yulun, L. (1992). *Pneumatic Capsule Transfer System, MNSR-DC-5*. China Institute of Atomic Energy,. Beijing, China.
- IAEA. (2005). *Safety of Research Reactors: Safety Requirements*. IAEA Safety Standards Series No. NS-R-4. <https://doi.org/http://www.iaea.org/books>
- IAEA SPECIFIC SAFETY GUIDE No. SSG-24. (2012). *Safety in the Utilization and Modification of Research Reactors*.

<https://doi.org/http://www.iaea.org/books>

IAEA SPECIFIC SAFETY GUIDE No.SSG-39. (2016). *Design of*

Instrumentation and Control Systems for Nuclear Power Plants.

<https://doi.org/http://www.iaea.org/books>

Ismail, S. S. (2010). A New Automated Sample Transfer System for Instrumental Neutron Activation Analysis. *Journal of Analytical Methods in Chemistry*, 2010. <https://doi.org/10.1155/2010/389374>

Joshi, G. ., & Agrawal, H. (1995). Multielemental Analysis of Soil Samples by Fast Neutron Activation'. *Radioanal. Nucl. Chem., Articles*, 198(2), 475–485.

Kerr, S. A., & Spyrou, N. M. (1978). Fluorine analysis of bone and other biological materials: A cyclic activation method. *Journal of Radioanalytical Chemistry*, 44(1), 159–173. <https://doi.org/10.1007/BF02517687>

Laughton, M. A., & Warne, D. F. (2003). *Electrical engineer's reference book*. Retrieved from <https://www.oreilly.com/library/view/el-ectrical-engineers-reference/9780750646376/>

Laul, J. C. (1979). *Neutron Activation Analysis of Geological Materials*, *Atomic Energy Review*.

Logo, P., & Logo, C. (2009). *Technical data Order numbers*. 1–286.

MIL-STD-1629A. (1980). *Procedures for performing a Failure Mode, Effects and Criticality Analysis*. https://doi.org/www.http://every-spec.com/MIL-STD/MIL-STD-16001699/MIL_STD_1629A_1556/

Nafaa Reguigui. (2006). (PDF) Gamma Ray Spectrometry. Retrieved May 10,

2019, from https://www.researchgate.net/publication/259533588_Gamma_Ray_Spectrometry

Notes, E. (2018). *Phototransistor Circuit Configurations | Applications | Electronics Notes*.

Odoi, H., Amponsah-Abu, E., Gyamfi, K., Osei-Mensah, W., Shitsi, E., Boafo, E., Osei, B. (2018). *LEU Safety Analysis Report for GHARR-1. Nuclear Research Institute, Ghana Atomic Energy Commission, Accra, Ghana*.

Onsemi. (2005). *Complementary Silicon Power Transistors*. Retrieved from <https://www.onsemi.com/pub/Collateral/2N3055-D.PDF>

Sarheel, A. M., Nassri, M., & Hatem, E. (2018). *Automated Sample Changer System connected with Gamma Spectroscopy System*. Damascus, Syria.

Schonfeld, E. (1966). Alpha—a computer program for the determination of radioisotopes by least-squares resolution of the gamma-ray spectra. *Nuclear Instruments and Methods*, 42(2), 213–218. [https://doi.org/10.1016/0029-554X\(66\)90188-1](https://doi.org/10.1016/0029-554X(66)90188-1)

Siemens. (2012). *Industry Sector Postfach 48 48 90026, LOGO 8 Siemens PLC manual pdf, Pp. 47-48*.

Spyrou, N. M. (1981). Cyclic activation analysis—A review. *Journal of Radioanalytical Chemistry*, 61(1–2), 211–242. <https://doi.org/10.1007/BF02517411>

Spyrou, N. M., & Kerr, S. A. (1979). Cyclic activation: The measurement of short-lived isotopes in the analysis of biological and environmental samples. *Journal of Radioanalytical Chemistry*, 48(1–2), 169–183.

<https://doi.org/10.1007/BF02519783>

Texas Instrument (2014). *Texas Instrument Incorporated*.

Tout, R. E., & Chatt, A. (1981). The effect of sample matrix on selection of optimum timing parameters in cyclic neutron activation analysis. *Analytica Chimica Acta*, 133(3), 409–419. [https://doi.org/10.1-016/S0003-2670\(01\)83212-8](https://doi.org/10.1-016/S0003-2670(01)83212-8)

Ward, N. I., & Ryan, D. E. (1979). Multi-element analysis of blood for trace metals by neutron activation analysis. *Analytica Chimica Acta*, 105(C), 185–197. [https://doi.org/10.1016/S0003-2670\(01\)83750-8](https://doi.org/10.1016/S0003-2670(01)83750-8)

Wytttenbach, A. (1971). Coincidence losses in activation analysis. *Journal of Radioanalytical Chemistry*, 8(2), 335–343. <https://doi.org/10.1007/BF02518199>

Yanik, P. (2017a). *Fundamentals of Programming*. United States of America.

Yanik, P. (2017b). *Overview of Programmable Logic Controllers*. United States of America.

Yiguo, L., Peng, D., Jin, L., Jingyan, H., Qian, H., Mengjiao, W., Aboh, I. J. (2017). *Loading of LEU core and Commissioning report for GHARR-1 facility with LEU core*. China / Ghana.

Zhang, H., Chai, Z. F., Qing, W. Y., & Chen, H. C. (2009). Cyclic neutron activation analysis for determination of selenium in food samples using ^{77m}Se. *Journal of Radioanalytical and Nuclear Chemistry*, 281(1), 23–26. <https://doi.org/10.1007/s10967-009-0087-6>

APPENDICES

APPENDIX A

THE OPERATING INSTRUCTIONS OF PTS CONTROLLER



Starting and stopping the PTS Controller

To start the PTSC:

First plug the power cord to 220 VAC power supply. Press the main switch to “ON” position, the main AC voltage supply meter move clockwise to 220 VAC.

Second step, toggle the +24 VDC switch up, the testing yellow LED and the power green bulb lights-up.

Third step, toggle the +12 VDC switch up and the system is ready for operation.

The test point red LED and the power green bulb lights-up.

Stopping procedure:

Toggle the +12 VDC switch down, the red LED and green power lights go-off.

The next step, toggle the +24 VDC switch down, the yellow LED and the green power bulb go-off; and

Lastly, press the main-switch to “OFF” position, the main power to the PTS controller is disconnected.

Controller front panel LEDs

Controller front panel Button knobs and switches

AC Power Supply

Applying power to the PTS controller, press the AC main switch to “ON” position. The AC meter at the left top of the system will point to about 220 volts, the relay bank indication bulb (red LED) will glow to indicate that the 8-way relay bank is powered.

DC Power Supply

The DC power supply consist of +24 VDC and +12 VDC respectively. To power the PLC, the +24 VDC switch is toggled up, the first green bulb glow along with a yellow LED in between a test point of the +24 VDC. The +12 VDC power supply which connect the PLC output to control the relays (relay bank) is switched on by toggling the second switch up. A red LED in between +12 VDC test point glows.

Control Switches

The control switches are composed of six momentary push buttons.

Four of the button knobs are yellow in colour and the other two are red, mainly for stop and reset purposes. Button I₁ (compressor-start) is pushed to start the air-compressor. White LED glows to indicate that the air-compressor is in operation. Button I₂ (compressor stop/reset) is pushed to interrupt the process by either to stop or reset, should any mistake occurs. Button I₃ (sample-in) is pressed to open the solenoid valves S₁ and S₃ to transfer sample into the reactor irradiation site. Button I₄ which represents a phototransistor on top of the reactor detect the sample capsule, switch a +24 VDC pulse signal to close the solenoid valves and start a timer (B005) for irradiation. Red LED bulb flashes up and buzzer beeps to alert the operator of sample irradiation. After the irradiation, the irradiation timer sends signal to open solenoid valves S₂ and S₄ to transfer the sample capsule onto the detector. Phototransistor on top of the detector detects the sample capsule and the counting process starts. Button I₅ is used to represent the said phototransistor. Sample-out green LED glows to indicate that the sample capsule is out of the reactor. Button I₆ is pressed to either stop or reset the sample transfer process.

Ethernet communication slot

The Ethernet communication slot is for the transfer of data from the PC to PLC and vice versa.

APPENDIX B

Weekly Maintenance Check-list

| Systems | Details of Scheduled Maintenance Checks | Weekly Assessment | | | | | |
|---|---|-------------------|--|--|--|--|--|
| | | | | | | | |
| AC METER | AC Voltage measurement i. At 220 VAC ii. Above 220 VAC iii. Below 220 VAC | | | | | | |
| DC VOLTAGE MEASUREMENTS -USING AVOMeter | i. Measure +24 VDC ii. " +12 VDC iii. Indication light functionality • +24 VDC • +12 VDC | | | | | | |
| -USING OSCILOSCOPE | i. Measure the amplitude of +24 VDC ii. " +12 VDC iii. The waveforms | | | | | | |
| SWITCHES FUNCTIONABILITY | i. +24 VDC ii. +12 VDC | | | | | | |
| CONTROL KNOBS (SWITCHES) | Depress to transfer a dummy capsule IN / OUT of the Reactor. i. Compressor start ii. Compressor stop / reset iii. Sample-in iv. Phototransistor-IN v. Phototransistor-OUT vi. Sample stop / reset | | | | | | |
| TEST CONTROL INDICATION LIGHTS | Test during control knobs operation i. Compressor start light ii. Relay bank light iii. Sample -IN iv. Sample -OUT v. Sample irradiation flash light | | | | | | |

Name (s) of Inspector(s):

Date:

Remarks:

Signature: Date:

(REACTOR MANAGER)

COMMENTS (IF ANY):

APPENDIX C

PTS CONTROLLER MAINTENANCE PROGRAM

The objective of PTS Controller maintenance, periodic testing and inspection is to ensure that the system and components (SCs) of the Controller function in accordance with the design intents and requirements.

The maintenance structure adopted for PTS Controller is PROACTIVE and REACTIVE based. The proactive component is based on preventive and predictive maintenance, while the reactive component is executed by corrective maintenance activities (IAEA, 2006). The maintenance program developed for the PTS Controller is hence divided into two: routine maintenance, during which preventive and predictive maintenance are carried out; and corrective maintenance. Maintenance logbook (check list) for routine and corrective maintenance activities should be kept to keep track of maintenance records of systems and components. The check list can be found, Appendix B.

Routine (Preventive) Maintenance

This is to ensure that the PTS Controller is always ready for safe operation in the week. Routine maintenance activities for the system should be carried out on weekly basis, depending on the frequency of use.

The preventive maintenance should include;

- Taking the reading of the AC meter
- Measuring of +24 VDC and +12 VDC respectively at the test points using AVOMeter

- Use oscilloscope at the test points to measure the amplitude of the voltages and check for fluctuations in the waveform
- Toggle the +24/12 VDC switches for their functionality
- Inspect the indication LEDs
- Depress the control knobs to send dummy capsule in and out of the reactor to ensure the functionality of the buttons, (if implemented).

Corrective maintenance

- If any of the control knobs fail, switch-off power to the controller, remove the six self-tapping screws and take off the controller metal cover. Take care of the PLC device fixed in the cover. Take AVOMeter, select Ohms and check the continuity by pressing the particular button. If it is malfunctioning, (then corrective maintenance) take soldering iron and a solder sucker, remove the affected switch and replace.
- If any of the indication LEDs fail, first connect an AVOMeter across the LED, select DC voltage and measure the voltage across it. Measure the voltage dropper resistor, if it is in good condition and the required voltage is measured, then remove the LED and replace. If the required voltage is present but the LED is not functioning, remove and replace.